



**HAL**  
open science

## Durabilité du polychloroprène pour application marine

Pierre Yves Le Gac

► **To cite this version:**

Pierre Yves Le Gac. Durabilité du polychloroprène pour application marine. Mécanique des matériaux [physics.class-ph]. Ecole nationale supérieure d'arts et métiers - ENSAM, 2014. Français. NNT : 2014ENAM0036 . tel-01132912

**HAL Id: tel-01132912**

**<https://pastel.hal.science/tel-01132912>**

Submitted on 18 Mar 2015

**HAL** is a multi-disciplinary open access archive for the deposit and dissemination of scientific research documents, whether they are published or not. The documents may come from teaching and research institutions in France or abroad, or from public or private research centers.

L'archive ouverte pluridisciplinaire **HAL**, est destinée au dépôt et à la diffusion de documents scientifiques de niveau recherche, publiés ou non, émanant des établissements d'enseignement et de recherche français ou étrangers, des laboratoires publics ou privés.

École doctorale n° 432 : Sciences des Métiers de l'Ingénieur

**Doctorat ParisTech**

**T H È S E**

pour obtenir le grade de docteur délivré par

**l'École Nationale Supérieure d'Arts et Métiers**

**Spécialité “ Mécanique – Matériaux ”**

Le 20 Novembre 2014

**Pierre-Yves LE GAC**

**DURABILITY OF POLYCHLOROPRENE RUBBER FOR MARINE  
APPLICATIONS**

Directeur de thèse : **Bruno FAYOLLE**  
Co-encadrement de la thèse : **Peter DAVIES**

**Jury**

**M. Costantino CRETON**, Directeur de Recherche CNRS, ESPCI ParisTech  
**M. Pieter GIJSMAN**, Directeur de Recherche, Laboratory Polymer Technology, Eindhoven  
**M. Toan VU-KHANH**, Professeur, École de Technologie Supérieure, Montreal  
**M. Matthew CELINA**, Directeur de Recherche, Sandia National Laboratories, Albuquerque  
**M. Peter DAVIES**, HDR, IFREMER, Brest  
**M. Bruno FAYOLLE**, Professeur, PIMM, ARTS & Métiers ParisTech  
**M. Jacques VERDU**, Professeur, PIMM, ARTS & Métiers ParisTech  
**M. Gérard ROUX**, Ingénieur, Thales Underwater System

Président  
Rapporteur  
Rapporteur  
Examineur  
Examineur  
Examineur  
Examineur  
Invité

**T  
H  
È  
S  
E**



*A mes enfants,  
Marius et Marceau*



# Remerciements

Ces quelques années dans le monde de la Recherche m'ont permis de découvrir que cette page de remerciements est probablement celle qui est la plus lue dans un manuscrit de thèse, malheureusement elle ne sera pas la plus intéressante donc surtout n'hésitez pas à lire la suite du document...

Une thèse n'est pas, contrairement à ce que l'on peut croire, un travail solitaire mais un travail d'équipe qui permet les échanges scientifiques et personnels. Je tiens donc à remercier très chaleureusement, et avec beaucoup de gratitude, tous les membres de cette fine équipe : Bruno Fayolle, Peter Davies, Jacques Verdu et Gérard Roux. Messieurs, quel bonheur de travailler avec vous ! Merci pour votre présence, votre confiance, vos connaissances et aussi tous ces moments agréables passés ensemble en réunion ou... au bar. Je suis certain que nous aurons l'opportunité de continuer à travailler ensemble et je m'en réjouis d'avance.

Ces travaux ont été évalués par un jury composé de Costantino Creton, Pieter Gijsman, Toan Vu-Khanh et Mat Celina. Je tiens à tous vous remercier pour le temps que vous avez passé à évaluer ce travail mais surtout pour la pertinence de vos questions et remarques qui me feront, sans aucun doute, avancer pour la suite. Un remerciement tout particulier pour Mat qui m'a accueilli au sein de son laboratoire et surtout pour toutes les discussions sur la science et le monde en général.

Une fois encore, les travaux présentés dans ce manuscrit sont le fruit d'un travail d'équipe ; je tiens donc à exprimer toute ma gratitude aux membres du Laboratoire « Matériaux » de l'Ifremer : Marie Michèle, Benoit, Florence, Nico, Mick, Bertrand, Denise, Tatiana, Morgane, Luc, Nico, Corentin, Mael, Yvon, Christophe, Albert, Nico, Patrick, Mathieu, Matthias, Philippe, Maelenn... Je sais que pour certains l'ordre de citation est important, ce n'est pas le cas ici : merci à la fonction aléatoire ! J'ai quand même une pensée particulière à Dominique qui est à l'origine de ce projet et qui a toujours su m'intégrer dans ses activités, merci pour ça ! Un petit clin d'œil pour 'le Laboratoire d'à côté' et nos moments passés en salle café.

Je remercie également ma hiérarchie de m'avoir permis de réaliser cette thèse dans le cadre de mon travail au quotidien.

Un petit mot également pour tous les membres du PIMM qui m'ont toujours réservé un accueil chaleureux et agréable à chacun de mes passages. Un merci particulier à Emmanuel et Xavier pour les nombreuses discussions et les bons moments passés ensembles. . .

Je souhaite remercier les personnes avec qui j'ai le plaisir de travailler en dehors de ce projet : Denis, Bertrand, Alan, Vincent, Yann, Romain, Romain, Bernard. . . et tous les autres.

Mais il n'y a pas que le « boulot » dans la vie, merci donc à tous ceux qui ont été ou sont présents à mes côtés au quotidien. En premier lieu, ma famille et plus particulièrement mes parents et ma sœur pour avoir toujours été disponibles, pour m'avoir soutenu dans mes choix et donné la possibilité de faire des études. J'ai également une pensée sincère pour Héloïse et ma belle famille. Et enfin merci à mes deux petits loups, pour leur présence et leur sourire au quotidien. . . quel bonheur !

Et puis les potes aussi. . . je ne peux faire ici une liste exhaustive (trop peur d'en oublier !) mais ils se reconnaîtront, j'en suis certain. Une pensée particulière pour Virginie, sans toi ce document n'aurait peut-être jamais été rédigé ; merci à toi pour ta présence.

Et enfin je terminerai en te remerciant toi, lecteur, cela me permet d'oublier personne et surtout de t'inciter à lire la suite. . .

# Contents

<b>Introduction</b>	<b>1</b>
<b>1 Long term behaviour of rubbers in a marine environment</b>	<b>5</b>
1.1 Physical degradations of rubber when immersed in sea water . . .	6
1.1.1 Water absorption in rubbers . . . . .	6
1.1.1.1 Water absorption due to concentration differ- ences . . . . .	6
1.1.1.2 Kinetics of water diffusion . . . . .	7
1.1.1.3 Water absorption due to osmotic processes . . .	9
1.1.2 Consequences of water absorption in rubber for mechan- ical properties . . . . .	11
1.1.3 Degradation mechanisms induced by water exposure . . .	12
1.2 Possible chemical degradation processes of rubber when used in a marine environment . . . . .	14
1.2.1 Hydrolysis . . . . .	14
1.2.2 Oxidation in sea water . . . . .	16
1.3 Oxidation of polymers . . . . .	19
1.3.1 Mechanisms of oxidation . . . . .	19
1.3.1.1 Initiation . . . . .	19
1.3.1.2 Propagation . . . . .	21
1.3.1.3 Termination . . . . .	22
1.3.2 Oxidation kinetics . . . . .	22
1.3.2.1 Time/Temperature superposition method . . . .	23
1.3.2.2 Mechanistic approach . . . . .	23
1.3.3 Consequences of oxidation for mechanical properties of rubbers . . . . .	27
1.3.3.1 Modulus . . . . .	27
1.3.3.2 Fracture properties . . . . .	30
1.4 Conclusion . . . . .	33
<b>2 Materials and Methods</b>	<b>35</b>
2.1 Materials . . . . .	36
2.1.1 Polychloroprene . . . . .	36
2.1.1.1 Raw material . . . . .	36
2.1.1.2 Vulcanized CR . . . . .	36

2.1.2	Polyurethane . . . . .	37
2.1.3	Chlorinated Polyethylene . . . . .	37
2.2	Ageing . . . . .	38
2.2.1	Ovens . . . . .	38
2.2.2	Sea water tank . . . . .	38
2.2.3	Dynamic Vapor Sorption . . . . .	39
2.3	Characterizations . . . . .	40
2.3.1	Chemical characterizations . . . . .	40
2.3.1.1	FTIR . . . . .	40
2.3.1.2	Chlorine content in raw CR . . . . .	41
2.3.1.3	Oxygen absorption . . . . .	41
2.3.1.4	HCl released during CR immersion . . . . .	41
2.3.2	Physical characterizations . . . . .	42
2.3.2.1	In situ modulus measurement . . . . .	42
2.3.2.2	Tensile test . . . . .	42
2.3.2.3	DMA . . . . .	42
2.3.2.4	Permeation . . . . .	42
2.3.2.5	Modulus profiles . . . . .	42
2.3.2.6	Fracture in mode I . . . . .	43
<b>3</b>	<b>Oxidation of unvulcanized polychloroprene</b>	<b>45</b>
3.1	Introduction . . . . .	46
3.2	Results . . . . .	51
3.2.1	Molecular modifications . . . . .	51
3.2.2	Chlorine content . . . . .	54
3.2.3	Effect of oxygen pressure . . . . .	55
3.2.4	Effect of temperature . . . . .	56
3.3	Oxidation kinetic modelling . . . . .	57
3.3.1	Effect of oxygen pressure . . . . .	59
3.3.2	Physical meaning of rate constant values and their hierarchy . . . . .	61
3.3.3	Comparison of polychloroprene with other polydienes . . . . .	62
3.3.4	Temperature effect . . . . .	63
3.4	Conclusion . . . . .	64
<b>4</b>	<b>Oxidation of vulcanized and unstabilized polychloroprene rubber</b>	<b>65</b>
4.1	Introduction . . . . .	66
4.2	Homogeneous oxidation at 100°C . . . . .	68
4.2.1	Results . . . . .	68
4.2.1.1	Oxidation mechanisms . . . . .	68
4.2.1.2	Effect of oxidation on CR modulus . . . . .	71
4.2.2	Discussion and Modelling . . . . .	73
4.2.2.1	Sulfur effect . . . . .	73
4.2.2.2	Predicted oxygen consumption rate . . . . .	75

4.2.2.3	Modulus prediction . . . . .	76
4.3	Temperature effect on oxidation of vulcanized polychloroprene . . . . .	80
4.3.1	Variation of $ks_1$ and $ks_2$ with temperature . . . . .	80
4.3.2	Effect of ageing temperature on modulus prediction . . . . .	82
4.3.3	Temperature effect on the overall oxidation kinetics . . . . .	84
4.4	Inhomogeneous oxidation . . . . .	87
4.4.1	Results . . . . .	87
4.4.1.1	Double bond concentration and modulus profiles . . . . .	87
4.4.1.2	Oxygen permeability . . . . .	88
4.4.2	Modelling . . . . .	89
4.5	Conclusion . . . . .	92
<b>5</b>	<b>Oxidation effect on fracture properties of rubbers</b>	<b>95</b>
5.1	Introduction . . . . .	96
5.2	Crack propagation experiments . . . . .	99
5.2.1	Description of the experiments . . . . .	99
5.2.1.1	Machine . . . . .	99
5.2.1.2	Sample geometry . . . . .	100
5.2.2	Influence of experimental parameters . . . . .	100
5.2.2.1	Influence of ligament length . . . . .	100
5.2.2.2	Effect of sample thickness . . . . .	101
5.2.2.3	Temperature effect . . . . .	102
5.2.2.4	Influence of strain rate . . . . .	103
5.3	Results . . . . .	104
5.3.1	Fracture properties from tensile test . . . . .	104
5.3.2	Fracture properties of CR from crack propagation characteristics . . . . .	105
5.3.3	Comparison of CR with other elastomers . . . . .	107
5.4	Discussion . . . . .	109
5.4.1	Period I: Decrease in $G_{IC}$ . . . . .	109
5.4.2	Period II: Increase in $G_{IC}$ . . . . .	109
5.4.3	Period III: Drop off in $G_{IC}$ . . . . .	111
5.4.4	Life time prediction . . . . .	112
5.5	Conclusion . . . . .	113
<b>6</b>	<b>Long term behaviour of polychloroprene in sea water</b>	<b>115</b>
6.1	Accelerated ageing of fully formulated CR in sea water . . . . .	116
6.2	Water clustering in polymers: a literature review . . . . .	119
6.3	Results and discussion . . . . .	121
6.4	Conclusion . . . . .	132
	<b>Conclusions</b>	<b>133</b>
	<b>Future work</b>	<b>135</b>
	<b>Bibliography</b>	<b>137</b>

<b>Appendix I: Differential equation system</b>	<b>151</b>
<b>Appendix II: French summary</b>	<b>153</b>

# Introduction

The oceans represent more than 70 % of the surface of the planet but so far less than 5% of their volume has been explored. Faced with diminishing resources of energy, food and rare metals the exploration and exploitation of the oceans is becoming a major issue for our society. However, the cost and complexity of maintaining structures immersed at sea makes long term exploitation of ocean resources difficult.

There are three main types of materials employed at sea: concrete, metals and polymers. The latter, which have the advantage of low density, help to reduce the weight of structures and thus simplify installation. The lifetime of polymers in a marine environment is a subject which is complex and has received little attention to date. The complexity is related to the many possible degradation mechanisms for these materials. For this reason, the definition of a methodology for lifetime prediction, based on accelerated laboratory aging, is crucial. Polychloroprene rubber (CR) is widely used for marine application due to its intrinsic properties such as large elongation, good fatigue behaviour, thermal properties and good durability compared to natural rubber.

The aim of this study is to analyse the long term behaviour of polychloroprene (CR) in a marine environment and in particular to evaluate the role of oxidation, so that a non-empirical methodology for the prediction of the evolution of mechanical properties with time can be established.

In the first part of this document the long term behaviour of elastomers will be presented based on published work. It will be shown that in theory elastomers pick up very little sea water when immersed. However, in practice through an osmotic cracking mechanism there may be large water absorption and a significant loss in fracture resistance. In addition, CR can undergo chemical degradation, in particular oxidation. The examination of samples aged in service has shown that oxidation is one of the main chemical degradation processes in elastomers used at sea. This study will therefore focus on the prediction of oxidation in polychloroprene, and the consequences for mechanical property predictions.

In the same chapter a description will be given of current methods used to predict elastomer oxidation. These will show that a mechanistic description of oxidation, coupled with a kinetic approach, is the only method which allows a non-empirical prediction to be made. However, this method is not simple and

requires a step by step approach. A reminder of the main bibliographic results will be given before each chapter in order to facilitate reading of the document.

The following chapter will describe the materials and methods used in this study. While the methods used to follow the chemical and mechanical changes are well known (IR spectroscopy, tensile tests) a particular effort has been made to follow these changes in-situ under accelerated oxidation conditions.

The first step in setting up the kinetic model is presented in Chapter 3, devoted to the oxidation of non-vulcanized polychloroprene. The aim of this part of the study is to determine the oxidation mechanisms and in particular to assess the role of chlorine and of the double bond which characterizes the polychloroprene monomer. After proposing a mechanistic scheme for oxidation of non-vulcanized polychloroprene, the rate constants associated with each chemical reaction have been determined at 100°C by an inverse method, using the experimental results at different oxygen pressures. Then the effect of temperature has been integrated in the kinetic model.

The second step in developing the kinetic model involves integrating the effect of vulcanization, and especially that of sulfur (Chapter 4). Sulfur acts as an anti-oxidant which slows down the oxidation rate of the elastomer. This effect has been taken into account by adding two new chemical reactions to the model and determining their associated rate constants. In addition, the presence of double bonds in the CR leads to extensive cross-linking during oxidation, which is revealed in a strong increase in modulus. This behaviour will be predicted quantitatively for the first time in CR by use of the kinetic model coupled with rubber elasticity theory. Finally, this chapter will also examine the physical effects involved in oxidation, and in particular the diffusion of oxygen, which must be included in order to predict the behaviour of thick components.

The following chapter (Chapter 5) will investigate the effect of oxidation on the fracture behaviour of elastomers. The final aim is to be able to predict the fracture behaviour from the mechanistic approach by considering the changes in cross-link density resulting from oxidation. First, an experimental study of crack propagation in CR will be presented in order to identify the parameters which influence these measurements. Then the evolution of fracture energy with oxidation will reveal an unexpected response, with a first drop in resistance, then an increase followed by a final drop. Understanding this behaviour is essential if reliable lifetime predictions are to be made. In order to test different hypotheses, two other materials will be compared to CR: a polyurethane containing double bonds liaisons and a chlorinated polyethylene. The latter will enable the role of oxidation on induced crystallization to be separated from cross-linking induced by double bonds. The results will

be compared with theoretical considerations and a prediction will be proposed.

The final chapter was originally intended to describe the adaptation of the model for oxidation in air to the marine environment (Chapter 6). However, the accelerated aging tests performed on a completely formulated polychloroprene (with stabilizers and carbon black) in sea water revealed a very large water absorption. As a result this chapter is devoted to explaining the origins of this large absorption, using dynamic vapor sorption tests. This indicated the formation of water clusters in the elastomer. The formation of these clusters will be discussed and modeled.

The document is completed by a general conclusion on the work presented here, and some ideas for future work. The aim of the latter will be to allow the completion of a long term behaviour model for industrially formulated elastomers.



## Chapter 1

# Long term behaviour of rubbers in a marine environment

This first chapter is dedicated to the description of existing data and knowledge about the long term behaviour of rubbers when used in a marine environment. First, physical degradations induced by water absorption will be considered. Then in a second section, chemical degradations that could occur when rubbers are used in a marine environment will be detailed and we will show that this kind of polymer is very sensitive to oxidation. Rubber oxidation will be described in the next section. Finally, based on data and results described here, a philosophy of work will be proposed for this study.

## 1.1 Physical degradations of rubber when immersed in sea water

Obviously when rubbers are used in a marine environment, they are immersed in sea water and the first point when considering long term behaviour is to examine the effect of this immersion. This section aims to present some generalities about rubber behaviour when immersed in water.

### 1.1.1 Water absorption in rubbers

When a polymer sample is immersed in water, water diffuses from the external media to the interior of the sample in order to balance chemical potentials. In fact the surface layer immediately absorbs the water and reaches almost instantaneously its equilibrium state. The distribution of water in the early stages is markedly non-uniform with most of the water absorbed being close to the surface of the sample. As time passes, water penetrates further and further into the bulk of the sample until equilibrium is reached when water concentration is uniform everywhere throughout the rubber. The movement of water usually obeys Fick's laws of diffusion and the kinetics of movement are characterized by a water diffusion coefficient. The quantity of water absorbed by a polymer at equilibrium is another characteristic of a polymer, which depends on the chemical structure. The capacity of water absorption of a given polymer is sometimes called hydrophilicity. Water uptake in polymers depends in a more or less complex way on two exposure parameters: temperature and water activity, often expressed as relative humidity. The aim of experiments is to establish the dependence of diffusivity and solubility (the property characterizing equilibrium) on these exposure parameters.

#### 1.1.1.1 Water absorption due to concentration differences

Water content in a polymer is directly linked to the polarity of the chemical groups present in the material and especially to the aptitude of these groups to establish hydrogen bonds [1] [2]. Roughly speaking, the more polar is the matrix, the more the polymer will absorb water. Elastomers are polymers with low polarity, otherwise their glass transition temperature  $T_g$  would be higher than ambient temperature and so they would not be elastomeric in their common use conditions, so water solubility in elastomer matrix is expected to be low. In fact, in the literature there are a few examples of low water absorption in rubbers. Both Kemp [3] and Boggs [4] found water absorption up to 0.5 % when natural rubber was immersed in water. For polyurethane, water absorption was less than 2 % [5] [6] and could even be reduced by using hydroxyl polybutadiene as a polyol [7] [8]. Briggs found that both polybutadiene and ethylene-propylene absorbed less than 1 % when immersed in water at 25°C [9]. Silicone rubbers also absorb a very small amount of water, less than 1 % according to the study of Riggs [10].

It appears that due to the low polarity of rubbers, the maximum water absorption in this kind of polymer is generally low. According to Henry's law the equilibrium water concentration is directly proportional to the solubility and water activity as shown below:

$$[H_2O]_{saturation} = S_{H_2O} \cdot p_{H_2O} \quad (1.1)$$

where  $[H_2O]_{saturation}$  is the concentration of water at saturation,  $S_{H_2O}$  is the water solubility in the polymer and  $p_{H_2O}$  is the partial pressure of water in the external media.

However the amount of water absorbed in a polymer is not the only aspect that has to be considered. It is also necessary to focus on the kinetics of the absorption: this is the aim of the next paragraph.

#### 1.1.1.2 Kinetics of water diffusion

Since water is present only in low concentrations in rubbers, it does not modify significantly the free volume and other polymer characteristics linked to macromolecular mobility. In such cases, diffusion obeys the simplest kinetic law i.e. Fick's second law in one dimension (equation 1.2) in which sorption kinetics at a given temperature depends only on two material parameters: the equilibrium water concentration and the water coefficient of diffusion  $D$  in the polymer. A typical sorption curve obeying Fick's law is shown in Figure 1.1, this is an example of water absorption in polyurethane sheets of two thicknesses at 80°C in sea water [5].

$$\frac{\partial [H_2O]}{\partial t} = D \cdot \frac{\partial^2 [H_2O]}{\partial x^2} \quad (1.2)$$

Where  $[H_2O]$  is the concentration of water,  $D$  the diffusion coefficient,  $t$  the time and  $x$  the position through the thickness.

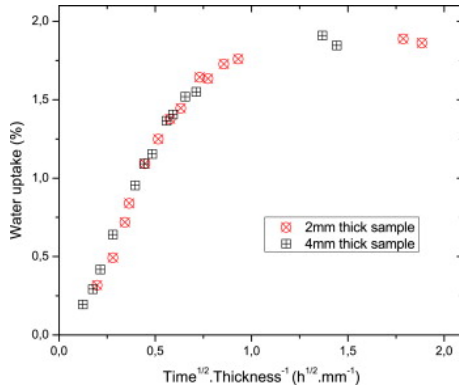


Figure 1.1: Water absorption in a polyether based polyurethane immersed in sea water at 80°C : a typical Fickian behavior [5].

Water diffusion results from activated jumps in holes opened by segmental motions. Since the glass to rubber transition is characterized by a strong increase in the cooperativity of molecular motions, it results that water diffusivity is higher (by at least one order of magnitude) in elastomers than in glassy polymers. For instance, in a polyurethane elastomer,  $D$  is of the order of magnitude of  $10^{-11} \text{ m}^2.\text{s}^{-1}$  at 25°C compared to about  $10^{-14} \text{ m}^2.\text{s}^{-1}$  for an amine cured epoxy [11].

Although a low hydrophilicity is the rule for elastomers, there are some exceptions [12] [13] [14], as shown by the example of polychloroprene immersed in water at 38°C (Figure 1.2). Here, the weight gain reaches about 30 % after 120 days without any sign of stabilization. This behaviour is presumably due to an osmotic process that will be described in the next section.

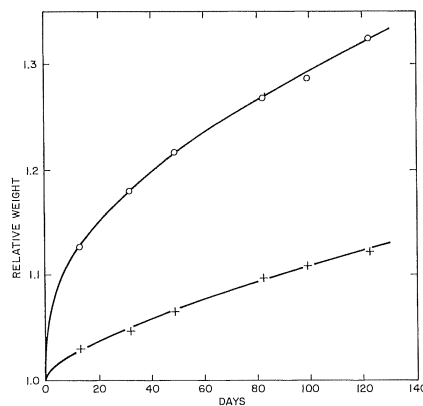


Figure 1.2: Water absorption in polychloroprene for fresh (o) and salt (+) water [12].

### 1.1.1.3 Water absorption due to osmotic processes

Water absorption due to an osmotic process in rubbers has been first described by Fedors [15] [16] and could be explained as follows: if one of the several additives used in a (filled) rubber formulation (for vulcanization, stabilization or reinforcing) is partially soluble in water, a solute layer will be formed in a droplet at the filler surface. This solute has its own osmotic pressure which differs from the one (generally almost zero) in the external medium. This means that water uptake is now driven by the difference in osmotic pressure between clusters and external water and not by concentration differences, this osmotic pressure can be written as follows:

$$P = \pi_i - \pi_o \quad (1.3)$$

Where  $\pi_o$  is the osmotic pressure of the external salt solution in which the rubber is immersed,  $\pi_i$  is the osmotic pressure of the internal droplet solution and  $P$  the hydrostatic pressure exerted by the rubber on the impurity droplet as shown in figure 1.3 and observed experimentally in Figure 1.4.

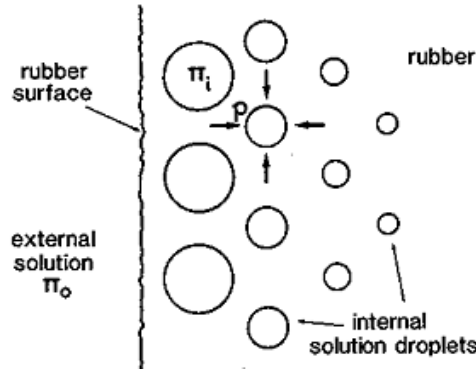


Figure 1.3: Schematic representation of the osmotic process in rubber according to Fedors [15].

Pressure inside the cavity leads to an increase of this cavity size according to a crack propagation mechanism, i.e. when pressure is superior to a critical value  $P_{CR}$  the cavity grows.

According to fracture mechanics, in rubbers, the critical pressure can be predicted from considerations of rubber elasticity. Indeed, considering a cavity as defined by Ball [17] and assuming a neohookian behaviour, the critical pressure to initiate the cavity ( $P_{CR}$ ) can be written as:

$$P_{CR} = \frac{5G}{2} \quad (1.4)$$

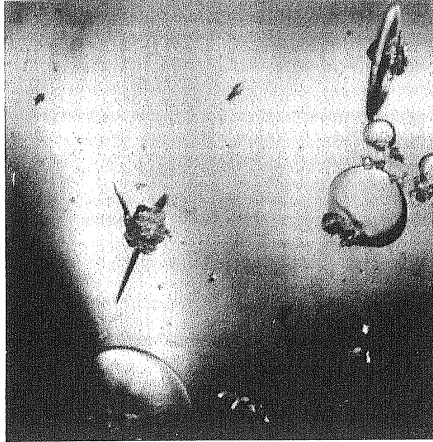


Figure 1.4: Experimental observation of cavities in a silicone elastomer containing cobalt chloride crystals as an inclusion [16].

After the cavity initiation, the pressure required for the cavity growth can be described as:

$$P_{CR} = \frac{G}{2} * \left( 5 - \frac{4}{\lambda} - \frac{1}{\lambda^4} \right) \quad (1.5)$$

Where  $P_{CR}$  is the critical pressure required to enlarge an isolated cavity in a large block of rubber,  $G$  the shear modulus and  $\lambda$  local extension ratio. One can notice here that the surface tension (related to the cavity surface) is not taken into account in the previous relationship.

This osmotic process stops when the pressure applied to the cavity is equal to the internal pressure in the cavity (i.e. when  $P=0$  in equation 1.5) meaning that in practice due to this phenomenon, the amount of water absorbed by a rubber could be high, up to 30 % in polychloroprene (CR) [14].

To conclude, water absorption in rubbers is a complex phenomenon because it depends on the nature and concentration of the partially soluble compounds [9], the rubber stiffness, and the nature of external medium. Due to this complexity it is not easy to model the kinetics of water absorption in rubbers when osmotic processes are involved. However, some ideas have been developed in the past, and interesting work can be found in [18] [19] [20]. A detailed study of cluster formation in rubber with consideration of kinetic aspects will be proposed in Chapter 6.

### 1.1.2 Consequences of water absorption in rubber for mechanical properties

Usually when considering polymers, the presence of water increases chain mobility due to plasticization effects, the main manifestations of these latter being a  $T_g$  and a modulus decrease, and often an increase of elongation at break [21] [22] [23]. As previously mentioned, because mobility is large in rubbers the water absorption is expected to have only small consequences for the mechanical behaviour. For example, Figure 1.5 shows the evolution of mechanical behaviour of a natural rubber aged in natural sea water at 40°C up to 3 months. This rubber absorbs about 1 % of water at saturation [24]. Water absorption in this natural rubber does not affect its mechanical behaviour.

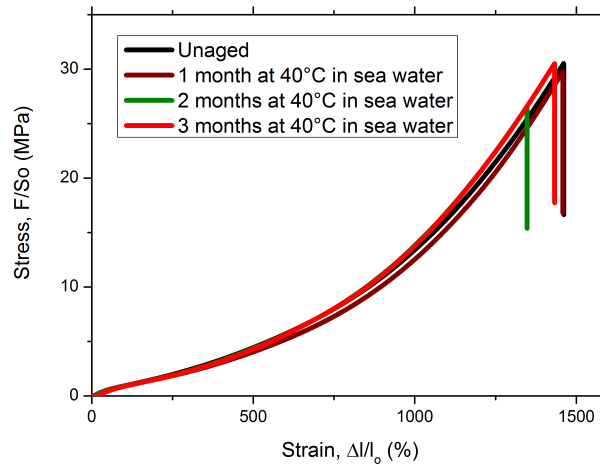


Figure 1.5: Mechanical behavior of a 2 mm thick natural rubber that absorbed 1% of water at saturation (saturation is reached in 20 days after immersion) [24].

However, when large water uptake occurs during an osmotic process, large changes occur in the mechanical behaviour of rubber. In fact, for a CR aged at 70°C, Leveque found a decrease of 80 % for the tensile products (tensile strength X elongation at break) for a volume swelling of 22 % as shown in Figure 1.6 [25]. Various studies have been performed on mechanical evolution of rubber when immersed in water [26] [27], such as fatigue [14] [28] and acoustic behaviour [13] showing that properties may or may not be affected by water depending on the degradation mechanism involved, this point will be detailed in the next section.

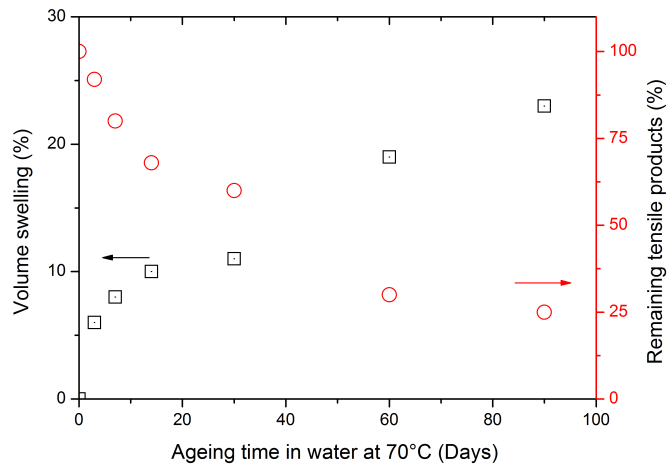


Figure 1.6: Tensile product (modulus X elongation at break) and swelling ratio evolution with water absorption in a CR immersed in water at 70°C [25].

### 1.1.3 Degradation mechanisms induced by water exposure

To summarize the previous sections, the mechanisms responsible for rubber degradation when the latter are exposed in sea water can be described as follows:

- When a rubber is used in sea water, water diffuses in the matrix according to a Fickian process in many cases. Because of the low polarity of the matrix the amount of absorbed water is usually low, and due to high molecular mobility in rubbers the water diffusion is fast compared to glassy polymers.
- This low amount of water absorbed by the rubber does not usually affect its properties much because mobility in such polymers is very high even in the absence of water.
- Meanwhile, in practice large water absorption has been observed in certain rubbers, this behaviour was explained by the existence of an osmotic driving force caused by the presence of partially soluble additives. In this case, the large amount of water and formation of droplets working as cracks lead to a large reduction of mechanical properties.

Moreover large variation in mechanical behaviour can also be observed even with low water absorption, due to chemical degradation occurring when rubbers are used in a marine environment. For example, Le Gac [29] reported a large evolution of properties of a silica filled CR used in sea water for 23 years even in the dry state (Figure 1.7). The next section will be dedicated to these chemical reactions in terms of mechanisms and their consequences.

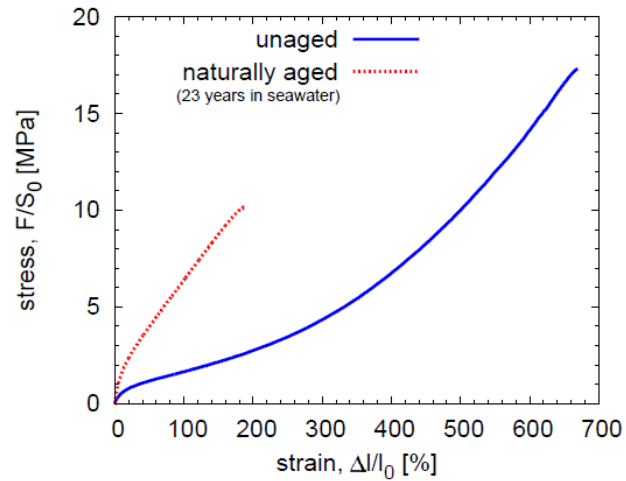


Figure 1.7: Tensile curves of a silica filled CR samples unaged (full line) and after 23 years in sea water (dotted line) tested in the dry state [29].

## 1.2 Possible chemical degradation processes of rubber when used in a marine environment

When rubbers are used in sea water, chemical degradation can also occur. This degradation is irreversible, i.e. when water is removed, properties remain permanently altered as shown in several studies [30] [31] [32]. This section will focus on the description of possible irreversible degradation processes that could occur when rubbers are used in sea water. The first one is the hydrolysis of the polymer.

### 1.2.1 Hydrolysis

Due to the presence of water within the rubber, one of the chemical degradation mechanisms that could theoretically occur is hydrolysis. This irreversible degradation can be defined as a chemical reaction between water and polymer that can be written as:



This reaction involves a chain scission in the polymer network and so a decrease of the crosslink density. As a result of these scissions, the mechanical behaviour of polymers is strongly affected, for rubber, stiffness and ultimate properties tend to decrease. Wet ageing of polyurethane based on polyester is probably the best known example of elastomer hydrolysis, chemical reactions involved in the degradation can be found in [33].

Hydrolysis equilibrium occurs at high conversion, far beyond the conversion domain of practical interest. There is a wide consensus that the reverse reaction is negligible at the conversions under consideration. Hydrolysis generates acid groups which accumulate in the polymer. This accumulation is responsible for auto-acceleration of the hydrolysis process in two ways:

- Carboxylic acids are able to establish strong hydrogen bonds with water, they contribute thus to an increase of the equilibrium concentration in the polymer [34]. Indeed the hydrolysis rate is proportional, in a first approximation, to the water concentration.
- Carboxylic acids generate  $\text{H}^+$  ions and hydrolysis is acid catalyzed. Indeed the proportion of dissociated acids is lower in a polymer matrix of relatively low dielectric permittivity than in water but it is high enough to have a significant auto-acceleration effect.

Hydrolysis kinetics can be established in a scheme in which non-catalyzed and catalyzed reactions coexist:



In this case the conversion ratio X can be written [35]:

$$X = \frac{1 - \exp(-K.t)}{1 + A. \exp(-K.t)} \quad (1.6)$$

with  $K = k_c. [H_2O]. ([Ester]_o + \frac{k_u}{k_c})$  and A is dimensionless auto-catalysis factor defined by:  $A = \frac{k_c. [Ester]_o}{k_u}$

This reaction leads to a large molar mass decrease when linear polyester-urethanes are used in humid environment, for example Murata found that degradation occurs within a month at 80°C (Figure 1.8)[36].

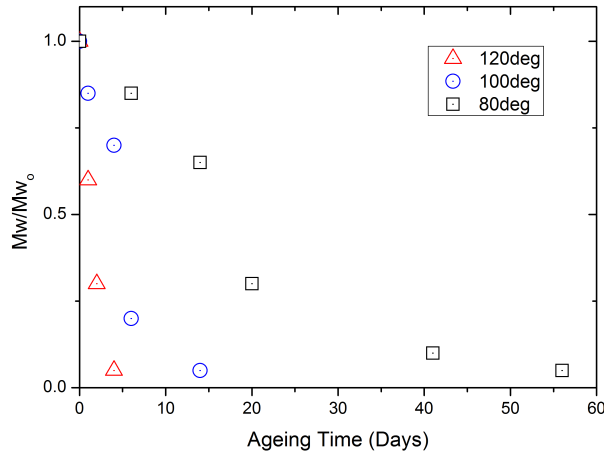


Figure 1.8: Decrease in molecular mass during polyester-urethane hydrolysis [36].

Due to hydrolysis, polyester based polyurethanes are not suitable for long term use in a marine environment; in contrast polyether-polyurethanes are considerably more stable owing to the non-hydrolyzable character (at low temperature) of ether linkages [31] [37] [38] when no amines are used.

Unlike PU, most of the usual elastomer materials do not undergo hydrolysis when used in water. However, because of the use of fillers in rubber formulation, hydrolysis has to be considered. For example, a hydrolysis of silica fillers used in a polychloroprene has been reported after both accelerated ageing in the laboratory and natural ageing [29]. In this case hydrolysis of the filler leads to an increase of polymer stiffness which is unusual. In the same way but without evidence, for some authors [20] the natural rubber evolution, when immersed in water, is due to hydrolysis of impurities such as esters. It is not easy to consider stability of each additive or filler used in rubbers;

however it has been shown that carbon black (which is the most used reinforcing filler in rubber) does not play a role in rubber degradation in water [39].

From previous considerations it appears that when rubbers are carefully formulated with appropriate fillers, hydrolysis should not be an issue for this material in a marine environment. However other kinds of irreversible chemical degradation processes could occur in rubbers when they are used in sea water, in particular oxidation.

### 1.2.2 Oxidation in sea water

Oxidative ageing of a polymer can be defined as a chemical reaction between the polymer and oxygen. This kind of degradation has been widely studied in the past in terms of mechanisms, kinetics and consequences, more information can be found in recent reviews [40] [41]. It clearly appears that oxidation is one of the most important sources of ageing for polymers because of the availability of oxygen in the environment and this kind of degradation is involved in many failures that have been reported in the literature [42]. In spite of extensive research and progress in this area for 70 years, polymer oxidation is not fully understood due to the complexity of the mechanisms involved in the degradation. When considering polydienic rubbers it appears that these are very sensitive to oxidation due to the presence of highly reactive carbon-carbon double bonds and high oxygen diffusivity, so when dealing with long term behaviour of these materials it is necessary to consider this type of degradation [43] [44] [45].

The idea that oxidation is one of the main chemical degradation mechanisms of rubber when they are used in sea water is supported by literature results. In fact, oxidation has been considered as the main degradation process during accelerated ageing of rubbers [28]. In a more detailed study Riaya clearly shows that oxidation occurs when SBR is used in water [46]. Regarding polychloroprene rubber, a recent characterization of a sample used in service for 23 years in sea water clearly indicates an oxidation of the external layer of about 200 microns [29]. This indicates that when long term behaviour in a marine environment is an issue, oxidation of rubber has to be considered.

When talking about rubber oxidation in sea water, the first point is the oxygen availability; the oxidation rate in polymers depends on the oxygen concentration within the material, the latter is proportional to the oxygen concentration in the surrounding water which is directly linked to the oxygen partial pressure in the surrounding atmosphere, according to Henry's law. According to thermodynamic principles, a water layer saturated by oxygen is as effective in polymer oxygenation as the atmosphere with which it is in equilibrium. In other words, polymers can undergo oxidation in water despite the low oxygen solubility in water. The maximum oxygen content in sea water depends on

temperature and salinity and can be calculated using the equation developed by Benson and Krause [47]. In practice the actual oxygen concentration in the ocean is usually lower than its theoretical value owing to oxygen consumption by living resources. Furthermore a coupling effect can exist between sea water and oxidation:

- On one hand, the presence of water in the rubber can affect the oxidation process. Water can lead to hydrolysis of certain oxidation products, for instance esters, and so to modification of chemical processes, but there is no evidence of any effect of water on the kinetics of oxidation or its consequences in the literature. However, the presence of water in elastomers and more broadly in polymers can induce leaching of additives, especially antioxidants. These organic molecules that aim to reduce oxidation rate are widely used in rubbers, they are usually amine or phenol molecules that can scavenge radicals and so increase time to failure. Leaching by water of these protective molecules has been highlighted in a few studies [48] [49] [50] in the past but there has been no particular study for rubbers in sea water to our knowledge.
- Rubber oxidation could also lead to a modification of water absorption behaviour in such materials. In fact oxidation leads to formation of polar products that could increase maximal water absorption in rubber. For example, Lake tested water absorption in Natural Rubber, Nitrile rubber and CR with and without a prior ageing of 4 days at 100°C in an oven (Figure 1.9) [14]. For all rubbers, water absorption is more important after oxidation; similar results have also been obtained by Tester [51].

Since polydiene rubbers are very sensitive to oxidation, even when they are used in sea water, this irreversible degradation has to be considered in order to be able to predict long term behaviour of polychloroprene in sea water. Furthermore other kinds of irreversible degradation could occur such as oxidation induced by UV exposure or degradation due to biological attack. Based on existing data these kinds of degradation seem to be less important compared to the effect of water and thermal oxidation and will not be considered here.

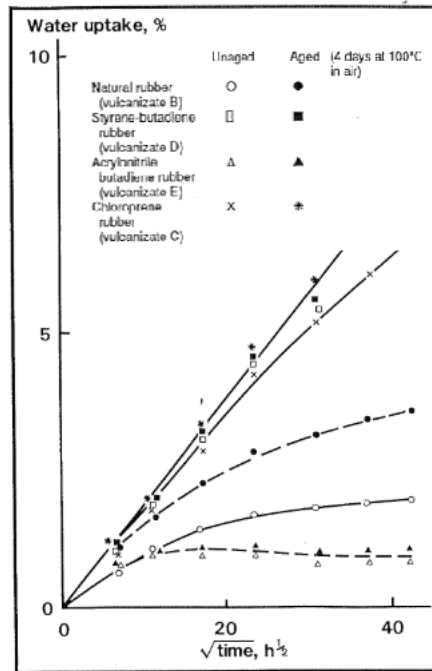


Figure 1.9: Effect of prior oxidation on the water absorption of 1.6mm thick rubbers in salt water (5%NaCl) [14].

To conclude we can consider that when rubbers are used in a marine environment, irreversible chemical degradation can occur resulting in a large modification of mechanical properties. Due to the presence of water, hydrolysis could occur, but when rubbers are formulated properly this kind of degradation should be avoided. However, rubbers are very sensitive to oxidation and data from literature highlight that this kind of degradation has to be taken into account when rubber durability in sea water is considered. So the next section will be dedicated to the description of this specific chemical degradation.

## 1.3 Oxidation of polymers

### 1.3.1 Mechanisms of oxidation

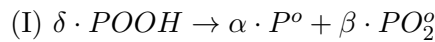
Here a quick presentation of the basic concepts of oxidation will be described, more information can be found in many books and reviews [40] [41]. Oxidation of polymers is a radical chain process that involves a reaction with oxygen. A radical chain process always involves three steps:

- Initiation: Non radical species  $\rightarrow$  Radicals
- Propagation: Radical type 1  $\rightarrow$  Radical type 2 + other products
- Termination: Radical + Radical  $\rightarrow$  Inactive Products

Each step of this process will be described hereafter.

#### 1.3.1.1 Initiation

The initiation step is the formation of radicals and is the most controversial step of the oxidation process in polymers. In the literature this step is often reported as  $\text{PH} \rightarrow \text{P}^\bullet$ , however this reaction is expected to be very slow at low temperature [52]. It has been proposed [43] that in this mechanistic approach radical formation occurs through decomposition of hydroperoxide according to:



This initiation step could be either unimolecular ( $\delta=1$ ,  $\alpha=2$  and  $\beta=0$ ) or bimolecular ( $\delta=2$ ,  $\alpha=1$  and  $\beta=1$ ). This choice is motivated by the fact that this kind of initiation could be used to predict the auto acceleration of oxidation in polymers through the "closed loop process" (Figure 1.10).

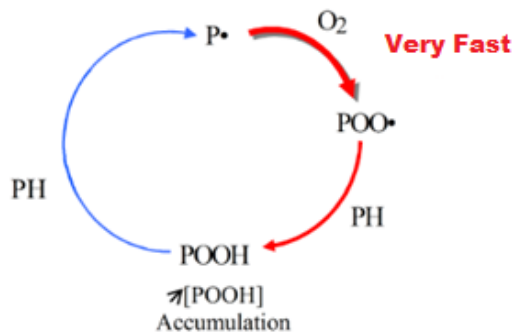


Figure 1.10: Schematic representation of the closed loop oxidation process.

Hydroperoxides are formed in the propagation step and destroyed in the initiation step, we can thus expect the existence of a pseudo-equilibrium POOH concentration:  $[POOH]_{equ}$  corresponding to the equality of both rates and thus to the existence of a steady state regime. In most cases, the nature of species responsible for the first initiation events and the corresponding initiation rate is unknown but what is sure is that a short time after exposure, hydroperoxides become the major radical sources owing to their high instability and their growing concentration. Tobolsky and coll. [43] proposed a simple but efficient kinetic model based on the following assumptions:

- Hydroperoxides are the unique radical sources, in other words there is an initial hydroperoxide concentration  $[POOH]_o$  kinetically equivalent to the radical sources initially present in the polymer;
- The global radical concentration  $[P^o] + [PO_2^o]$  rapidly reaches a stationary state but each concentration can vary. This last hypothesis is, indeed, questionable but Tobolsky and coll. obtained very a simple analytical relationship having a high heuristic value.

We can see that if the initial hydroperoxide concentration is lower than the steady state concentration ( $[POOH]_o < [POOH]_{equ}$ ), then the reaction will begin at low rate and auto-accelerate to reach a steady state. In extreme cases ( $[POOH]_o \ll [POOH]_{equ}$ ), the kinetics can display an initial induction period during which the concentration of oxidation products will remain lower than the sensitivity threshold of common analytical methods. In principle, the kinetic model describes only the variation of POOH concentration. Stable oxidation products can come only from initiation or termination but since initiation and termination rates are almost equal during most of the exposure time, it can be postulated that all the oxidation products come from hydroperoxide decomposition.

One major point is that chain scissions are among the most important oxidation products; a schematic representation of this chain scission is shown in Figure 1.11. It is noteworthy that the POOH decomposition mechanism leading to the chain scission process involves several steps, the overall kinetics being controlled by the slowest reaction. This random chain scission will affect mechanical properties of rubbers significantly as will be shown later.

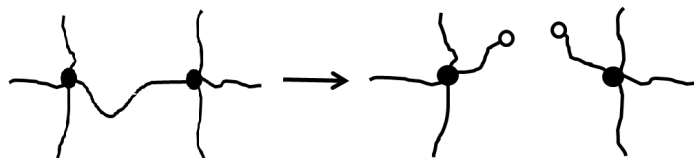
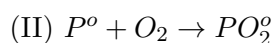


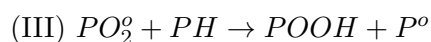
Figure 1.11: Schematic representation of the random chain scission that occurs when POOH is decomposed.

### 1.3.1.2 Propagation

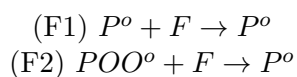
Several reactions are involved in the propagation process, the fastest one is the reaction of oxygen with radicals; in fact because oxygen is a biradical in its ground state it will have a high reactivity with free radicals ( $P^\circ$ ) created during the initiation step according to the following reaction:



Then two kinds of propagation could occur, one is general for all polymers and involves an abstraction of hydrogen from the substrate (PH) that can be written as follows:



The other occurs only in unsaturated substrates (such as polychloroprene),  $PO_2^\circ$  and  $P^\circ$  radicals add to double bonds (noted F) according to the following equations:



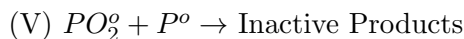
When this reaction is intermolecular, new crosslinks are formed in the network of the rubber as shown in Figure 1.12. These additions could also be intramolecular giving cycles instead of crosslinks [53]. This point will be detailed in Chapter 4.



Figure 1.12: Representation of the formation of new crosslink during intermolecular reaction of radicals on double bond.

### 1.3.1.3 Termination

Radicals can deactivate each other through bimolecular combinations that lead to formation of non radical species. Since two radicals ( $P^\bullet$  and  $PO_2^\bullet$ ) are considered, three termination reactions are possible:



Each termination type may involve several different elementary reactions that have been detailed in [41]. Among possible termination processes, radical coupling contributes to crosslinking. Non-empirical lifetime prediction needs a kinetic model based on a more or less complex mechanistic scheme of which the main elementary reactions are the ones shown above.

## 1.3.2 Oxidation kinetics

The question here is how to be able to predict long term oxidation (over about 20 years) of polymers and more especially rubbers on the basis of relatively short (of the order of one year) accelerated ageing tests. This section will briefly describe the most frequently used approaches with their limits, and then the mechanistic approach will be introduced.

### 1.3.2.1 Time/Temperature superposition method

In order to reduce ageing time the ageing temperature is often increased and then a Time/Temperature superposition is applied, usually based on the use of the Arrhenius law considering that lifetime  $t_f$  can be written as:

$$t_f = t_{fo} \cdot \exp\left(\frac{H}{RT}\right) \quad (1.7)$$

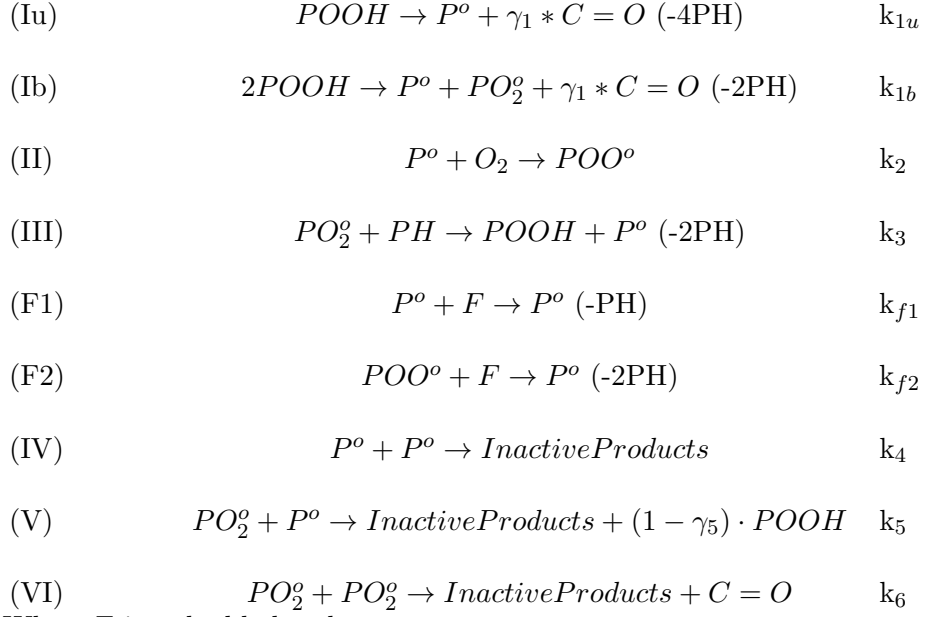
where  $t_{fo}$  is a preexponential factor,  $H$  is the activation energy,  $R$  is the perfect gas constant and  $T$  is absolute temperature.

However it is essential to keep in mind that the Arrhenius law is established for an elementary reaction but not for complex ageing processes that involve several phenomena and chemical steps. Due to its ease of use, this approach has been used many times in the field of polymer ageing and rubber oxidation [54] [55] [56], it has even been the subject of various international standards. However many experimental studies have shown the limitations of predictions based on this approach [57] even for ageing in sea water [58]. Reasons for these failures have been detailed in the literature [59]; to summarize, the use of Arrhenius' law to predict ageing might be possible when one and only one process is involved in the degradation. In order to overcome this limitation two main approaches have been developed during the last 30 years. One is the mechanistic approach that will be described in the next section. The other very interesting one has also to be mentioned here, it is based on the development of an ultrasensitive oxygen absorption measurement that allows the measurement of oxidation rate even at room temperature and so factors of acceleration are known and not extrapolated [59]. However this latter methodology has also some limitations when predictions of mechanical properties are needed, this point will be discussed later.

### 1.3.2.2 Mechanistic approach

Many kinetic models have been developed in the last 50 years, a review is available in [41] but the two more advanced approaches will be described and compared here.

- In the ENSAM group, the kinetic model is derived from a mechanistic scheme, applying the basic principles of chemical kinetics. This scheme is generally close to the basic one that has been described in the previous section. The main idea is to attribute a rate constant for each step of the overall process as shown below in the case of an unsaturated substrate:



Where F is a double bond.

Obviously the general kinetic scheme has to be adapted to the polymer considered and its specificities, in the case of polychloroprene this will be done in Chapter 3.

From this scheme, it is possible to establish the differential equation system for reactive species, especially  $P^o$ ,  $POO^o$ , and  $POOH$  that could be resolved numerically in order to make predictions of oxidation over long periods. This approach has been developed for 40 years by the ENSAM group, the differential equation system according to the mechanistic scheme described above can be written:

$$\frac{d[P^o]}{dt} = 2 \cdot k_{1u} \cdot [POOH] + k_{1b} \cdot [POOH]^2 + k_3 \cdot [PH] \cdot [PO_2^o] + k_{f2} \cdot [F] \cdot [PO_2^o] - k_2 \cdot [P^o] \cdot [O_2] - 2 \cdot k_4 \cdot [P^o]^2 - k_5 \cdot [P^o] \cdot [PO_2^o]$$

$$\frac{d[POOH]}{dt} = -k_{1u} \cdot [POOH] - 2 \cdot k_{1b} \cdot [POOH]^2 + k_3 \cdot [PH] \cdot [PO_2^o] + (1 - \gamma_5) \cdot k_5 \cdot [P^o] \cdot [PO_2^o]$$

$$\frac{d[PO_2^o]}{dt} = k_{1b} \cdot [POOH]^2 + k_2 \cdot [P^o] \cdot [O_2] - k_3 \cdot [PH] \cdot [PO_2^o] - k_{f2} \cdot [F] \cdot [PO_2^o] - k_5 \cdot [P^o] \cdot [PO_2^o] - 2 \cdot k_6 [PO_2^o]^2$$

The main difficulty of this approach is the determination of each rate constant, this point will be considered later.

- In the meantime, the Sandia group has developed a simpler kinetic model based on an analytical solution of a similar mechanistic scheme called Basic Oxidation Scheme [60]. Wise et al. [61] have proposed a kinetic model based on an analytical solution of the previous system of differential equations. The oxygen consumption rate  $d[O_2]/dt$  under ambient equilibrium (non DLO) conditions is then:

$$\frac{d[O_2]}{dt} = \frac{C_1 \cdot [O_2]}{1 + C_2 \cdot [O_2]} \quad (1.8)$$

Where  $C_1 = \frac{k_1 \cdot k_2}{k_5}$  and  $C_2 = \frac{k_2 \cdot (k_4 - 2 \cdot k_3)}{k_5 \cdot (k_3 + k_4)}$  with  $k'_3 = k_3$ . [PH]

Contant rates  $k_i$  are the same as the ones defined in oxidation scheme. By multiplying both sides of the previous equation by  $L^2/p_{O_2} \cdot P_{O_2}$ , one obtains the following expression:

$$\frac{d[O_2]}{dt} \cdot \frac{L^2}{p_{O_2} \cdot P_{O_2}} = \frac{\alpha}{1 + \beta} \quad (1.9)$$

Where  $L$  is the sample thickness,  $p_{O_2}$  the oxygen partial pressure and  $P_{O_2} (= D_{O_2} \cdot S_{O_2})$  the oxygen permeability. Because according to Henry's law  $[O_2] = S_{O_2} \cdot p_{O_2}$ , the parameters  $\alpha$  and  $\beta$  are given by:

$$\alpha = \frac{C_1 \cdot L^2}{D_{O_2}} = \frac{L^2}{D} \cdot \frac{k_1 \cdot k_2}{k_5} \quad (1.10)$$

$$\beta = C_2 \cdot [O_2] = C_2 \cdot S_{O_2} \cdot p_{O_2} = \frac{k_2 \cdot (k_4 - 2 \cdot k_3)}{k_5 \cdot (k_3 + k_4)} \cdot S_{O_2} \cdot p_{O_2} \quad (1.11)$$

It is noteworthy that the main feature of this model is that oxidation rate is strongly dependent on the oxygen partial pressure. This model aspect is fundamental to describe the case where oxidation is controlled by oxygen diffusion (DLO regime). To simulate oxidation profile for the DLO regime (thick samples), the authors consider a fickian behaviour and steady state conditions with constant diffusivity. In this case, one obtains:

$$D \cdot \frac{d^2 [O_2(x)]}{dx^2} = \frac{C_1 \cdot [O_2]}{1 + C_2 \cdot [O_2]} \quad (1.12)$$

If  $X = x/L$  and  $\Theta = [O_2]/[O_2]_0$  are the dimensionless position and concentration variables, respectively, the previous equation is then:

$$\frac{\partial^2 \Theta}{\partial X^2} + \frac{1}{D} \cdot \frac{\partial D}{\partial X} \cdot \frac{\partial \Theta}{\partial X} = \frac{\alpha \cdot [O_2]}{1 + \beta \cdot [O_2]} \quad (1.13)$$

After the assessment of  $\alpha$  and  $\beta$  by measuring the oxygen absorbed on homogeneous samples and oxygen permeability (solubility and diffusivity), it is then possible to calculate the absorbed oxygen profile through

a thick sample in the DLO regime by solving numerically the previous equation [61] [62].

This approach proposed by the Sandia group seems to be simpler (only two parameters) however some of the hypotheses are questionable, differences between the two approaches will be detailed below.

The main differences between the two approaches are their assumptions. In order to be able to resolve this model analytically it has been assumed that:

- the only initiation mechanism is given by  $PH \rightarrow P^\circ$  ( $k_1$ ) and not by POOH decomposition meaning that the autoacceleration can not be predicted;
- the reaction linked to the addition reactions between double bonds and radical (F1 and F2) is not taken into account;
- long kinetic chain lengths (many propagation cycles compared to termination reactions) and  $k_5^2 = 4 \cdot k_4 \cdot k_6$ ;
- the steady state hypothesis ( $d[P^\circ]/dt + d[PO_2^\circ]/dt = 0$ ).

In the ENSAM approach, these assumptions are not made, so analytical resolution is not possible. It has been proposed to solve numerically the differential equation system [63]. In this case, hydroperoxides have been considered as responsible for the initiation. It has been shown that this pure numerical model can predict the autoacceleration behaviour observed for the oxidation kinetics. For instance, simulated concentrations of POOH,  $P^\circ$  and  $POO^\circ$  during polypropylene oxidation have been found not to be constant during exposure [64]. In this work, we propose to use this approach allowing not only to simulate oxidation products but also to simulate double bond (F) and substrate (PH) consumption during the oxidation process. In order to overcome the difficulty to determine each rate constant the main idea is to increase oxygen pressure in order to promote the (very fast) reaction of alkyl radicals with oxygen (reaction II) and so all reactions that involve alkyl radicals except reaction II can be neglected. A detailed description of the methodology of determination of the rate constants will be given in Chapter 3.

However this approach cannot be directly applied to industrial polymers owing to the complexity of the kinetic problem. It requires a step by step method, the first step corresponding to a model material, for instance the “pure”, uncrosslinked polymer, for which the rate constants of the main reactions can be determined. Then, the components and structural elements characterizing the industrial material (vulcanization, fillers and stabilization [65]) will be progressively added. This is the approach which will be used in this work. It is worth noting that the final goal of this approach is not to predict the formation of oxidative products but changes in mechanical properties. This is why the next section is devoted to the evolution of mechanical properties induced by rubber oxidation.

### 1.3.3 Consequences of oxidation for mechanical properties of rubbers

Because oxidation leads to a modification of the crosslink density, it affects the global mechanical behaviour of rubbers. This section aims to describe changes in mechanical properties induced by oxidation in rubbers and more especially polychloroprene with consideration of the modulus first and then fracture properties.

#### 1.3.3.1 Modulus

Many studies highlight a large increase of the polychloroprene modulus during oxidation. For example Ha-Anh observed a modulus close to 30 MPa after 4 days of ageing at 140°C on 2 mm samples with an initial modulus of 3 MPa (see Figure 1.13,) but this value was an average and much higher values were observed [54]. In fact, Celina has shown that at 140°C the oxidation is limited by the diffusion of oxygen meaning that modulus changes are non-uniformly distributed across the sample thickness. The local surface modulus is about 100 MPa after 8 days at 140°C compared to a 1 MPa initial (and core) value [62]. This large increase of modulus is due to the predominance of crosslinking events over chain scission, and more especially the free radical additions on unsaturations [53].

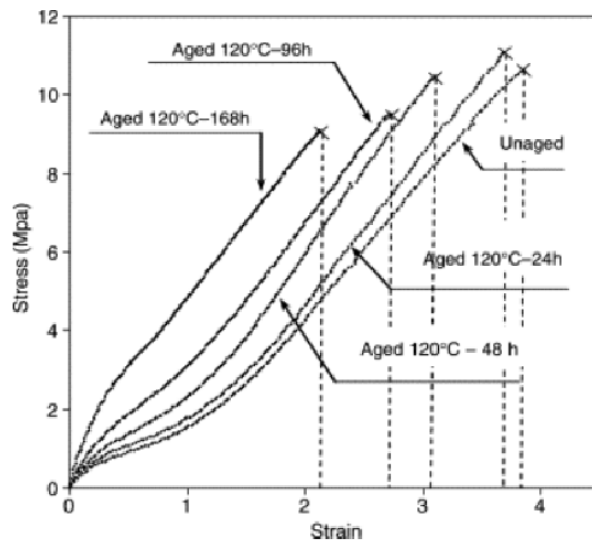


Figure 1.13: Tensile behavior changes during oxidation of stabilized polychloroprene at 120°C [54].

Because Natural Rubber is an unsaturated rubber and has been widely studied in the past (much more than CR) it is interesting to focus on changes of mechanical properties of this material during oxidation. During NR oxidation, the change in modulus is not simple: in a first stage a decrease of the modulus is observed and then a large increase occurs. The initial decrease is usually attributed to scission of intermolecular sulfur-sulfur bonds that have been created during vulcanization. The following large increase is attributed to the reaction of free radicals on the double bonds that creates new intermolecular bonds and so increases crosslink density [66]. This rapid description of the natural rubber behaviour during oxidation highlights the fact that both reactions on sulfur-sulfur bonds and double bonds have to be considered in order to describe network evolution. Because these reactions do not have the same activation energy, the temperature dependence of the mechanical properties is non-monotonic, as shown by Shelton [67] who found the modulus to increase at 40°C, decrease at 110°C and to vary non-monotonically at 90°C. The role of sulfur in rubber oxidation will be detailed in Chapter 4. But here the question is: *how to predict this behaviour?*

Usually two main approaches are used in literature, the first one is mainly used by ‘mechanics’ researchers and considers the evolution of parameters of a constitutive model. As an example, Ha-Anh proposed a prediction of the modulus based on the evolution of the two parameters of the Mooney Rivlin equation as a function of oxidation conditions. This approach could appear interesting because it is simple, however there is no consideration of the chemistry involved in the degradation and it could lead to a relatively poor prediction. In fact, at high temperature in thick samples, oxidation is not homogeneous because it is diffusion limited, meaning that the actual measured behaviour is the resultant of the different local behaviours of elementary thickness layers. Moreover, the prediction is made using Arrhenius law that could not be used a priori (see previous section). And finally, it is worth noting that this method has to be performed again if there is a small change in the formulation of the material.

The second approach that is more used by ‘chemistry’ researchers is based on a correlation between the build-up of oxidative products and modulus changes [68] [69], so if we are able to determine this correlation and then predict oxidation product formation it will be possible to make a prediction of the modulus. This approach has been used by Wise and Celina on polychloroprene to predict the increase of modulus, assuming the increase to be linked to the quantity of oxygen absorbed by the oxidation process by measuring experimentally the oxygen consumed by oxidation in the non DLO regime [61] [62]. Since a correlation between oxygen absorbed and modulus (at the edge of the sample) has been established in the case where oxidation is not controlled by oxygen diffusion, the authors are able to simulate modulus profiles through the sample thickness thanks to their analytical kinetic model coupling oxidation and oxygen diffusion. This methodology is very interesting because it is based on the chemistry of oxidation and moreover the actual acceleration factor is

measured over a large temperature range in order to perform reliable predictions. However, the actual correlation between the concentration of oxygen absorbed and modulus lacks the physical insights needed to build a complete non empirical model.

From the literature it appears that modulus prediction during rubber oxidation is a complex subject and existing methodologies are based either on quantitative consideration but without any chemistry involved or on qualitative predictions when chemistry is considered. Because the mechanistic model allows the prediction of chain scission and crosslinking, it should be possible to establish a quantitative relationship between oxidation chemistry and network evolution at the macromolecule scale. But now the question is: *is it possible to quantitatively link the evolution of the network to the rubber modulus?*

Fortunately and thanks to the theory of rubbery elasticity the modulus of an unfilled elastomer is directly linked to the crosslink density as shown below. In fact based on thermodynamic considerations, assuming that deformations occur at constant volume and that macroscopic deformations are affine of microscopic ones, it is possible to show [70] that the stress/strain behaviour at low deformation of unfilled rubber is, in simple extension, given by:

$$\sigma = R.T.\rho.\nu.(\lambda - \lambda^{-2}) \quad (1.14)$$

with  $\sigma$  the stress in Pa defined as  $F/S_o$  with  $F$  the load and  $S_o$  initial section,  $R$  the perfect gas constant,  $T$  the absolute temperature,  $\rho$  the density of the material,  $\nu$  the crosslink density, i.e. the concentration of elastically active chains, and  $\lambda$  the extension ratio.

From this equation it appears that the Young's modulus of an unfilled rubber in ideal conditions is directly linked to the crosslink density of the rubber.

$$E = 3.R.T.\rho.\nu \quad (1.15)$$

At reasonably low conversions, the actual crosslink density changes with time can be written as:

$$\nu(t) = \nu_0 - \delta \cdot s(t) + \gamma \cdot x(t) \quad (1.16)$$

Where  $\nu_0$  is the initial crosslink density,  $s(t)$  and  $x(t)$  are respectively the numbers of chain scission and crosslinking events at time  $t$ , the  $\delta$  and  $\gamma$  coefficients depend on the nature of the rubber and will be discussed later (Chapter 4).

So it appears that, in theory, by using the mechanistic approach coupled with theoretical considerations on structure-property relationships it is possible to predict quantitatively the evolution of rubber modulus during oxidation. This approach will be applied in Chapter 4 on vulcanized polychloroprene. As a conclusion, oxidation induces a large increase of polychloroprene modulus due to crosslinking by free radical addition on double bonds. Although the origin of this modulus increase is well known the prediction of change in

modulus as a function of oxidation in rubber is not straightforward. Existing methodologies are interested in either quantitative evolution without any consideration of oxidation mechanisms and could be partially wrong, or on qualitative evolutions. Using a mechanistic approach coupled with the theory of rubber elasticity a quantitative prediction of modulus considering chemistry involved during oxidation seems to be possible and will be developed in this study. At the same time, most lifetime predictions of rubbers are based on fracture properties, so the next section will be dedicated to changes in fracture properties of rubber with oxidation.

### 1.3.3.2 Fracture properties

During oxidation rubber undergoes large modification of the network structure and so changes in mechanical behaviour are induced. For most rubber applications, lifetime prediction is usually performed based on changes in elongation at break with ageing [28] [42]. The exact origin of this choice is not clear, in fact for most of their applications rubbers are used far from their ultimate elongation and failure must occur from crack propagation initiated at a defect. One reason for the choice of ultimate tensile elongation as an ageing sensitive property could be the simplicity of the experimental method for its measurement rather than its usefulness in practice where crack propagation properties are obviously more pertinent. This section will present generalities about changes in fracture properties with oxidation for polychloroprene.

In an extensive study of a fully formulated polychloroprene, Gillen tested change in elongation at break during oxidation of polychloroprene over a large range of temperature from 130°C to room temperature [71]. For all temperatures, elongation at break decreased with ageing time as shown in Figure 1.13. A prediction based on a correlation between absorbed oxygen and elongation at break was then proposed, here again this prediction was based on the hypothesis of a direct link between absorbed oxygen and elongation at break, and the fact that this link is independent of the ageing temperature. Similar ultimate elongation decreases have been observed many times in the literature for CR [54] [71] or other polydienic rubbers [42].

As previously mentioned ultimate tensile elongation is not an intrinsic material property. In fact, due to edge effects and the presence of cutting defects, elongation at break is more a 'sample' characteristic than a 'material' characteristic. In order to overcome this limitation it is possible to consider the energy necessary to propagate an existing crack that is directly related to rubber structure rather than sample preparation. Evolution of critical fracture energy in mode I (which is the opening mode, the most sensitive to mechanical property changes) ( $G_{IC}$ ) of polychloroprene during oxidation has already been reported in the literature [72]; it appears that a large decrease of  $G_{IC}$  occurs when the rubber undergoes oxidation as shown in Figure 1.14. Tearing energy decreases from 8 to 1 kJ/m<sup>2</sup>. Although these data are very interesting and show a large decrease of the tearing energy induced by oxidation it is not straightforward to propose a prediction mainly because oxidation is not

homogeneous through the sample thickness at these temperatures.

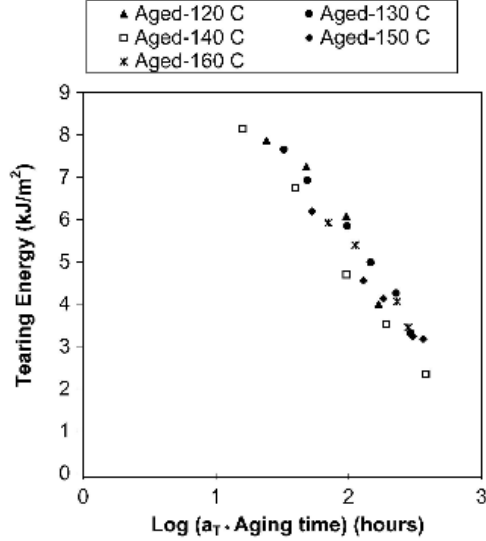


Figure 1.14: Change in tearing energy during oxidation of polychloroprene at temperature from 160°C to 120°C [72].

As a partial conclusion, it appears that fracture properties of rubber are of major interest for lifetime prediction. However the use of elongation at break can be considered more a sample characterization than a measurement of intrinsic material properties, it is thus interesting to consider the evolution of crack propagation properties as function of ageing. Here again the main idea is to be able to predict changes in the network structure through the mechanistic model and then use a physical theory to predict fracture energy. It is thus necessary to focus on the link between  $G_{IC_0}$  and the network structure. In a quasi ideal network with a unimodal distribution of the molar masses of elastically active chains (EACs), it is possible to show, based on network statistical theory and theory of entropic elasticity, that the threshold tear strength ( $G_{IC_0}$ ) is directly linked to the molar mass of EACs ( $M_c$ ) through the following equation [73]:

$$G_{IC_0} = K.M_c^{1/2} = K.\nu^{-1/2} \quad (1.17)$$

Where  $G_{IC_0}$  is the threshold tear strength that characterizes fracture free of viscoelastic dissipation or strain induced crystallization effects.  $K$  is mainly related to the rupture energy of a single chain.

This kind of relationship has been experimentally checked by various authors [74] [75] [76], but counter-examples have also been found [77] [78] due to

the fact that many phenomena could influence the fracture energy of a rubber such as viscoelasticity, strain induced crystallization or double networks. It appears that based on a prediction of network modification induced by oxidation it should be possible, in theory, to predict the decrease in fracture strength observed in the literature based on equation 1.17; this point will be investigated in Chapter 5 with special attention to the homogeneity of the degradation through the sample thickness.

## 1.4 Conclusion

When a rubber is immersed in sea water it will absorb water. The mechanisms and kinetics of water sorption depend strongly on the exact formulation of the rubber; if the material does not contain water soluble impurities it will absorb a very low amount of water with a high diffusion rate because of low polarity of the rubber. This low water uptake does not significantly affect mechanical properties. On the contrary due to the presence of partially soluble impurities an osmotic process could occur, this new driving force for water absorption can lead to a significant water uptake often without stabilization with immersion time. This large water absorption could lead to large modification of mechanical properties with a loss of elongation at break and change in stiffness due to swelling. This osmotic process is complex and not fully understood yet, however it can be avoided by using appropriate rubber formulations.

In addition to water absorption, rubbers can undergo irreversible chemical degradation when they are used in a marine environment. Due to the presence of water, hydrolysis may occur in both matrix and fillers but here again if the rubber formulation is chosen carefully this kind of degradation can be avoided. However because of the very high sensitivity of rubbers to oxidation, this latter degradation occurs even when rubbers are used in marine environment. In fact, the few results available after 42 years natural ageing of natural rubber show that oxidation was the most important cause of degradation [26]. Rubber oxidation is a mode of chemical degradation that cannot be avoided by changing the formulation, obviously rates can be reduced, but this degradation will occur eventually.

Furthermore, oxidation of polychloroprene leads to a large change in mechanical properties with a large increase of the modulus and a decrease of fracture properties that will lead to crack formation. So oxidation is of major interest for long term behaviour of polychloroprene in a marine environment and needs to be considered in order to make a life time prediction.

Despite a large interest for more than 50 years, prediction of oxidation in polymers and more especially the prediction of mechanical changes induced by oxidation is not straightforward due to the complexity of chemical and physical processes involved. Existing methodologies to predict change in mechanical properties during oxidation are usually empirical and limited. This study aims to overcome some of these limitations by using a prediction of mechanical properties, such as modulus and fracture energy, based on a mechanistic approach to describe the degradation.

This approach, that includes all the chemical steps that are kinetically important in the oxidation, is complex and cannot be directly applied to a fully formulated rubber, the model has to be set up step by step:

- In a first step (Chapter 3) oxidation of raw polychloroprene is considered in terms of both mechanisms and kinetics in order to set up the core of the model.
- Then in a second step (Chapter 4), the effect of vulcanization will be considered using a vulcanized CR without any stabilization, in order to take into account the sulfur effect on oxidation kinetics. Using this model coupled with the rubber theory a new non empirical methodology to predict modulus modification induced by oxidation will be described and discussed.
- The next step will be dedicated to the understanding of the evolution of fracture properties in rubber during oxidation (Chapter 5) with the aim of being able to make a property prediction.
- The last step to predict the long term behaviour of a fully formulated CR will be to take into account the effect of stabilizers, this will not be considered in this study.

In the meantime, the model developed for oxidation in air has to be adapted to sea water, this is why polychloroprene rubber has been immersed in heated sea water. Results obtained during these accelerated ageing tests reveal that, in this case, oxidation is not the only degradation process; a large amount of water is absorbed by the rubber. The last chapter (Chapter 6) discusses the origin and the prediction of this large water uptake.

## Chapter 2

# Materials and Methods

This chapter describes all the materials and techniques used during this study. First, all the gum and rubbers used here are presented, then the ageing conditions are described, and finally both chemical and mechanical characterization techniques are detailed.

## 2.1 Materials

This study is mainly focussed on polychloroprene degradation, however in order to understand the behaviour of this rubber better several other types of materials were also used, their characteristics are listed below.

### 2.1.1 Polychloroprene

#### 2.1.1.1 Raw material

Among the specialty elastomers polychloroprene [poly(2-chloro-1,3-butadiene)] is one of the most important, with an annual consumption of nearly 300 000 tons worldwide. First production was in 1932 by DuPont (“Duprene”, later “Neoprene”) and since then CR has an outstanding position due to its favorable combination of technical properties. Nowadays, polychloroprene is based on butadiene that is converted into the monomer 2-chlorobutadiene-1,3 (chloroprene) via 3,4-dichlorobutene-1, monomers are then polymerized using free radical emulsion according to:

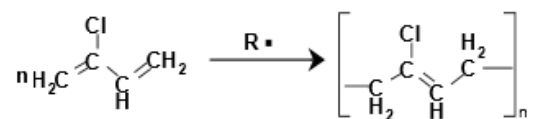


Figure 2.1: Polychloroprene polymerization.

The first part of this study (Chapter 3) was performed on the simplest polychloroprene gum, i.e. a raw linear polychloroprene referenced as Baypren 116. The polymer density is equal to  $1250 \text{ kg}\cdot\text{m}^{-3}$  and weight average molar mass, assessed by GPC, is close to  $140 \text{ kg}\cdot\text{mol}^{-1}$ .

#### 2.1.1.2 Vulcanized CR

##### *With MgO*

The most used material in this study is a polychloroprene vulcanized with sulphur. The formulation of the rubber is very basic and common, with vulcanization accelerators (MgO, ZnO and stearic acid). The actual sulphur concentration in the rubber was calculated theoretically based on formulation and measured, both values are in accordance and equal to  $0.45 \text{ mol}\cdot\text{l}^{-1}$ . The main characteristics of the rubber are given in Table 1.

### ***Without MgO***

Because MgO plays a role in the water absorption induced by the osmotic process [13] a new formulation was used, in order to evaluate the origin of water absorption in polychloroprene (Chapter 6). The material is exactly the same as above but without MgO.

### ***Fully formulated***

The fully formulated material was not studied in detail here but it includes the addition of 50 phr of carbon black and an amine as stabilizer (the nature of the amine is not known but that information is not needed here).

## **2.1.2 Polyurethane**

The PU is made of hydroxyl terminated polybutadiene (PBHT) cured by the diisocyanate derived from methylene dianiline (MDI) in a stoichiometric ratio. Samples were cured at room temperature for 24 hours and post cured at 100°C under a nitrogen atmosphere for 24 hours. The main characteristics are shown in Table 1.

## **2.1.3 Chlorinated Polyethylene**

An industrial partner provided a chlorinated polyethylene which was manufactured using a peroxide vulcanization process. No reinforcing fillers or stabilizers were used, characteristics are again given in Table 2.1.

Elastomer	Acronym	Modulus (MPa)	$M_c$ ( $\text{kg}\cdot\text{mol}^{-1}$ )	$T_g$ °C	Elongation at break (%)	Stress at break (MPa)
Polychloroprene	CR	1.89	5.50	-40	1400	9.8
Chlorinated Polyethylene	CPE	2.91	2.99	-21	500	8.2
Polyurethane	PU	3.78	1.77	-63	200	1.4

Table 2.1: Initial characteristics of rubbers used in this study.

## 2.2 Ageing

### 2.2.1 Ovens

Thermal oxidation was performed in Memmert ovens with forced convection at temperatures from 60 to 140°C ± 2 °C. Exposures were performed on both films and thicker samples. The films were cut from bulk samples, cooled by liquid nitrogen, with a Leica microtome.

### 2.2.2 Sea water tank

Samples were immersed in natural renewed sea water at different temperatures from 25 to 80 °C ± 2 °C (Figure 2.2). Sea water can be considered, (see Chapter 6), as pure water with an activity of 0.98 according to Robinson [79]. The water absorption was determined from the weight evolution of square samples (50 mm × 50 mm) with two different thicknesses (1.8 and 3.8 mm). Mass gain was followed by periodic weighing on a Sartorius LA 310 S balance (precision 0.1 mg). Samples were removed from the ageing containers and wiped with paper towels to dry the surfaces before weighing. The mass percent of absorbed water  $M(t)$  of each sample at time  $t$  is expressed using equation 2.1. For each condition 3 samples were tested and results averaged.

$$M(t) = \frac{m(t) - m_0}{m_0} \cdot 100 \quad (2.1)$$

where  $m(t)$  is sample mass at time  $t$  and  $m_0$  is the mass of the dry sample.



Figure 2.2: Circulating natural sea water tanks.

### 2.2.3 Dynamic Vapor Sorption

Dynamic Vapor Sorption measurements were performed with TA Instruments (Q5000SA) equipment to characterize water absorption in 0.1 mm thick films. This allows water uptake to be monitored using a microbalance with a  $0.1 \mu\text{g}$  resolution placed in a humidity chamber that can be controlled in both temperature (from 5 to  $80^\circ\text{C}$ ) and humidity (from 0 to 95%).

The DVS measurements were made at  $40^\circ\text{C}$ . After a drying period until the sample reached equilibrium, water activity in the chamber was increased step by step using a flow of nitrogen-dry water vapor mixture at  $200 \text{ mL}\cdot\text{min}^{-1}$ . Mass evolution  $m(t)$  was recorded at a frequency of about 0.1 Hz and translated into mass percent of the absorbed water  $M(t)$  calculated according to equation 2.1. The drying process was performed in situ by setting the humidity level to 0.

## 2.3 Characterizations

### 2.3.1 Chemical characterizations

#### 2.3.1.1 FTIR

##### *In-situ measurement (Raw CR)*

The tool used in order to perform in-situ chemical characterization during oxidation was an ageing chamber (Harrick TFC MXX-3 equipped with IR transparent windows) that can be controlled in both temperature (up to 240°C) and atmosphere composition and pressure (up to 3 MPa). This ageing cell was placed in a Perkin Elmer Spectrum 2 Infrared spectrophotometer where the sample spectra were periodically collected. Each spectrum resulted from the averaging of 32 scans with a resolution of 4 cm<sup>-1</sup>.

Polychloroprene was first dissolved in chloroform and then a film was cast on a ZnSe window, residual solvent was dried out prior to ageing. Sample thickness was about 15 microns. Exact sample thickness was evaluated using the intensity of the band of double bonds situated at 1660 cm<sup>-1</sup>, using the Beer–Lambert law with a molar absorptivity value of 25 l.mol<sup>-1</sup> cm<sup>-1</sup> (calculated from [65] and checked in this study).

For the determination of double bond concentration, a deconvolution was necessary owing to the overlapping of their band (which decreases) with the carbonyl one (which increases). Deconvolution was performed using the automatic software tool Origin. The global peak situated between 2000 cm<sup>-1</sup> and 1500 cm<sup>-1</sup> was deconvoluted into three peaks situated at 1660 cm<sup>-1</sup>, 1725 cm<sup>-1</sup> and 1790 cm<sup>-1</sup> respectively attributed to carbon–carbon double bonds, ketones and acid chlorides.

##### *Ex-situ measurement (Vulcanized CR)*

###### *Kinetics*

Chemical modifications such as double bond consumption and carbonyl formation have been followed by FTIR spectroscopy in transmission mode using thin films (about 10 microns). During exposure, FTIR analyses have been performed on a Perkin Elmer Spectrum 2 with a resolution of 4 cm<sup>-1</sup> and double bond concentration has been assessed by using the peak at 1660 cm<sup>-1</sup> using the same deconvolution method as described above. In order to convert the absorbance at 1660 cm<sup>-1</sup> into a concentration value, the Beer–Lambert law has been used.

###### *Profiles*

The oxidation profiles of the samples were measured with a Perkin-Elmer Spectrum SpotLight 300 in transmission mode through 20 microns thick films with a spatial resolution of about 30 microns. The films were cut from bulk samples (4.8 mm thick) aged at 120°C, cooled by liquid nitrogen, with a Leica microtome. Spectra were collected using 16 scans per pixel in a wavenumber range between 4000 and 750 cm<sup>-1</sup>.

### 2.3.1.2 Chlorine content in raw CR

Sample thickness was chosen in order to avoid any limitation of degradation by O<sub>2</sub> diffusion, 100 microns thick samples of raw polychloroprene were aged in an oven at 80°C. Chlorine content was measured externally using a potentiometric method with a DL50 device from Mettler, with an accuracy estimated around 0.6%.

### 2.3.1.3 Oxygen absorption

The consumption of oxygen (i.e. oxidation rate measurement) during thermal aging was determined using a commercial Oxzilla instrument with the experimental approach described previously [80]. The technique has been established as a routine analysis in Sandia National Laboratories with the instrumental response being calibrated using standard gas mixtures under a specific range setting. Total oxygen loss in a sample and the resulting rates can also be compared against other materials with known oxidation rates. Known amounts of samples ( $\sim 0.1$  g at the highest and 1 g at the lowest temperature) were sealed at room temperature in ampoules of  $\sim 21$  cc volume and filled with air from a gas cylinder to provide consistent composition. In order to maintain air conditions of equal partial pressure at the elevated temperatures the samples were quickly vented when hot; hence aging was always conducted at 630 mm-Hg air pressure (ambient conditions in Albuquerque with  $p_{O_2} = \sim 130$  mm-Hg) independent of temperature. At each aging temperature, the same sample was used sequentially to obtain time-dependent results. As an important requirement, the sample must be sufficiently thin to avoid diffusion-limited oxidation conditions, so that a homogenous oxidation reaction occurs throughout the sample, and the measured rate can be adequately expressed as per total mass of the sample. Experiments were performed by the author during a 2 months stay in Albuquerque.

### 2.3.1.4 HCl released during CR immersion

In order to investigate the possible release of HCl due to hydrolysis of C–Cl bonds, 1.8 mm thick samples of CR (cut in small squares) were aged in a small bottle (100 ml) of pure water at 95 °C for more than 200 h. After aging, silver nitrate was used to reveal the presence of HCl in the water bath. For these experimental conditions, the measurement sensitivity was lower than  $10^{-4}$  mol.l<sup>-1</sup> meaning that the lowest rate of HCl formation that could be detected was  $1.2 \times 10^{-5}$  mol.l<sup>-1</sup>.

## **2.3.2 Physical characterizations**

### **2.3.2.1 In situ modulus measurement**

Modulus change during oxidation was measured in-situ on 100  $\mu\text{m}$  thick films using a TA Instruments DMA (2980). Samples were tested in tensile mode at a frequency of 1 Hz, with a displacement amplitude of 5  $\mu\text{m}$ . Specimen dimensions were 10 mm length and 4 mm width.

### **2.3.2.2 Tensile test**

Tensile tests were performed using standard dog bone specimens (type 2 from ISO 37) on an Instron machine with a displacement rate of 10 mm/min. Sample deformation was measured using crosshead displacement and load was measured with a 500 N load cell. For each condition, three samples were tested and results averaged.

### **2.3.2.3 DMA**

Dynamic mechanical analysis was performed on a Q800 device from TA Instruments. Measurements were performed in tensile mode at 1 Hz with a dynamic strain amplitude of 0.2 and a static force of 1 N on 17 mm  $\cdot$  5 mm  $\cdot$  0.9 mm samples. Heating rate was 2°C/min between  $-80$  and 100°C.

### **2.3.2.4 Permeation**

Oxygen permeation experiments were performed on a disk samples of approximately 64 mm diameter and 2 mm thickness using a custom-modified, commercial Oxtran-100 coulometric permeation apparatus (Modern Controls MOCON, Inc., Minneapolis, MN, USA), which is based on an ASTM standard. To allow for high temperature analysis a modified sample holder was positioned in a common laboratory oven. These experiments were performed in Sandia National Laboratories by M. Celina.

### **2.3.2.5 Modulus profiles**

Modulus profiles were performed in Sandia National Laboratories in Albuquerque (USA). The modulus profiler apparatus, which monitors the penetration of a paraboloid-shaped tip into a polymer sample, has been described in detail elsewhere [81]. Penetration data are converted to inverse tensile compliance values, which approximate the modulus. The instrument allows for convenient scanning across a sample with a resolution of approximately 50  $\mu\text{m}$ . The rubber specimens were cut in cross-sections, encapsulated in epoxy resin to improve sample handling, mounted in a custom-made clamp and then

metallographically polished. The modulus profile was then obtained by measuring individual modulus values across the polished cross-section of the sample. Identical profile results were obtained when using the original approach of positioning three identical samples side-by-side to enable a more precise edge modulus determination. This indicates that any possible edge effects due to epoxy-encapsulation do not significantly affect the modulus measurements. Experiments were performed by the author during a 2 months stay in Albuquerque.

### 2.3.2.6 Fracture in mode I

$G_{IC}$  measurements were performed on a Metravib DMA 150 N machine using a 2 N load cell (XFTC300) from Measurement Specialists, in double notched tensile mode, with a strain rate of  $6.7 \cdot 10^{-4} \text{ s}^{-1}$ . Samples were 200  $\mu\text{m}$  thick with a typical length of 10 mm and a width of 5 mm. They were notched on each side using a new razor blade, distance between the two notches (ligament length,  $L$ ) was about 1 mm. The validity of these tests was established in a preliminary study which examined the effect of strain rate and ligament length, more details are presented in Chapter 6. Tests were performed inside a transparent oven, in order to record experiments with a high resolution camera (Camera Basler PIA 2400-12GM). Images from the camera were used to measure the actual ligament length ( $L$ ) before testing and fracture energy was measured from the load/displacement curve. The following expression was used to determine  $G_{IC}$ .

$$G_{IC} = \frac{\int P dU}{t \cdot L} \quad (2.2)$$

where  $P$  is the load in Newtons,  $U$  is displacement in m,  $t$  is sample thickness in m and  $L$  distance between the two notches in m.



## Chapter 3

# Oxidation of unvulcanized polychloroprene

This chapter presents a mechanistic model that could be used to describe and predict oxidation of unvulcanized polychloroprene. First, existing data and knowledge about CR oxidation will be considered. Then, a specific characterization of raw polychloroprene oxidation under different conditions in terms of temperature and oxygen pressure will be presented using a new ageing tool that allows in situ measurements. Next a mechanistic model of raw CR oxidation will be set up based on both experimental results from this study and data available in the literature, with determination of the associated elementary rate constants and their temperature dependence. Finally, comparison of these rate constant values with those of other polydienic elastomers will be used in order to highlight specificities of raw CR oxidation.

### 3.1 Introduction

Elastomers derived from vulcanized poly 2 chloro butadiene (polychloroprene) have been known for almost 80 years. They show better resistance to ozone and oil than common hydrocarbon polydienic elastomers and are particularly appreciated for their good properties in aqueous media (gloves, joints, etc.). It is now well recognized that radical chain oxidation is one of the most important modes of thermal ageing for this polymer, and that has led to a significant amount of literature in the past half century. Despite that, certain aspects of their degradation mechanisms remain obscure and the available quantitative data are largely insufficient to envisage a non-empirical lifetime prediction based on an indisputable kinetic model. The aim of this work is to try to contribute to the elaboration of such a model. It has been chosen to decompose the investigation into several steps, corresponding to material structure and composition of increasing complexity. The first step corresponds to the starting linear polychloroprene (ICR) polymer. In the industrial samples under study, all the other material components (crosslinks, fillers) are in relatively low concentration or unreactive and are thus expected to have an influence of second order on oxidation behaviour. This latter will be thus described as the oxidation of ICR monomer units (and/or structural irregularities) possibly disturbed by crosslinking agents and additives. The second step of the investigation will focus on additive-free vulcanisates (vCR) in order to appreciate the effect of crosslinking agents (here sulfur, of which the effect on oxidation has already been the object of many studies for other elastomers), in the next chapter. The third step consists of studying the effect of stabilizers on the oxidation of industrial vulcanisates (iCR).

Considering the relatively recent literature on polychloroprene thermal ageing, we dispose first of data relative to thermal degradation in neutral atmosphere at 150°C [82]. NMR and IR data indicate the important role of 1-2 /1-4 sequences (Figure 3.1). Commercial grades of ICR are essentially composed of 1-4 sequences but some 1-2 isomers are present, and are characterized by the presence of a labile chlorine atom destabilized by its tertiary placement and by the presence of a double bond in an  $\alpha$  position. The homolytic splitting of the C-Cl bond is favored by the resonance stabilization of the resulting allyl radical.  $\text{Cl}^\bullet$  radicals can add to double bonds or abstract hydrogens to give hydrogen chloride and thus propagate oxidation. Miyata and Atsumi [82] show a correlation between the yields of 1-2 isomerizations and HCl evolution indicating that the 1-2 isomer is the precursor of both species. *How can we exploit these results in the framework of a study of thermal oxidation?*

The first approach is to suppose that oxidation radical chains could be initiated by the thermolysis of a labile polymer bond. The dissociation energy of C-Cl bonds attached to double bonds, as in the monomer unit, is very high; these bonds cannot participate in initiation events. Secondary C-Cl bonds in regular monomer units of PVC for instance have a dissociation energy of  $320 \pm 10 \text{ kJ.mol}^{-1}$ , lower than that of C-H bonds in saturated compounds but stable at least at temperatures lower than  $80^\circ\text{C}$ . Tertiary C-Cl bonds or allylic C-Cl bonds are destabilized by respectively inductive and mesomeric effects; they are often cited as weak points in the thermal degradation of PVC. Indeed tertiary C-Cl bonds in allylic placement, combining both destabilizing effects, must be especially unstable. Their dissociation energy is expected to be of the order of  $250 \text{ kJ.mol}^{-1}$ . They can therefore play a role in initial steps of ICR or CR thermal oxidation. However, it must be recalled that oxidation leads to the formation of peroxides (including hydroperoxides) of which the dissociation energy is of the order of  $180 \text{ kJ.mol}^{-1}$  in hydrocarbon peroxides and significantly lower in  $\alpha$  chloro peroxides of which the explosive behaviour at temperatures close to ambient temperature has been the cause of major catastrophes, in PVC polymerization plants for instance.

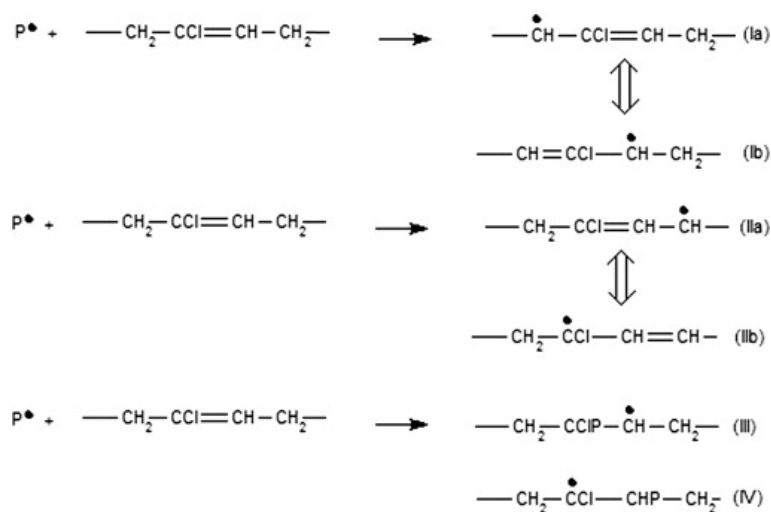


Figure 3.1: Possible reaction of the 1/4 monomer with a radical.

Let us now consider thermal oxidation. A significant difficulty in the study of polydiene oxidation is the occurrence of two kinds of radical propagation processes: hydrogen abstraction on allylic carbons and addition reactions on double bonds. In the case of a dissymmetric monomer unit such as the polychloroprene one, this opens the way to at least four reaction pathways, even six if isomerizations of allyl radicals are taken into account, Figure 3.1.

Let us first note that radicals Ia and Ib are identical, they will be called I here. In the following, only radical Ia will be considered. The existence of intermediary allyl radicals has been recognized for a long time [83]. According to Shelton et al. path II is favored relative to path I [84] owing to the stabilizing effect of the chlorine atom in the  $\beta$  position of the reacted methylene. Concerning addition reactions, we dispose of the example of PVC polymerization [85] to appreciate the relative probability of the formation of radicals III or IV. It is clear that the anti Markovnikov process - in which it is the less substituted carbon which is attacked - is favored. Additions are thus expected to give predominantly radical IV. To summarize, we expect the presence of essentially three primary radicals: IIa, IIb and IV (Figure 3.2).

These radicals react very fast with oxygen to give considerably less reactive peroxy radicals. The latter can remove hydrogens from allylic methylenes or add to double bonds. As in the case of polyisoprene [86], additions can be inter or intramolecular; in the first case they give crosslinks, in the second they give cycles. In the case of  $\alpha$  chloroperoxy radicals, an interesting peculiarity is the possibility, for the cyclization, to propagate as a zip reaction along the chain. It is noteworthy that, except for hydroperoxides coming from radical IIa, all the other peroxides or hydroperoxides have a chlorine atom in the  $\alpha$  position. The high instability of  $\alpha$  chloro peroxides is well known; it is presumably responsible for the absence of an induction period in LPCR oxidation. Finally, we expect for each primary radical three kinds of products: hydroperoxides, intermolecular peroxide bridges and cyclic peroxides, which may form sequences.

The nature of stable oxidation products has been investigated by Delor et al. [87] mainly using infrared measurements. As expected the spectra reveal the disappearance of double bonds and the appearance of a variety of oxygen containing structures, among which acid chlorides absorbing at  $1790\text{ cm}^{-1}$  the presence of which has been confirmed by derivatization (transformation into primary amides by reaction with ammonia). Delor et al. proposed a mechanistic scheme for processes starting from a hydrogen abstraction event; addition processes were neglected, probably because peroxides resulting from these processes have very discrete IR spectra, their decomposition products are not necessarily different from those of hydroperoxides so that peroxides often need to be identified by indirect methods.

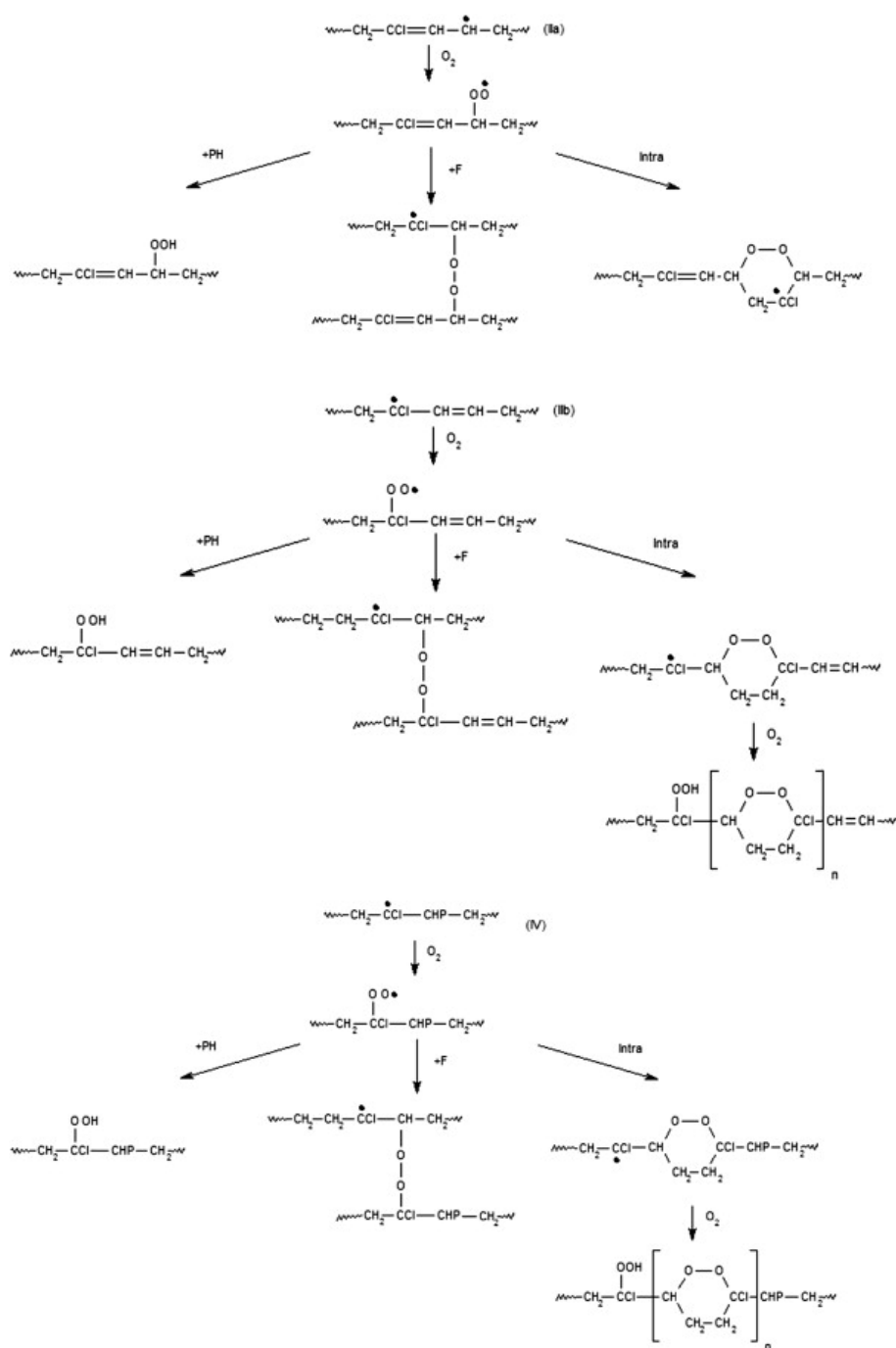


Figure 3.2: Hydroperoxide and peroxide formation from principal radicals.

When comparing iCR with hydrocarbon polydienes, the most striking difference is the presence of the peak at  $1790\text{ cm}^{-1}$  attributed to acid chlorides. It seems logical to attribute their formation, as proposed by Delor et al. [87] to the oxidative attack of the carbon bearing a chlorine atom.

As previously noted, the corresponding hydroperoxides are highly unstable, their decomposition gives an  $\alpha$  chloroalkoxyl which, according to Delor et al. [87] would lead to the acid chloride by  $\beta$  scission. However splitting of the C-Cl bond can be a competitive  $\beta$  scission process leading to a ketone. Anyhow, it is difficult to imagine another mechanism for acid chloride formation. Gillen et al. [71] have also measured the quantity of  $\text{CO}_2$  evolved. The ratio  $\text{CO}_2$  evolved/ $\text{O}_2$  absorbed is of the order of 0.13 at  $50^\circ\text{C}$  and 0.3 at  $95^\circ\text{C}$ . The presence of  $\text{CO}_2$  can result only from secondary processes involving very unstable structures, for instance from a secondary hydroperoxide (Figure 3.3).

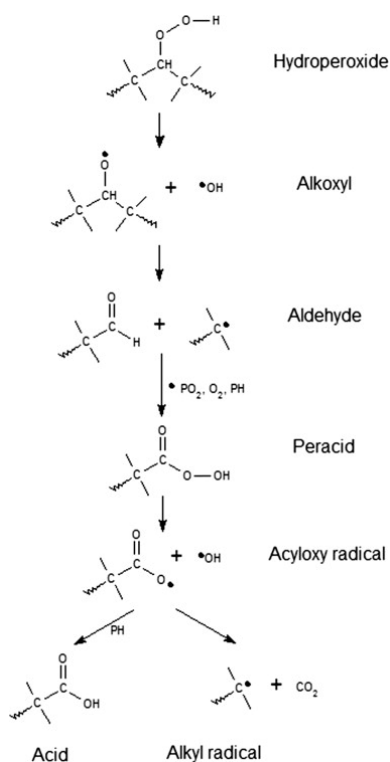


Figure 3.3: Possible route for  $\text{CO}_2$  formation.

Aldehydes are extremely reactive in radical processes; peracids are very unstable hydroperoxides and acyloxy radicals undergo decarboxylations at very high rates [88].  $\text{CO}_2$  (and acid) formation is thus governed by the slowest step, i.e. presumably the formation of the starting secondary hydroperoxide or its decomposition. With a mechanism of such complexity, it is not surprising to observe variations of the relative yields, such as  $\text{CO}_2/\text{O}_2$  with temperature, as found by Gillen et al. [71].

The next section will focus on characterization of raw polychloroprene oxidation in terms of both mechanisms and kinetics. The influence of both temperature and oxygen pressure will be considered.

## 3.2 Results

### 3.2.1 Molecular modifications

Examples of IR spectra are shown in Figure 3.4. They display the same features as the spectra presented by Delor et al. [87]. The main changes are summarized in Table 3.1 with the assignments and the estimated values of the corresponding molar absorptivity values used to translate absorbance values into approximate concentrations. Special attention has to be paid to the modifications in the 1500-2000  $\text{cm}^{-1}$  spectral region corresponding to carbonyls and double bonds (zoom in Figure 3.4). In the spectral domain corresponding to the carbonyl stretching band (1680-1800  $\text{cm}^{-1}$ ) two peaks can be clearly distinguished: one at 1725  $\text{cm}^{-1}$ , generally attributed to aliphatic, saturated ketones and the other at 1790  $\text{cm}^{-1}$  attributed to acid chlorides. It is interesting to plot the ketone concentration against acid chloride concentration for all the exposure conditions under study (Figure 3.5). It appears that, in the domain of moderate conversions, both concentrations are proportional irrespective of temperature or oxygen pressure, which leads us to suppose that both species could have the same precursor and that their build-up kinetics could be closely linked to their formation rate.

Wave Number ( $\text{cm}^{-1}$ )	Evolution	Attribution	References	Molar Absorptivity ( $\text{l.mol}^{-1}.\text{cm}^{-1}$ )
1660	Decrease	C=C	[65], [89], [90]	25
1725	Increase	C=O in saturated ketone	[87], [89], [90]	320
1790	Increase	C=O in chlorine acid	[87], [89], [90]	300

Table 3.1: Attribution of main infrared bands that evolve during CR oxidation.

From the quantitative analysis of IR spectra, it is possible to follow carbonyl build up and double bond consumption during oxidation of raw CR. Figure 3.6 shows an example of such an evolution for a sample exposed to air at 80°C. An increase in carbonyl content is observed during CR oxidation whereas a large decrease of double bond concentration occurs. These results clearly show that the consumption of double bonds cannot be neglected in a kinetic analysis.

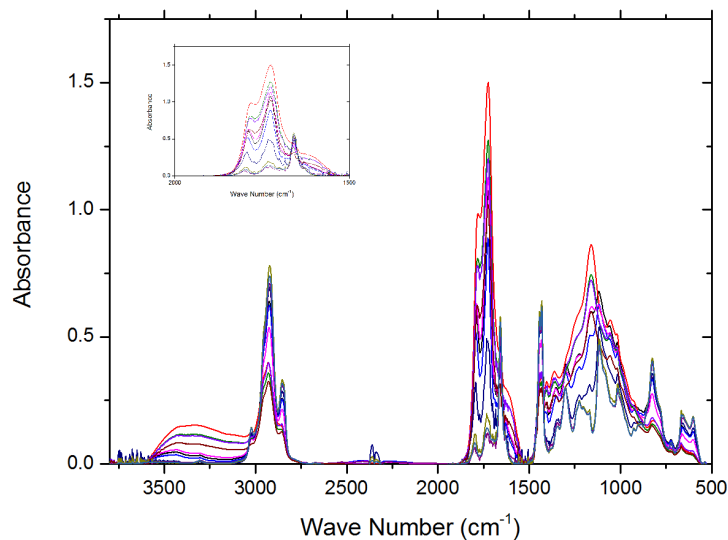


Figure 3.4: Infrared spectra evolution during raw polychloroprene oxidation.

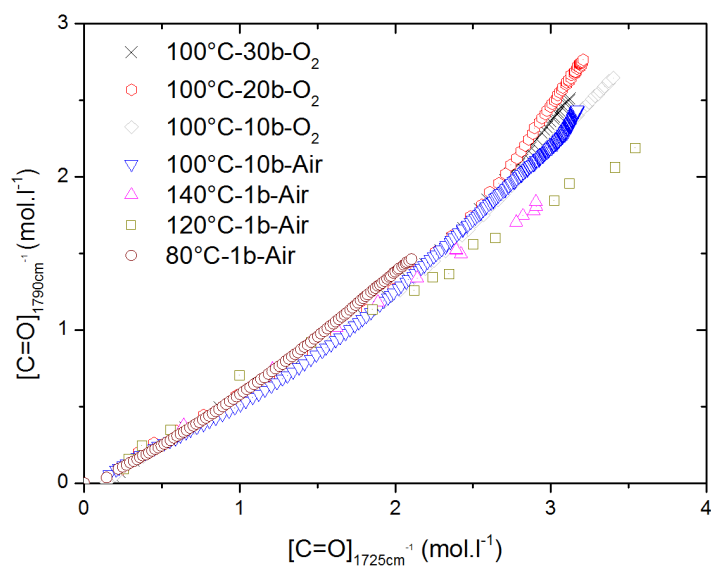


Figure 3.5: Evolution of chloride acid concentration versus ketone concentration for different ageing conditions.

The kinetic curves of Figure 3.6 show the absence of an induction period, that can result from hydroperoxide instability or from a high initial hydroperoxide concentration. Since the second hypothesis can be rejected, it can be concluded that the hydroperoxides formed during ICR oxidation are particularly unstable. This is consistent with the hypothesis that  $\alpha$  chlorohydroperoxides are formed.

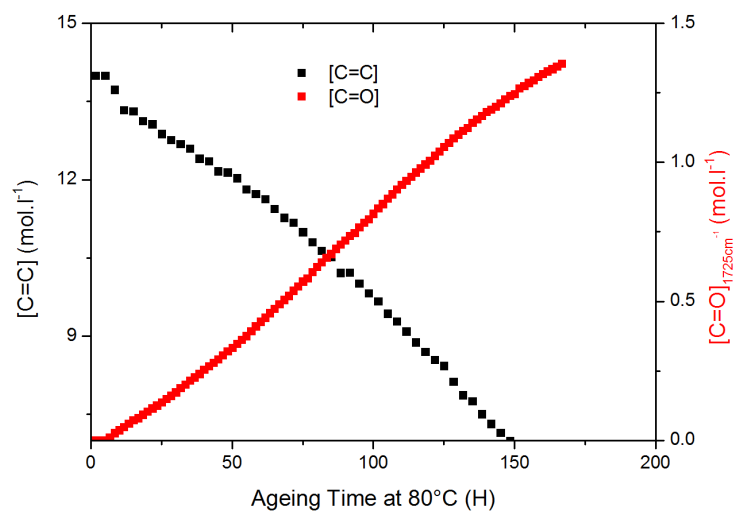


Figure 3.6: Carbonyl build-up and double bond consumption during oxidation of raw CR in air at 80°C.

Based on these results, it appears that stable polychloroprene oxidation products are essentially ketones and acid chlorides which are formed in closely related chemical events. Furthermore, double bond consumption is a major oxidation process and has to be considered in a mechanistic scheme. But one of the main questions when considering polychloroprene is the effect of chlorine on polymer oxidation.

### 3.2.2 Chlorine content

In order to evaluate this effect and more especially the possible formation of hydrogen chloride during oxidation, chlorine concentration in CR has been measured for different oxidation levels when exposed to air at 80°C. Results are plotted in Figure 3.7, where chlorine content is plotted as a function of acid chloride concentration. It appears that chlorine content does not decrease much, even for high oxidation level; this result is in accordance with previous observations made by Celina [62]. It has to be noted that a very small decrease could be suspected, this small decrease needs confirmation using more accurate experimental techniques and will not be considered here.

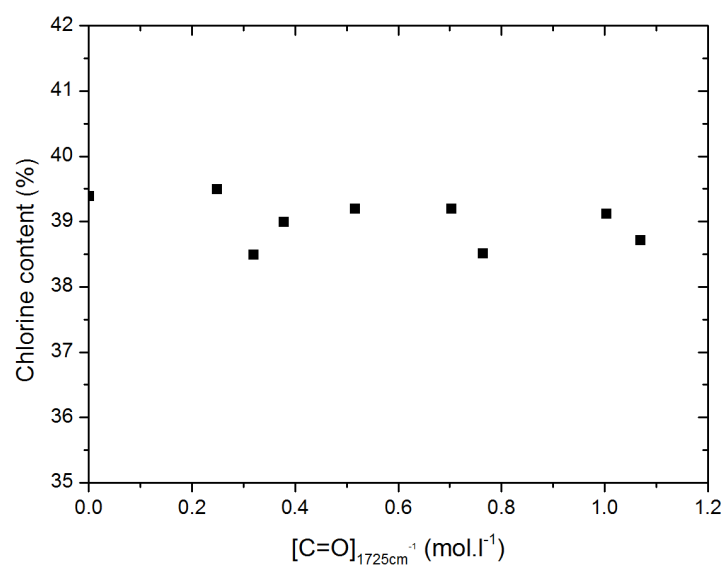


Figure 3.7: Chlorine content versus carbonyl concentration during CR oxidation at 80°C.

### 3.2.3 Effect of oxygen pressure

The effect of oxygen pressure on oxidation kinetics of raw polychloroprene has been considered at 100°C. The curves of double bond depletion versus time are plotted in Figure 3.8. These results clearly show that the higher oxygen pressure is, the faster double bonds are consumed, meaning that raw CR is not in an oxygen-excess regime in air at atmospheric pressure. This oxygen pressure effect has been shown many times in the literature for many polymers [91] [64] [92].

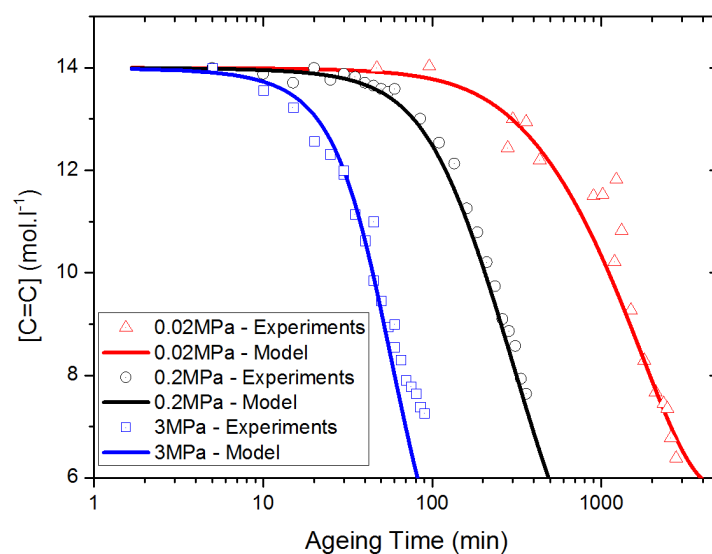


Figure 3.8: Effect of oxygen pressure on double bond consumption during CR oxidation at 100°C.

### 3.2.4 Effect of temperature

Obviously by increasing ageing temperature, oxidation rate is increased leading to a faster increase in carbonyl concentration (Figure 3.9a) and faster double bond consumption (Figure 3.9b). From these results, it appears that carbonyl build-up and double bond consumption occur in the same timescale at all temperatures.

The experimental part of this study highlighted the fact that polychloroprene oxidation begins rapidly and is characterized by a complex mechanism that presumably involves a double propagation process through peroxy addition to double bonds and hydrogen abstraction by peroxy radicals. It appears that chlorine atoms remain bonded to the polymer; their splitting-off can be neglected. The next section will focus on the possibility to model this complex behaviour in order to set up a life time prediction scheme.

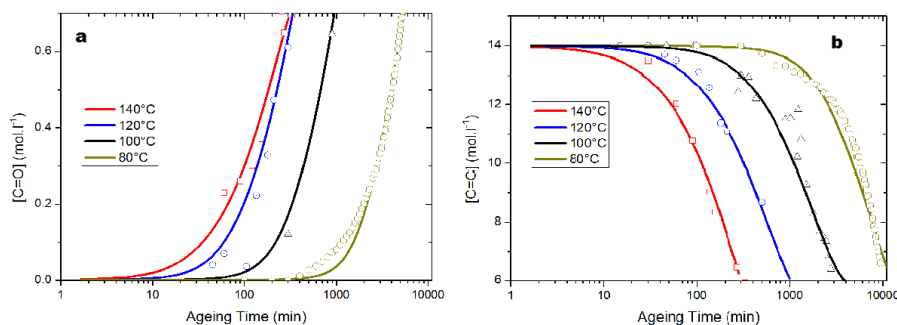
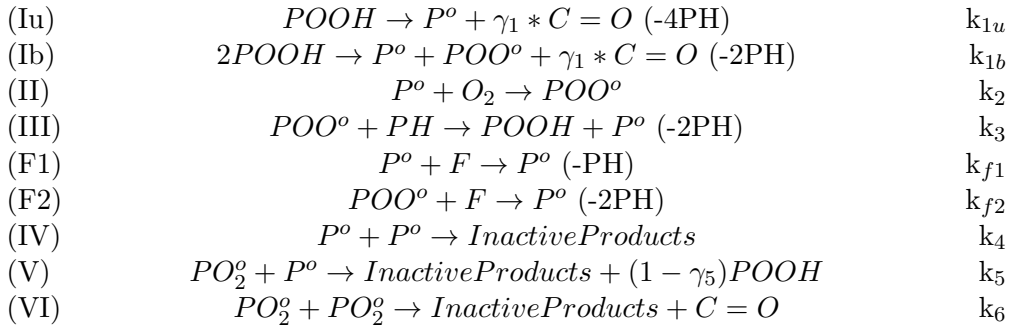


Figure 3.9: Effect of temperature on carbonyl build-up double bond consumption.

### 3.3 Oxidation kinetic modelling

This study aims to set up a mechanistic model of raw polychloroprene oxidation based on results from the literature presented in the introduction of this chapter and data presented in the previous section. The proposed mechanism can be considered as simply as possible taking into account all information available; it is based on the classical mechanistic scheme of oxidation to which radical addition to double bonds has been added and both unimolecular and bimolecular modes of hydroperoxide decomposition have been considered:



The system of differential equations derived from this scheme (Appendix 1) is resolved with the following initial parameters:

- $[P^o] = [POO^o] = 0$  at  $t = 0$ ;
- $[POOH] = [POOH]_o = 5.10^{-3} \text{ mol.l}^{-1}$  at  $t = 0$ . This value does not result from a measurement but rather from the inverse approach (Appendix 1);
- $[PH]$  is the concentration of methylenes in allylic placement. Thus  $[PH]_o = 2\rho * M_o = 28 \text{ mol.l}^{-1}$  where  $M_o$  is the molar mass of the monomer unit ( $85 \text{ g.mol}^{-1}$  and  $\rho$  is the polymer density ( $1250 \text{ g.l}^{-1}$ );
- The equilibrium oxygen concentration has been estimated from the solubility coefficient value reported by Van Krevelen [1]:  $S = 3.10^{-8} \text{ mol.l}^{-1}.\text{Pa}^{-1}$ , using Henry's law  $[O_2] = S.p_{O_2}$  where  $p_{O_2}$  is the partial pressure of oxygen;
- No stationary state hypothesis is made; substrate  $[PH]$  consumption is taken into account. At high conversions, secondary reactions can interfere with the above chain mechanism. To avoid such complications, simulations were stopped when the double bond concentration reached half of its initial value i.e.  $7 \text{ mol.l}^{-1}$ .

The determination of elementary rate constants is based on the following approach:

- Propagation rate constants are extracted from the literature:  $k_2$  because it does not depend strongly on structure (when  $P^\circ$  radicals are not too conjugated or hindered) and small variations of  $k_2$  have a negligible effect on simulations. Here, we have chosen  $k_2 = 10^8 \text{ l.mol}^{-1}.\text{s}^{-1}$ .
- It has been shown [93] that  $k_3$  does not depend strongly on molecular mobility and is almost the same for polymers and their model compounds. For these latter,  $k_3$  and its activation energy  $E_3$  are closely linked to the C-H dissociation energy  $D(\text{P-H})$  and can be estimated using an empirical relationship [94].

$$\log k_3 = 15.4 - 0.2 \cdot D[\text{P-H}] \quad (3.1)$$

$$E_3 = 0.55 \cdot (D[\text{P-H}] - 62.5) \quad (3.2)$$

Where  $k_3$  is expressed in  $\text{l.mol}^{-1}.\text{s}^{-1}$ ,  $E_3$  and  $D[\text{P-H}]$  in  $\text{kcal.mol}^{-1}$ . In CR,  $D[\text{P-H}]$  is equal to  $87 \text{ kcal.mol}^{-1}$  [95]. Application of these relationships to the case of CR leads to:

$$k_3 = 4.4 \cdot 10^7 \cdot \exp\left(-\frac{56000}{RT}\right) \quad (3.3)$$

All the other rate constants have been determined from experimental data, using the kinetic scheme in an inverse approach. A two-step procedure is used:

- In the oxygen excess regime (see below), all the reactions involving radicals  $P^\circ$  except  $\text{O}_2$  addition can be neglected, the inverse approach gives access to initiation  $k_{1u}$  and/or  $k_{1b}$ ,  $\text{POO}^\circ$  addition to double bonds ( $k_{f2}$ ) and  $\text{POO}^\circ + \text{POO}^\circ$  termination ( $k_6$ ) rate constants.
- These values being known, one can determine the remaining rate constant values:  $k_{f1}$ ,  $k_4$  and  $k_5$ , applying the inverse approach to the results obtained in the oxygen deficient regime.

### 3.3.1 Effect of oxygen pressure

According to Figure 3.8, the oxidation rate at 100°C has reached its asymptotic value at the highest O<sub>2</sub> pressure values, so that it can be considered that oxidation occurs in an oxygen excess regime at 3 MPa oxygen pressure. The determination of the corresponding rate constant values was then made. These values are listed in Table 3.2. The kinetic scheme was then used with these rate constant values to simulate the consumption of double bonds. The result of the simulation is shown in Figure 3.10 together with the experimental curve, showing an acceptable agreement.

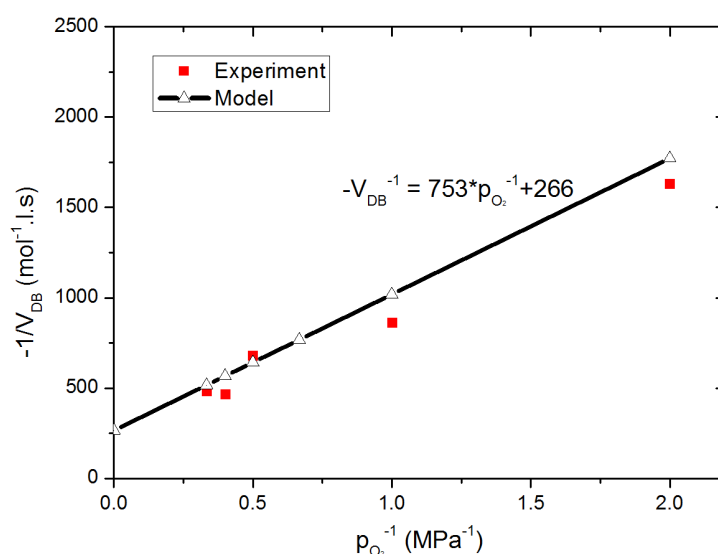


Figure 3.10: Reciprocal of the double bond consumption rate versus reciprocal of the oxygen pressure.

The whole kinetic scheme was then used to simulate oxidation in an oxygen deficient regime. The curves of double bond consumption at O<sub>2</sub> partial pressures of 0.2 and 0.02 MPa (this latter corresponding to air at atmospheric pressure) are also plotted in Figure 3.10. Here again a good agreement between model and experimental data is observed.

	Polychloroprene	Polyisoprene	Polybutadiene
$[POOH]_o$ (mol.l <sup>-1</sup> )	$5 \cdot 10^{-3}$	$5 \cdot 10^{-3}$ to $5 \cdot 10^{-2}$	$8 \cdot 10^{-4}$ to $1 \cdot 10^{-2}$
$k_{1u}$ (s <sup>-1</sup> )	$3 \cdot 10^{-4}$		
$k_{1b}$ (l.mol <sup>-1</sup> .s <sup>-1</sup> )	$1 \cdot 10^{-3}$	$6 \cdot 10^{-5}$	$1.6 \cdot 10^{-6}$
$\gamma 1$	0.5	0.27	0.4
$k_2$ (l.mol <sup>-1</sup> .s <sup>-1</sup> )	$1 \cdot 10^8$	$1 \cdot 10^8$	$1 \cdot 10^9$
$k_3$ (l.mol <sup>-1</sup> .s <sup>-1</sup> )	0.65	8.4	1.5
$k_{f1}$ (l.mol <sup>-1</sup> .s <sup>-1</sup> )	500	$5.9 \cdot 10^4$	$1 \cdot 10^4$
$k_{f2}$ (l.mol <sup>-1</sup> .s <sup>-1</sup> )	4.5	37	24
$k_4$ (l.mol <sup>-1</sup> .s <sup>-1</sup> )	$1.7 \cdot 10^{11}$	$1 \cdot 10^9$	$3 \cdot 10^8$
$k_5$ (l.mol <sup>-1</sup> .s <sup>-1</sup> )	$1.7 \cdot 10^{10}$	$4.8 \cdot 10^8$	$1.2 \cdot 10^8$
$k_6$ (l.mol <sup>-1</sup> .s <sup>-1</sup> )	$5 \cdot 10^4$	$6.6 \cdot 10^4$	$1 \cdot 10^4$

Table 3.2: Rate constants used for modelling oxidation at 100°C.

In Figure 3.10 the reciprocal rate of double bond consumption has been plotted against reciprocal O<sub>2</sub> pressure. When propagation occurs only by hydrogen abstraction, it has been demonstrated a long time ago [96] that under certain conditions (stationary state, no POOH decomposition, long kinetic chains,  $k_5^2 = 4k_4.k_6$ ) the dependence must be linear [52]. It has been shown many times, subsequently, that this relationship remains linear even when the validity conditions are not obeyed, but this is the first time, to our knowledge that this relationship has been applied to a case of dual propagation, revealing its universality. The corresponding equation is:

$$r_{ox} = r_{ox\infty} \cdot \frac{\beta \cdot [O_2]}{\beta \cdot [O_2] + 1} \quad (3.4)$$

or

$$\frac{1}{r_{ox}} = \frac{1}{r_{ox\infty}} + \frac{1}{r_{ox\infty} \cdot S \cdot \beta \cdot p_{O_2}} \quad (3.5)$$

It is possible to define approximately a critical pressure  $p_c$ , for instance:

$$p_c = \frac{1}{q \cdot S \cdot \beta} \quad (3.6)$$

$q$  being an arbitrarily chosen number higher than unity, for instance  $q = 10$ .

This critical pressure separates arbitrarily the regime of oxygen lack and the regime of oxygen excess. Here this pressure is about 2 MPa i.e. a pressure about 100 times higher than the oxygen partial pressure in air at atmospheric pressure. It is clear that in the case of exposure in air, kinetic modelling must take into account terminations (IV) and (V).

Obviously by increasing ageing temperature, oxidation rate is increased leading to a faster increase in carbonyl concentration (Figure 3.9a) and faster double bond consumption (Figure 3.9b). From these results, it appears that

carbonyl build-up and double bond consumption occur in the same timescale at all temperatures.

The experimental part of this study highlighted the fact that polychloroprene oxidation begins rapidly and is characterized by a complex mechanism that presumably involves a double propagation process through peroxy addition to double bonds and hydrogen abstraction by peroxy radicals. At the same time, it appears that chlorine atoms remain bonded to the polymer; their splitting-off can be neglected. The next section will focus on the possibility to model this complex behaviour in order to set up a life time prediction scheme.

### 3.3.2 Physical meaning of rate constant values and their hierarchy

We have no rigorous proof that the set of rate constants resulting from the inverse determination is a unique solution of the problem. A check of their physical validity is thus desirable. Let us first consider the hierarchy of values:

$$k_4 > k_5 > k_2 \gg k_6 \gg k_3 \gg k_{1b} \text{ and } k_2 > k_{f1} > k_{f2} > k_3$$

These inequalities reflect several general rules:

1. If radicals are called R and non-radicals are called N, reaction rates are generally in the order: R+R > R+N > N+N. Transposed to the domain of polymer oxidative ageing: termination > propagation > initiation.
2. Alkyl radicals are considerably more reactive than the corresponding peroxy radicals. This is valid for terminations ( $k_4 > k_5 > k_6$ ). According to Gillen and Clough [61] for radical mobility reasons, one expects  $k_5^2 > 4k_4k_6$  as observed here.
3. Let us recall that O<sub>2</sub> is a biradical in ground state, in other words an O<sub>2</sub> addition on a radical can be also considered as a termination. O<sub>2</sub> would behave as a peroxy but less reactive than a POO<sup>o</sup> so that:  $k_5 > k_2 \gg k_6$ .
4. Additions of peroxy radicals to double bonds are (slightly) faster than hydrogen abstractions to saturated groups as found for other polydienic polymers [97].

5. Hydroperoxide decomposition is, by far, the slowest elementary process that can be explained schematically by the fact that (in the domain of thermal reactions) radical creation is the most thermo-chemically disfavored process. Concerning the mode of hydroperoxide decomposition, we know that at a given temperature, it is possible to define a critical hydroperoxide concentration  $[POOH]_c = k_{1u}/k_{1b}$  at which both the unimolecular and the bimolecular POOH decomposition processes have equal rates. Here,  $[POOH]_c = 0.3 \text{ mol.L}^{-1} \gg [POOH]_o$  ( $5 \cdot 10^{-3} \text{ mol.l}^{-1}$ ). It can be deduced that oxidation begins in unimolecular mode and turns to bimolecular mode when  $[POOH]$  becomes equal to the critical value.

### 3.3.3 Comparison of polychloroprene with other polydienes

From Table 3.2, it is clear that the initiation process is much faster in polychloroprene than in other polydiene rubbers; this difference could be attributed to the destabilizing effect of chlorine atoms on hydroperoxide decomposition. As a consequence, the induction period has almost completely disappeared in ICR while it is present in other polydienes. Despite its high initiation rate, CR displays a steady state rate lower than in other polydienes (Table 3.3) because all propagation processes are slower. That is also obviously due to the presence of chlorine, presumably through inductive effects.

Nature of rubber	Time to consume half of double bonds at 100°C (Hours)
Polyisoprene	2
Polychloroprene	50
Polybutadiene	4

Table 3.3: Time for consumption of half double bonds in several rubbers at 100°C.

### 3.3.4 Temperature effect

The effect of temperature on oxidation rate has been considered from 80°C to 140°C in air. Rate constant values have been adjusted for all tested temperatures separately and then temperature dependence has been considered; results of modelling are plotted in Figure 3.9. It is worth noting that temperature dependence of  $k_3$  is fixed according to literature results (equations 3.1 and 3.2) and temperature effects on  $k_2, k_4$  and  $k_5$  can be neglected. The Arrhenius parameters of the rate constants are given in Table 3.4. Literature values of the activation energy of POOH decomposition [98] range between 80 and 140 kJ.mol<sup>-1</sup> meaning that the value in Table 3.4 is in accordance with previous results. However, if we compare this value with those of other polydienic elastomers it appears that the activation energy of the unimolecular decomposition of POOH is of the same order but lower. This is presumably due to the destabilizing effect of chlorine in  $\alpha$  chlorohydroperoxides. The decreasing chlorine effect on the activation energy of unimolecular POOH decomposition process is such that it becomes almost equal to the bimolecular one. As a consequence, both decomposition processes participate in initiation at every temperature in the 80°C-140°C interval.

		<b>Polychloroprene</b>		<b>Polyisoprene</b>	<b>Polybutadiene</b>
	$k_0$	$E_a$ (kJ.mol <sup>-1</sup> )	$R^2$	$E_a$ (kJ.mol <sup>-1</sup> )	$E_a$ (kJ.mol <sup>-1</sup> )
$k_{1a}$	$1.0 \cdot 10^{12}$	111	0.993	134	
$k_{1b}$	$9.4 \cdot 10^{11}$	107	0.995	102	137
$k_{f1}$	$2.1 \cdot 10^7$	33	0.996	11	0
$k_{f2}$	$1.1 \cdot 10^{10}$	67	0.998	34	94
$k_6$	$9.0 \cdot 10^{12}$	59	0.966	23	71

Table 3.4: Temperature dependence of kinetic rates.

### 3.4 Conclusion

The thermal oxidation of unstabilized, uncrosslinked, unfilled polychloroprene has been studied in the 80-140°C temperature interval in air at atmospheric pressure and in the 0.02-3 MPa pure oxygen pressure interval at 100°C. Carbonyl (including acid chloride) build-up and double bond consumption were monitored by IR spectrophotometry. No significant chlorine release was observed. The discussion of results has been based on a mechanistic scheme mainly characterized by dual propagation (Hydrogen abstraction plus peroxy addition to double bonds). Certain rate constant values ( $k_2$  and  $k_3$ ) were extracted from the literature, the others were determined from experimental results using the kinetic scheme in an inverse approach. Among the observations made on rate constant values, the following appear particularly important:

1. Hydroperoxides are especially unstable, that can be attributed to the presence of chlorine in  $\alpha$  placement.
2.  $\text{POO}^\circ$  addition on double bonds is significantly faster than hydrogen abstraction by  $\text{POO}^\circ$ .
3. Propagation is slower in polychloroprene than in other polydienes.

This model of raw polychloroprene will now be adapted in order to be able to describe oxidation of vulcanized rubber and perform life time predictions, this is the aim of the next chapter.

## Chapter 4

# Oxidation of vulcanized and unstabilized polychloroprene rubber

Because kinetic modelling of oxidation in polymers is complex it has to be set up step by step. First, oxidation of raw polychloroprene has been considered, both mechanisms and kinetics (chapter 3). This chapter is the second step, i.e. the characterization and integration of vulcanisation on oxidation of polychloroprene rubber in order to make a prediction of modulus evolution. A first part is dedicated to oxidation in homogeneous conditions at 100°C with a presentation of experimental results and adaptation of the model. Then results from this model will be compared to experimental oxygen absorption rate for the first time in order to evaluate advantages and limitations of this prediction. Next, using this model and theoretical considerations, a new methodology will be proposed in order to predict quantitatively changes in modulus during oxidation of rubbers. In a second part, temperature effects will be considered with the aim of making life time predictions at low temperature, special attention will be paid to the temperature effect on oxidation rate. And finally, in the last part oxygen diffusion will be implemented into the model in order to predict modulus profile when oxidation is heterogeneous in thick samples.

## 4.1 Introduction

When rubbers undergo oxidation, a large change in their modulus is observed, this is due to the fact that in the rubbery state the modulus is directly related to the crosslink density and this latter is affected by a relatively small number of scission or crosslinking events. In the case of polychloroprene, a large increase of the modulus is observed during oxidation; as an example Celina measured a local modulus at the surface equal to 100 MPa after 8 days at 140°C compared to 1 MPa for an unaged sample [62]. This large increase of modulus in CR during oxidation is mainly due to the reaction of free macro-radicals on the double bonds that creates new crosslinks (Figure 4.1), this kind of reaction has been reported many times in the literature. But the main question here is *how to predict such a modulus change during oxidation?*



Figure 4.1: Crosslink formation due to double bond consumption during oxidation of CR

Usually two methods are used:

- The first one does not involve any chemical considerations and is based on the empirical prediction of the variation of the parameters of a constitutive model with ageing time at high temperature. Then a time/temperature superposition is performed using a linear Arrhenius extrapolation. This approach is simple but may be limited by several factors: for example, the temperature dependence of the build-up of oxidation products does not necessarily obey an Arrhenius law [59] [41] [71], and degradation is not necessarily homogeneous [99] [61].
- The second method is based on chemical considerations, and considers that a simple correlation exists between the concentration of oxidation products and modulus. If it is possible to predict oxidation product formation it should be also possible to predict a change in modulus. But the existence of this correlation between the concentration of a given reaction product and modulus is not proven, only shown in a qualitative way. This approach has been used by Celina on polychloroprene using oxygen absorption to predict edge modulus quantitatively and modulus profile qualitatively. This methodology is very interesting because it is based on the chemistry of oxidation and the actual acceleration factor is measured over a large range of temperatures in order to perform reliable predictions, but the prediction remains partially qualitative.

The idea here is to use a new approach in order to predict quantitatively the change in modulus for unfilled CR as a function of degradation.

This new approach is based on the use of a mechanistic description of the oxidation of the rubber that aims to describe each step of the degradation that is kinetically important. The oxidation process is described according to a basic oxidation scheme [43] [45] that takes into account the specificity of each polymer [100]. The main idea is to attribute a rate constant for each step of the overall process. The determination of the rate constants is performed based on experimental data, physical considerations and values from the literature as shown in Chapter 3. Because this kind of model describes important chemical steps it is possible to predict both chain scissions and crosslinking events that occur simultaneously during oxidation. In this way, it can be used to predict crosslink density changes in the rubber. This kind of study has been partially considered previously for polyisoprene, but with chain scission largely predominant compared to crosslinking [86], and for polyurethane based on polybutadiene but only for heterogeneous oxidation and a very low oxidation level [53].

In the previous chapter, the mechanistic and kinetic oxidation schemes of uncrosslinked polychloroprene have been considered and it was highlighted that the behaviour could be predicted based on the general oxidation scheme coupled with radical addition reactions on the double bonds. This model will be used here as a basis for the prediction of vulcanized CR behaviour. Vulcanization of the rubber here was performed using a typical formulation, i.e. sulfur and accelerators (MgO and ZnO). First, a kinetic model will be set up at one temperature (i.e. 100°C) in order to predict modulus change during oxidation of the rubber. Then, the effect of temperature on reaction rate will be investigated and predictions at low temperature will be compared to experimental data. And finally, heterogeneous oxidation that occurs when both oxygen input (through diffusion) and oxygen consumption (through oxidation) are in competition, will be considered.

## 4.2 Homogeneous oxidation at 100°C

This section is devoted to the prediction of modulus change during oxidation of an unstabilized polychloroprene rubber when degradation is homogeneous. First, the effect of vulcanization on both oxidation mechanisms and kinetics will be considered using experimental results including FTIR, oxygen consumption and in-situ modulus characterization. Then a mechanistic model will be set up using the consumption of the double bonds during oxidation, taking into account the sulfur effect. And finally a quantitative modulus prediction will be performed and results will be compared to experimental data.

### 4.2.1 Results

#### 4.2.1.1 Oxidation mechanisms

During oxidation of uncured polychloroprene two main products are formed, carbonyl and acid chloride as shown in the FTIR spectra in Figure 4.2-a at  $1725\text{ cm}^{-1}$  and  $1790\text{ cm}^{-1}$  respectively. At the same time a decrease of the double bond concentration is observed at  $1660\text{ cm}^{-1}$ , the determination of double bond concentration being obtained by deconvolution of the IR spectrum. Considering now the oxidation of vulcanized polychloroprene, these two products are again formed, however a new band can also be observed in Figure 4.2-b at  $1590\text{ cm}^{-1}$ . This new band has already been observed in the literature [87] [101] and can be attributed to the reaction of carboxylic acids or acid chlorides with ZnO.

So the oxidation products of vulcanized CR are similar to those observed in the uncured material. However a complication of the oxidation process occurs due to the presence of ZnO as a filler in the rubber. This new reaction, which will not be considered here in detail, means that oxidation product concentrations cannot be used to set up the kinetic model. For this reason, the model presented here will be considered only in terms of double bond consumption.

As an example, Figure 4.3 shows this consumption of double bonds as a function of ageing time in ovens at 100°C for both uncured and vulcanized polychloroprene. A strong reduction in double bond consumption rate is observed when considering vulcanized CR compared to the uncured material. It is worth noting that here the double bond consumption due to the vulcanization process can be neglected, and cannot be considered to be the cause of this large rate reduction. In fact the  $0.45\text{ mol.l}^{-1}$  of sulfur used in formulation does not consume a large amount of double bonds during vulcanization.

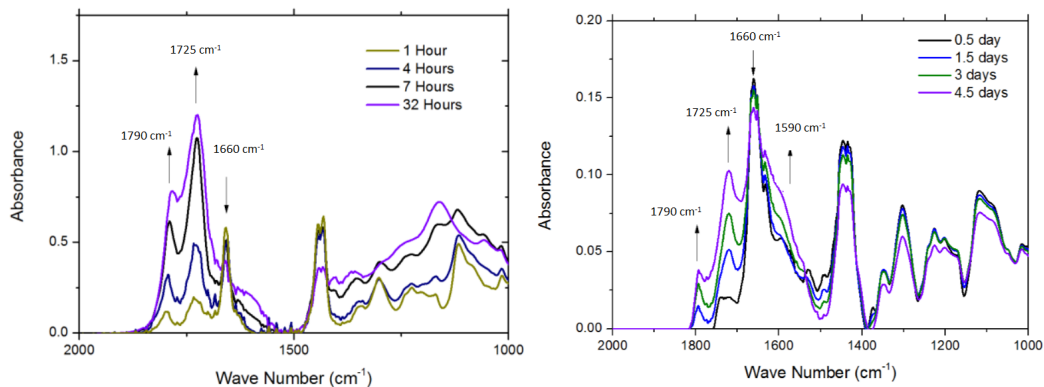


Figure 4.2: Change in FTIR spectrum during thermal oxidation at 120°C of uncured (a) and vulcanized (b) polychloroprene.

This reduction in double bond consumption rate is attributed to the oxidation rate decrease linked to the presence of sulfur that is involved in the vulcanization process; this is based on two facts. First, it has been shown many times that sulfur can destroy hydroperoxides by non-radical processes and so has a stabilization effect as it will be shown in Figure 4.8. In addition, Figure 4.4 shows that oxidation occurs in the first three days whereas the double bond concentration remains constant. About  $0.5 \text{ mol.l}^{-1}$  of oxygen have been consumed when double bond depletion begins.

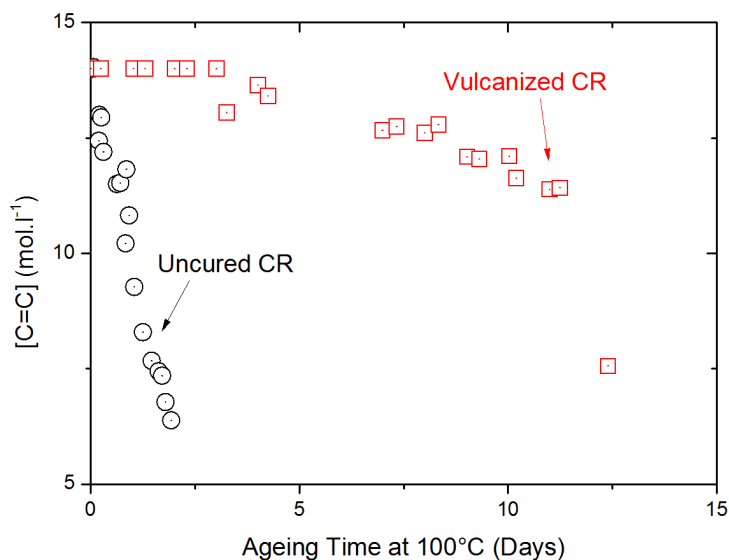


Figure 4.3: Loss in double bond content for uncured and vulcanized polychloroprene during thermo-oxidative aging at 100°C showing the increased stability of the cured material.

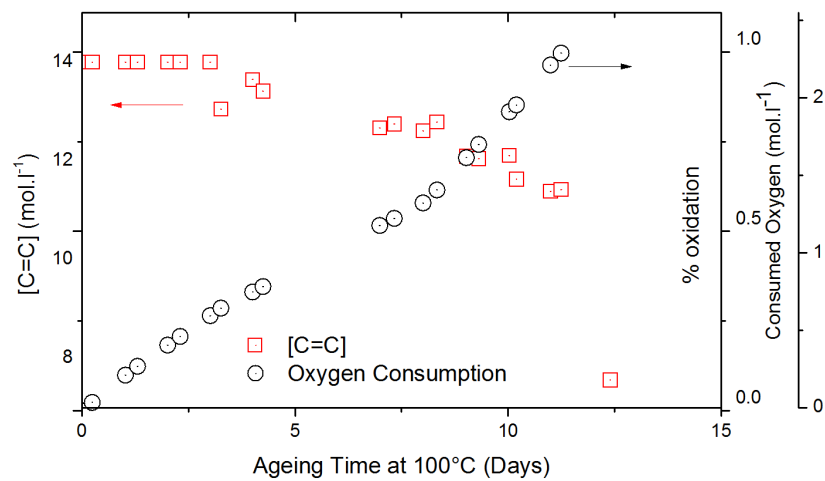


Figure 4.4: Oxygen consumption and double bond consumption during thermal oxidation at 100°C.

#### 4.2.1.2 Effect of oxidation on CR modulus

Based on FTIR results it appears that polychloroprene oxidation is affected by the vulcanization; the presence of ZnO leads to a modification of oxidation products through complex reactions that will not be considered here. This implies that the kinetic model will be based only on the double bond consumption that is much slower in vulcanized CR due to a stabilization induced by the presence of sulfur bonds, the effect has to be considered in the model. Because we want to be able to predict changes in mechanical properties induced by oxidation, the effect of oxidation on modulus of the rubber has been considered with special care, results are presented in the next section.

In order to characterize the effect of oxidation on the modulus of vulcanized CR, a new in-situ measurement has been used. This experiment allows an automatic, accurate and reproducible measurement of modulus variation during oxidation using a dedicated DMA. The modulus changes as a function of ageing time at 100°C, for a sample thin enough to avoid the existence of concentration gradients in the thickness, as shown in Figure 4.5. A large increase in modulus up to 200 MPa is observed, this phenomenon is in accordance with published data [54] [102] [62] and mainly attributed to widespread crosslinking during oxidation due to the addition of macroradicals on the double bonds (Figure 4.1). Modification of the network in the rubber might also occur at high temperature mainly due to formation of monosulfide bonds from polysulfide ones, this network modification would also lead to modulus change. This effect can be neglected here, in fact Figure 4.5 shows that no large modulus modification occurs when this rubber is aged at 140°C for 12 days under inert atmosphere (nitrogen).

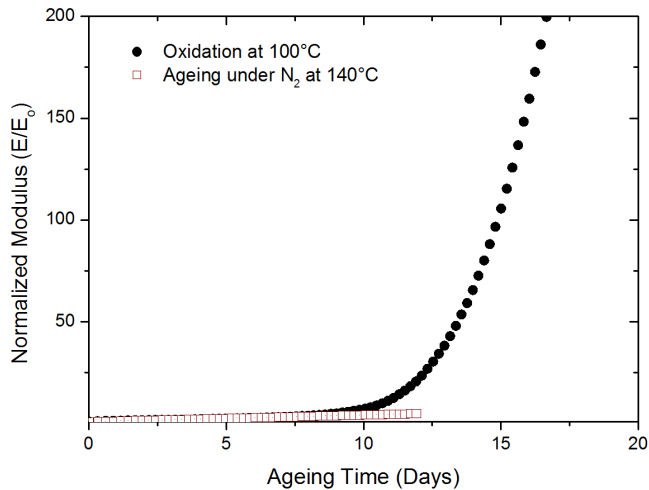


Figure 4.5: Changes in modulus as a function of time during oxidation of vulcanized CR at 100°C .

To understand the origin of this large modulus increase, DMA measurements were performed on homogeneous samples after several ageing times at 100°C; results provide interesting complementary information as illustrated by the plots of real ( $E'$ ) component of the complex tensile modulus against temperature for various ageing durations at 100°C (Figure 4.6). For low ageing duration a typical rubbery behaviour is observed with a  $T_g$  around  $-30^\circ\text{C}$  (Figure 4.6).  $T_g$  increases slightly with ageing time, as expected for a crosslinking process, but the most striking fact is that for long durations (i.e. 288 h and more), the rubbery plateau tends to be masked by a broadening of the glass transition. Between  $-30^\circ\text{C}$  and  $+60^\circ\text{C}$ , the modulus increases by a factor of at least 10 after 816 h of exposure. Such a broadening of the glass transition zone could be explained as follows: crosslinking leads to a progressive glass transformation (at  $-30^\circ\text{C} < T < 100^\circ\text{C}$ ) of the polymer but this transformation is not homogeneous, it occurs first in randomly distributed micro-domains and then progressively invades the sample volume. The fact that these changes cannot be explained by homogeneous crosslinking is attested by the numerical modulus value at  $30^\circ\text{C}$  after 816 h: about 100 MPa. Applying the basic theory of rubber elasticity this leads to a molar mass of elastically active chains of  $M_c = 105$  g/mol when the molar mass of monomeric units is 88.5 g/mol. It would be difficult to imagine a network displaying this average crosslink density in which the more densely crosslinked regions would not be glassy. This means that the prediction has to be limited to a range before the formation of such glassy domains. Thus in the next section modulus increases will be considered only up to 50 MPa.

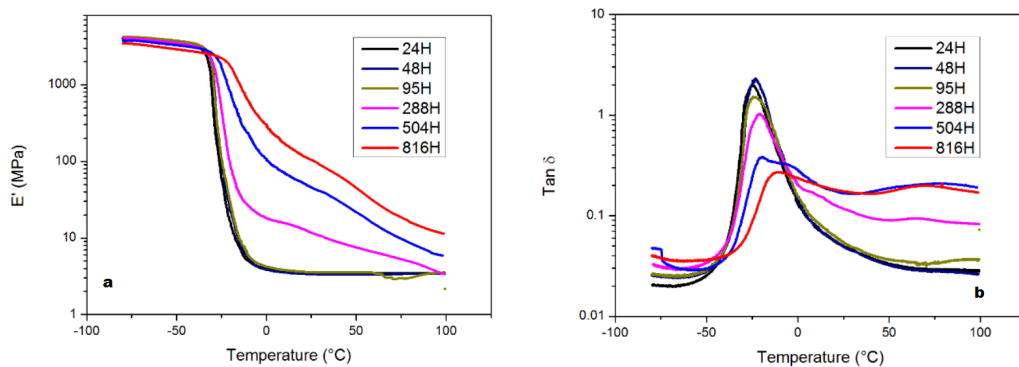


Figure 4.6: Evolution of DMA results (modulus and  $\tan \delta$ ) for different ageing durations at 100°C.

Using a logarithmic scale for modulus (Figure 4.7a) as proposed by Wise et al. [61], one obtains a curve which could be approximated by the intersection of two straight lines, in other words the modulus changes could be described by the sum of two exponentials of time. Even though this kind of behaviour

has already been observed for rubbers [68], the physical meaning of this sum of two exponentials remains unclear. However, if we consider the evolution of modulus (on a log scale) as a function of oxidation level in the rubber, it now appears that the curve is closer to a single exponential (Figure 4.7b) for low oxidation, i.e. up to 2%. This means that this kind of empirical relationship could be interesting to link the modulus with the amount of oxygen consumed by the degradation.

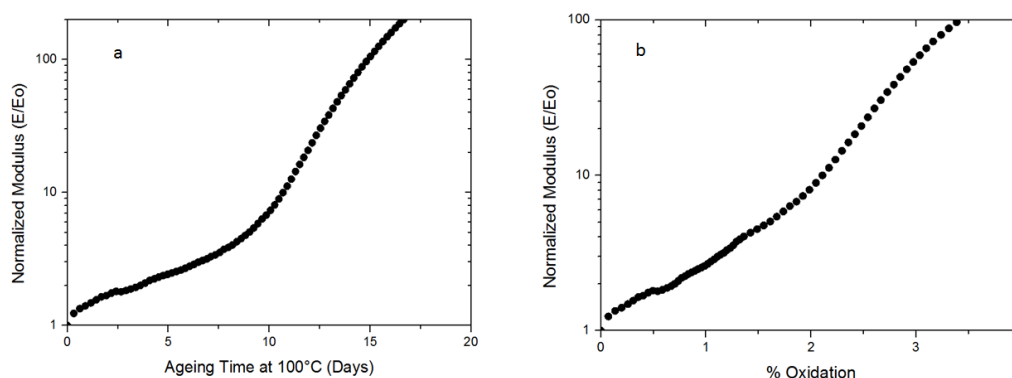


Figure 4.7: Change in modulus on a log scale as a function of time (a) and oxidation level in the rubber (b).

From these experiments we observed that a large increase in polychloroprene modulus occurs during oxidation, showing a complex evolution with ageing time. This modulus increase is not induced by an inert modification of the network. The next section will be dedicated to the prediction of this modulus evolution during oxidation based on mechanistic modelling. This latter is based on the kinetic model that has been set up for the uncured material with a consideration of sulfur effects in terms of both oxidation rates and network structure modifications. Then, based on these latter coupled with rubber elasticity theory, a prediction of modulus increase will be proposed and discussed.

## 4.2.2 Discussion and Modelling

This study aims to propose a new methodology in order to predict modulus evolution during oxidation of rubber, in the previous part both chemical and mechanical evolution have been characterized. We will now focus on the adaptation of the kinetic model to take into account the sulfur effect in order to create a new tool that allows prediction of modulus change.

### 4.2.2.1 Sulfur effect

The sulfur effect on oxidation rate is attributed to the reduction of POOH by sulfur, a part of this latter being present in intermolecular bridges [67] [103].

Since hydroperoxides are responsible for the initiation of radical chain oxidation, their destruction by non-radical processes is a stabilization mechanism. The mechanisms of POOH reactions with sulfur can be written as follows in the case of a mono-sulfide link:

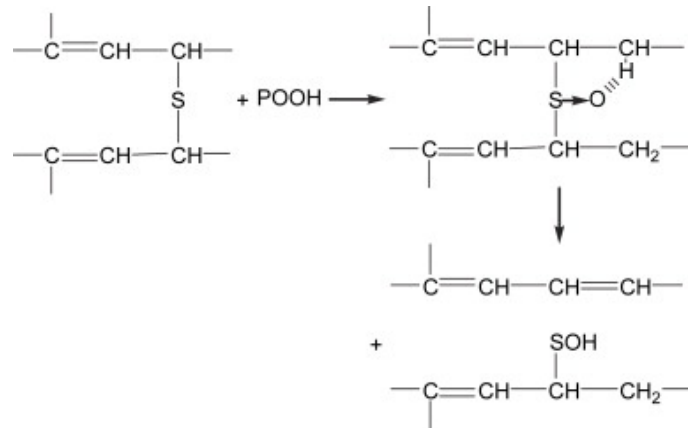
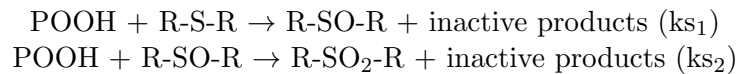


Figure 4.8: Reaction of POOH with sulfur in the case of natural rubber [86].



These two new equations are added to the general oxidation scheme of uncured polychloroprene, from this oxidation scheme a system of differential equations can be derived. Both  $ks_1$  and  $ks_2$  are determined using an inverse method based on double bond consumption, as shown in Figure 4.9. Values of  $ks_1$  and  $ks_2$  are reported in Table 4.1. It is worth noting that the only differences between the kinetic model of uncured CR and the one presented here are these two new reactions, i.e. all other rate constant values are the same as in [104], Table 3.3 in Chapter 3.

Contants rate	Values ( $\text{l.mol}^{-1}.\text{s}^{-1}$ )
$ks_1$	0.025
$ks_2$	0.005

Table 4.1: Optimal values for  $ks_1$  and  $ks_2$  used to model oxidation in polychloroprene at 100°C.

The influence of the  $ks_1$  value on the double bond consumption during oxidation is plotted in Figure 4.9a with two values of  $ks_1$ . By decreasing the value of  $ks_1$ , the reaction between sulfur and POOH is slower meaning that the double bond consumption induced by oxidation is faster. Figure 4.9b shows the evolution of both reacted sulfur atoms and double bonds; as soon as sulfur atoms are largely consumed a strong acceleration of double bond consumption occurs.

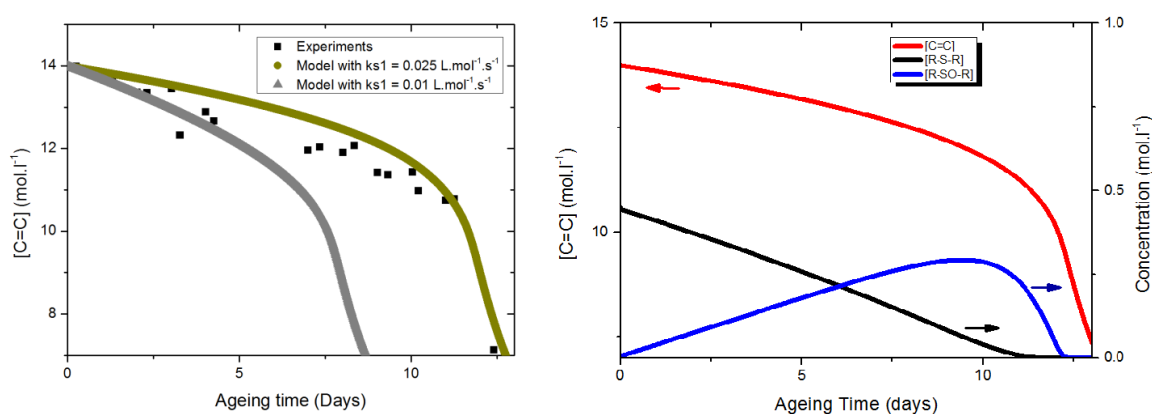


Figure 4.9: Double bond consumption during oxidation of vulcanized polychloroprene (a) Comparison between experiments and model prediction and (b) a representation of sulfur bond consumption that explains the slow decrease in double bonds and the autoacceleration for  $ks_1 = 0.025 \text{ l.mol}^{-1}.\text{s}^{-1}$ .

By adding two chemical reactions, the stabilization effect induced by the presence of sulfur within the polychloroprene rubber has been implemented in the model meaning that a kinetic model of oxidation in CR is now available. The two related rate constants have been determined at 100°C using an inverse method. In order to evaluate the limits of this new oxidation model for CR, the predicted oxygen consumption rate has been compared to experimental data generated at Sandia National Laboratories.

#### 4.2.2.2 Predicted oxygen consumption rate

Using the kinetic model described above, a comparison between measured and predicted oxygen consumption rates is shown in Figure 4.10. The key feature is that, without any adjustment, the order of magnitude of predicted consumed oxygen is close to that of measured values.

However, it appears that the predicted absorption is slightly above the measured one. This overestimation might be explained by measurement scatter, uncertainty on the initial double bond concentration and the presence of double bond consumption through a non-oxidizing reaction. In fact due to the complexity of the reaction between ZnO and oxidation products the model has

been set up only with double bonds whereas the actual initial double bond concentration in the rubber comes from theoretical calculation and not from experimental measurement. A difference between theoretical and actual double bond concentration would lead to a variation of the predicted absorbed oxygen rate. This experimental measurement is not straightforward but NMR will be used in the future to check this point.

Moreover we could imagine a reaction occurring in the absence of oxygen but induced by oxidation (this inert reaction does not occur if there is no oxidation of the rubber) but with no evidence to support this hypothesis. Adding complexity to the model might improve the prediction of absorbed oxygen, but this is not the aim here: the goal here is to predict modulus changes as a function of oxidation, as will be described below.

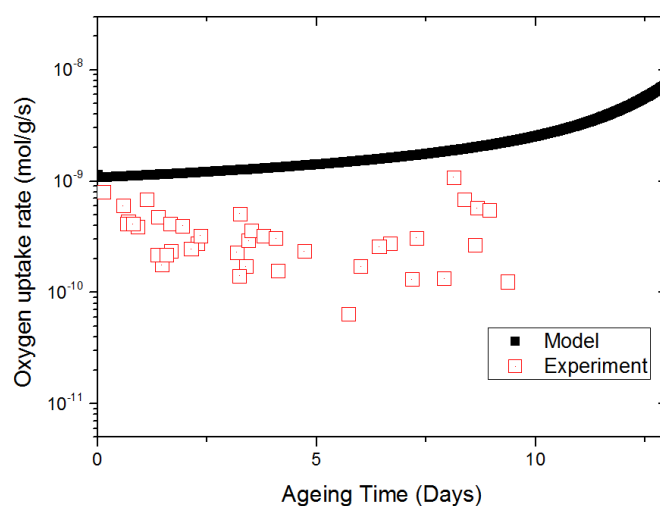


Figure 4.10: Predicted and measured oxygen consumption rate at 100°C for vulcanized polychloroprene.

Oxygen absorption rate measurements are very useful when considering polymer oxidation, here these data have been compared to predicted values for the first time in order to evaluate limitations of the prediction. The predicted oxygen absorption rate is of the same order of magnitude as the one measured experimentally, even if a slight overestimation is observed. The question is now *how to use this model to predict evolution of mechanical behaviour such as modulus*.

#### 4.2.2.3 Modulus prediction

The modulus prediction is based on a description of both chain scissions and crosslinking events for each chemical step involved in the mechanistic scheme considered here.

Two types of chain scissions are considered; the first one is random chain scission and occurs during the initiation step, i.e. the decomposition of hydroperoxides. The second one is selective chain scission, and occurs when hydroperoxides react with sulfur as described above (Figure 4.8). At the same time crosslinking occurs in the rubber, these events are due to both a termination reaction by macroradical coupling and the addition of free macroradicals on double bonds as described in Figure 4.1. All these events are schematically represented in Table 4.2 below.

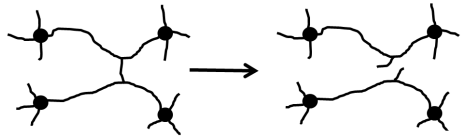
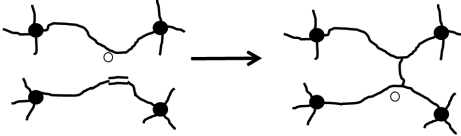
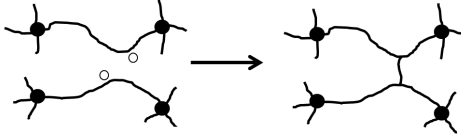
Nature of the reaction	Schematic representation	Value of $\delta$	Value of $\gamma$
Random chain scission during initiation steps		1	0
Selective chain scission during reaction with sulfure bonds		2	0
Crosslink due to reaction on the double bond		0	2
Crosslink due to termination steps		1	0

Table 4.2: Schematic representation of chain scissions and crosslinking events considered in this study.

This means that using a kinetic model, it is possible to predict the number of both chain scissions and crosslinks so as to obtain the evolution of the actual crosslink density in the rubber during oxidation that can be written (at low conversions):

$$\nu(t) = \nu_0 - \delta \cdot s(t) + \gamma \cdot x(t) \quad (4.1)$$

Where  $\nu_0$  is the initial crosslink density,  $s(t)$  and  $x(t)$  are respectively the numbers of chain scissions and crosslinking events at time  $t$ ,  $\delta$  and  $\gamma$  are coefficients depending on the nature of the rubber and determined from architecture modification in the rubber network. Parameter values are reported in Table 4.2. Because all reacted double bonds do not lead to a new crosslink [65] a yield  $\tau$  is introduced to take into account this effect so the previous equation (4.1) becomes:

$$\nu(t) = \nu_0 - \delta \cdot s(t) + x_{termination}(t) + 2 \cdot \tau \cdot x_{C=C}(t) \quad (4.2)$$

Based on the theory of rubbery elasticity the modulus of an unfilled elastomer is directly linked to the crosslink density as shown below. In fact based on thermodynamic considerations, assuming that deformations occur at constant volume and that macroscopic deformations are affine of microscopic ones, it is possible to show [70] that the stress/strain behaviour of unfilled rubber is, in simple extension, given by:

$$\sigma = R \cdot T \cdot \rho \cdot \nu \cdot (\lambda - \lambda^{-2}) \quad (4.3)$$

with  $\sigma$  the stress in Pa equal to  $F/S_0$  with  $F$  the load and  $S_0$  the initial section,  $R$  the perfect gas constant,  $T$  the absolute temperature,  $\rho$  the density of the material,  $\nu$  the crosslink density, i.e. the concentration of elastically active chains.

Assuming that deformations occur at constant volume (i.e.  $E = 3G$ ) the Young's modulus of an unfilled rubber at small deformation is directly linked to the crosslink density of the rubber.

$$E = 3 \cdot R \cdot T \cdot \rho \cdot \nu \quad (4.4)$$

From equations 4.2 and 4.4 it is thus possible to express the change in the modulus of an unfilled rubber with an ideal network as a function of time during oxidation. And so it appears that by using the mechanistic approach coupled with theoretical considerations it is possible to predict quantitatively the evolution of rubber modulus during oxidation. This has been done for the rubber considered in this study, a comparison between predicted and measured changes in modulus during oxidation is plotted in Figure 4.11. A good

agreement is observed when  $\tau$  is equal to 0.35, this yield is used as an efficiency factor for the crosslinks created by addition of macroradicals on double bonds (Figure 4.11). There is not much information available in the literature about this factor; this value of 0.35 could be explained by several parallel reactions such as intramolecular disproportionation [65]. But the important point is that now it is possible to predict quantitatively changes in modulus during polychloroprene oxidation based on both chemical and physical considerations.

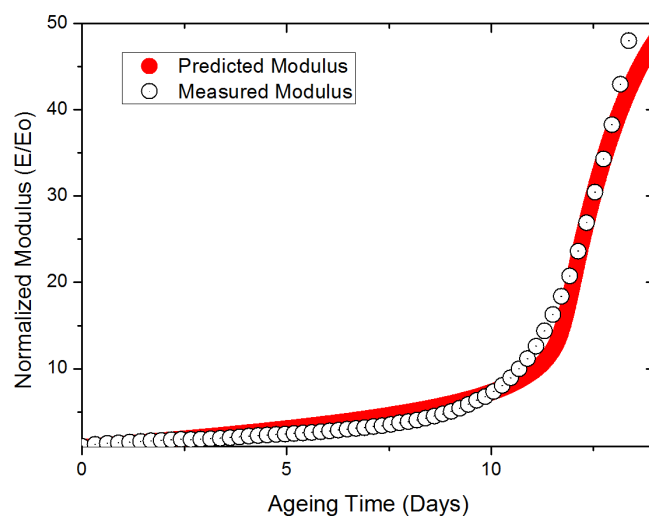


Figure 4.11: Comparison between predicted modulus change and measured values.

To conclude, a new methodology for the prediction of modulus changes in polychloroprene rubber oxidation has been developed here. The stabilization effect induced by the presence of sulfur used for the vulcanization process has been added to the kinetic model and modelling results have been compared to experimental oxygen absorption rate for the first time. Then, considering both chain scission and crosslinking events for each chemical step in the model, it is now possible to predict changes in crosslink density in the rubber as a function of oxidation and hence to predict modulus through theoretical considerations. This modulus prediction has been compared to experimental data and shows a good agreement when a specific ratio between double bond consumption and crosslink formation is used. This ratio,  $\tau$  is equal to 0.35 at 100°C but one of the remaining questions is how this ratio evolves with ageing temperature. In order to be able to make a lifetime prediction at low temperature this point has to be addressed, this is the aim of the next section.

## 4.3 Temperature effect on oxidation of vulcanized polychloroprene

This part of the study considers the temperature effect on both stabilization kinetics (i.e. evolution of  $ks_1$  and  $ks_2$  with temperature) and the ratio between double bond consumption and created crosslinks ( $\tau$ ) in order to be able to make reliable life time prediction at low temperature. First, evolution of kinetic rates with temperature is determined based on experimental FTIR data in the range from 140°C to 60°C. Then in a second step, using the kinetic model, predicted modulus values are compared to measured ones in the range from 140°C to 100°C in order to evaluate the possible variation of  $\tau$  with temperature. And finally temperature effect on the overall oxidation process will be described and discussed with a comparison between predicted and measured oxygen consumption rates.

### 4.3.1 Variation of $ks_1$ and $ks_2$ with temperature

The effect of temperature on oxidation kinetics has been considered in the range from 140°C to 60°C; Figure 4.12 plots the double bond consumption measured by FTIR as a function of ageing time for all temperatures considered here (plotted as points). For all temperatures, the behaviour is the same, i.e. a slow initial decrease of the double bond concentration and then a large auto acceleration that corresponds to the consumption of most of the sulfur groups. Using an inverse method, values of both  $ks_1$  and  $ks_2$  have been determined at these temperatures and plotted on an Arrhenius graph (Figure 4.13). From these results it appears that both reactions display Arrhenius behaviour and activation energies can be determined equal to 130 and 85 kJ/mol respectively for  $ks_1$  and  $ks_2$ . Although direct values in the literature are very scarce, these activation energy values are consistent with others assessed by inverse methods [105] [106].

All others parameters of the kinetic model are the same as for the uncured polychloroprene described in the previous chapter. The results of modelling are plotted on the same figure as continuous lines (Figure 4.12), a good agreement is observed indicating that the model is good enough to describe the double bond consumption in vulcanized polychloroprene without stabilization over the range from 140 to 60°C. Temperature effect on oxidation rate is now included in the kinetic model. However in order to make a prediction of the modulus at low temperature it is also necessary to evaluate the temperature effect on the ratio  $\tau$  that describes the fact that all double bond consumption events do not create a new crosslink; this point is considered in the next section.

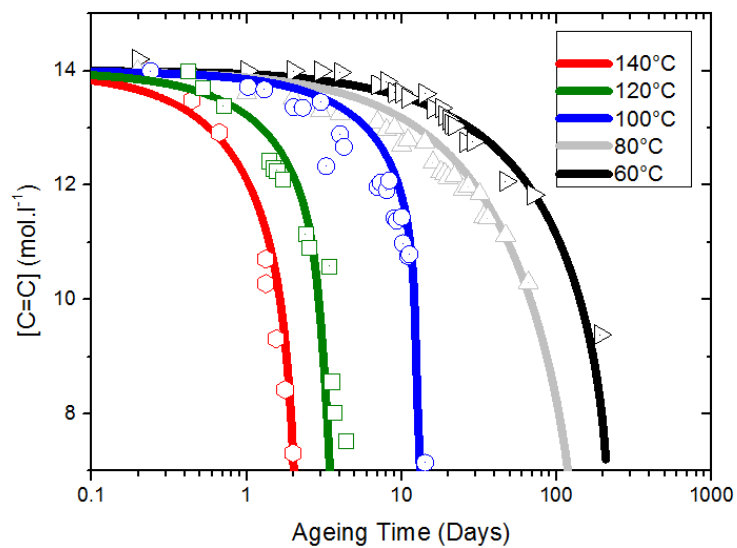


Figure 4.12: Effect of temperature on double bond consumption (symbols are experimental values and lines correspond to modelling).

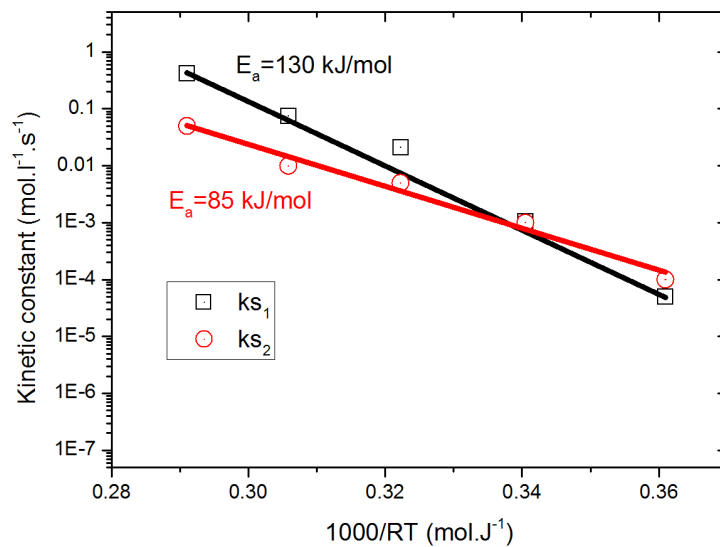


Figure 4.13: Evolution of  $ks_1$  and  $ks_2$  with temperature in an Arrhenius plot.

### 4.3.2 Effect of ageing temperature on modulus prediction

The model developed here can be used to predict modulus at 100°C (see above) and can describe the temperature effect based on double bond consumption, but it can also be used to predict the temperature effect on modulus change during oxidation. In-situ modulus characterization has been performed in the range of 140°C to 100°C in order to evaluate the ability of this approach to describe the effect of temperature. For all tested temperatures the same behaviour is observed i.e. a period in which modulus is almost unchanged and then a large increase occurs (Figure 4.14). This behaviour is predicted well by the model with the same yield (the  $\tau$  value) of crosslink creation per double bond consumed for all temperatures (i.e. 0.35 as described for 100°C). Another representation of this behaviour is shown in Figure 4.15 where the crosslink density is plotted as a function of consumed double bonds in the rubber. A nonlinear relationship between the crosslink density increase and the double bond consumption is observed for all tested temperatures; in fact the ratio between double bond consumption and crosslink density increase evolves with the oxidation level in the rubber. This behaviour could be explained by considering that in the early stages of degradation the two main modifications in the rubber network are chain scission on the sulfur bonds (Figure 4.7) and crosslinking from additions on the double bonds (Figure 4.1). Whereas for more advanced degradation, all sulfur bonds have been consumed and thus crosslinking due to reaction on the double bond is the main modification in the network. This interpretation is supported by modelling results when chain scissions on sulfur bonds are not taken into account in the modelling (red line in Figure 4.15); results clearly show a proportional relationship between double bond consumption and increase in cross link density with a higher ratio in the early stage of the degradation. This is a typical example of how kinetic modelling could be used for a better understanding of the oxidation process itself.

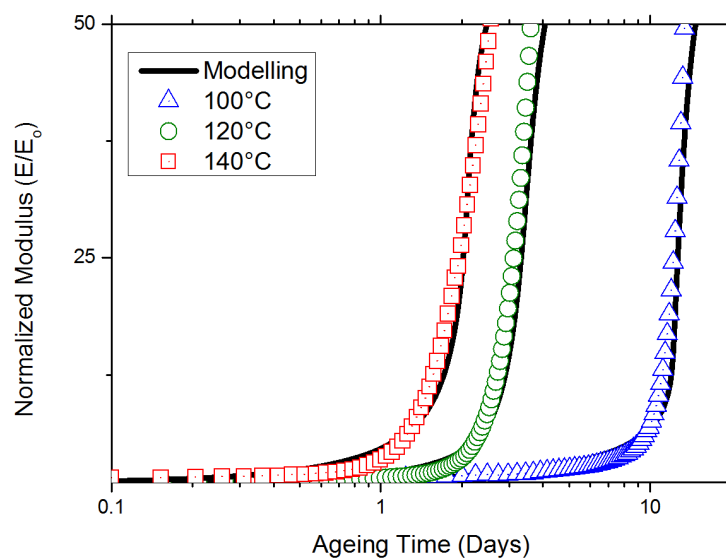


Figure 4.14: Effect of temperature on modulus increase measured in-situ (symbols are experimental values and lines correspond to modelling).

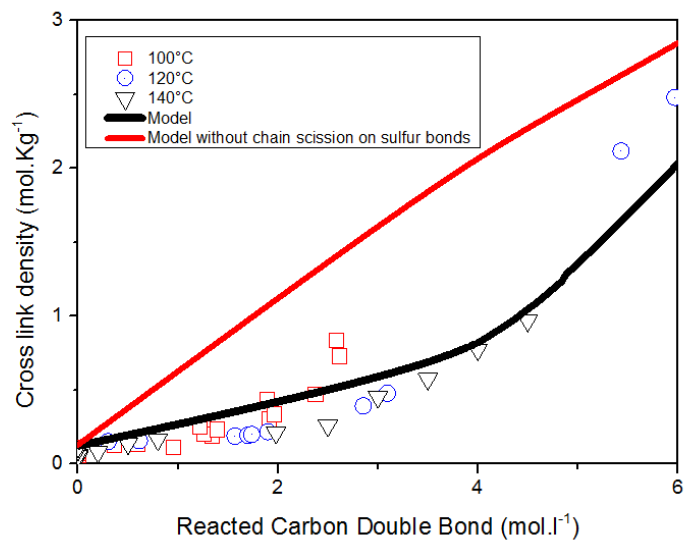


Figure 4.15: Crosslink density evolution during oxidation related to reacted double bonds in polychloroprene rubber

To conclude, a kinetic model has been developed for vulcanized CR and this can be used to predict modulus variation during oxidation over a large range of temperature. But when considering accelerated ageing of polymers, the temperature effect on mechanisms and kinetics is always a crucial point, and it is controversial. Based on the model developed here that allows prediction at low temperature coupled with oxygen absorption data measured in the range from 140°C to 25°C, the temperature effect on oxidation in rubber is discussed in the next section.

### 4.3.3 Temperature effect on the overall oxidation kinetics

Using this model, it is possible to evaluate the oxidation kinetics over an extended range of temperature, and to make predictions for lower temperatures. Figure 4.16 plots the average absorption rate of oxygen at the beginning of the oxidation (before the autoacceleration). Results from the model clearly show an Arrhenius behaviour with activation energy of 64 kJ per mol. These predicted results are compared to experimental data obtained using the Oxzilla respirometer at Sandia National Laboratories. Despite a difference in terms of values that has already been discussed, experimental results clearly show the same behaviour as the model, i.e. an Arrhenius behaviour in the range of temperature considered here with an activation energy of 66 kJ per mol. This behaviour raises some questions, which will be discussed below; in fact data from Celina [62] with stabilized polychloroprene show a departure from linear Arrhenius behaviour.

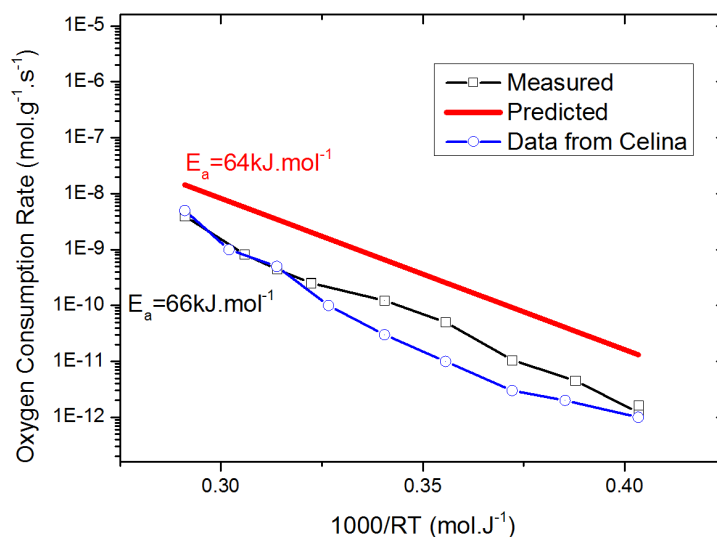


Figure 4.16: Arrhenius plots of both measured and predicted oxygen absorption rate in this study and values from Celina [62] on stabilized CR.

- First, how can we explain this behaviour although a non-arrhenian behaviour has been observed in literature with polychloroprene [62][61]. The main difference between the material studied by Celina and the one used in this study is the presence of stabilizer. In fact the CR that presents a curvature on the Arrhenius plots (in Figure 4.16) contains 2phr of phenol as stabilizers whereas the one that shows a linear behaviour does not contain any stabilizer. From these results it appears that the non linear behaviour does not come from the chemistry involved in the oxidation of polychloroprene but probably from the stabilizer efficiency at different temperatures. In fact, two phenomena are involved in the stabilizer reduction during oxidation; the first one is the reaction of phenol with radicals [107] [108] and the second is the physical loss by evaporation of the stabilizer [109]. Both phenomena are in competition and are influenced to different extents by temperature. This competition could be at the origin of the non linear behaviour observed by Celina. Here, the comparison of samples with and without stabilizers suggests that nonlinear behaviour is due to stabilizers.
- Second, why is the activation energy low ? Activation energies for oxygen consumption rate of vulcanized and unstabilized polychloroprene were measured equal to 66 kJ/mol and close to the value obtained from modelling. This value is quite low compared to other polymers, Table 4.3 summarizes experimental activation energy measured based on oxygen consumption rate especially at high temperature. The low value here could be partially explained by considering an analytical solution of the basic oxidation scheme. In steady state and in oxygen excess it is possible to write:

$$r_{ox} = 2 \cdot \frac{k_3^2 \cdot [PH]^2}{k_6} \quad (4.5)$$

that leads to

$$E_{ox} = 2 \cdot E_3 - E_6 \quad (4.6)$$

From the previous chapter we know that  $E_3$  and  $E_6$  are respectively equal to 56 kJ/mol and 53 kJ/mol meaning that  $E_{ox}$  should be, according to this analytical approach, equal to 53 kJ/mol. The difference between this value from analytical considerations and the values measured and predicted in air can be attributed to the fact that polychloroprene rubber is not in oxygen excess in air. Despite a lack of accuracy this analytical approach is useful to understand the origin of the low activation energy in polychloroprene. Considering that the temperature effect on propagation is similar for this rubber compared to others (Table 4.3), this low activation energy could be attributed to the large effect of temperature on the termination reaction that involves two  $PO_2^\bullet$ . Because this behaviour has not been observed with polyisoprene [86] it might be

attributed to the presence of the chlorine atom in the rubber, but the mechanism of this effect is unclear. As one hypothesis, we could imagine that the large size of the chlorine atom might reduce radical motions in the rubber and so increase the temperature effect; this hypothesis would need more experiments in order to validate it or not.

Nature of polymer	Activation Energy (kJ.mol <sup>-1</sup> )	Temperature range (°C)	References
PA 6	123	120-170	[110]
Polyurethane based on PBHT	119	80-120	[69]
	65	25-60	[69]
Butyl rubber	100	80-120	[111]
	75	30-70	[111]
Nitrile rubber	90	70-120	[68]
Etylene propylene rubber	100	50-125	[112]

Table 4.3: Activation energy of oxidation measured by oxygen absorption for several polymers.

One of the most interesting outcomes of the model developed here is that it can be used to understand the oxidation process. A comparison of prediction and experimental data gives information about the origin of the non linear Arrhenien behaviour: in the case of CR the curvature observed in Figure 4.16 can be attributed to the stabilization effect. This point has to be studied further (role of the nature of stabilization, effect of stabilizer concentration) in the future in order to understand and predict the long term behaviour of rubbers.

Up to here we have been concerned with thin film samples, but oxidation in polymers is usually limited by diffusion when thick samples are used, it is thus important to consider modelling of Diffusion Limited Oxidation (DLO), this is the aim of the next section.

## 4.4 Inhomogeneous oxidation

The first parts of this chapter were devoted to the prediction of modulus change during polychloroprene oxidation using a kinetic model when degradation is homogeneous. However it is well known that thick samples can undergo heterogeneous oxidation due to the competition between oxygen diffusion from the external media to the bulk of the material and oxygen consumption by the chemical degradation. This phenomenon is named Diffusion Limited Oxidation (DLO) and it is of great importance in practice because rubbers are usually employed in thick section parts. Also, when considering a study of oxidation, this kind of heterogeneous oxidation is very useful to validate any predictions.

### 4.4.1 Results

#### 4.4.1.1 Double bond concentration and modulus profiles

Local concentration of the double bonds in thick (4.8 mm) samples during ageing at 120°C has been measured using FTIR. Results, plotted in Figure 4.17a, show a heterogeneous consumption of the double bonds, i.e. the oxidation is limited to the first millimeter from each surface due to the DLO effect. As long as ageing time increases the double bond concentration at the surface decreases. Because oxidation of CR leads to an increase in the crosslink density and thus an increase in modulus, a modulus profile through the sample thickness is observed, and a good correlation between double bond consumption and modulus profiles can be observed. Although these results cannot be directly compared to those obtained by Celina [62] (because of the difference in ageing temperatures and the presence of stabilization), the thickness of oxidized layer is of the same order of magnitude.

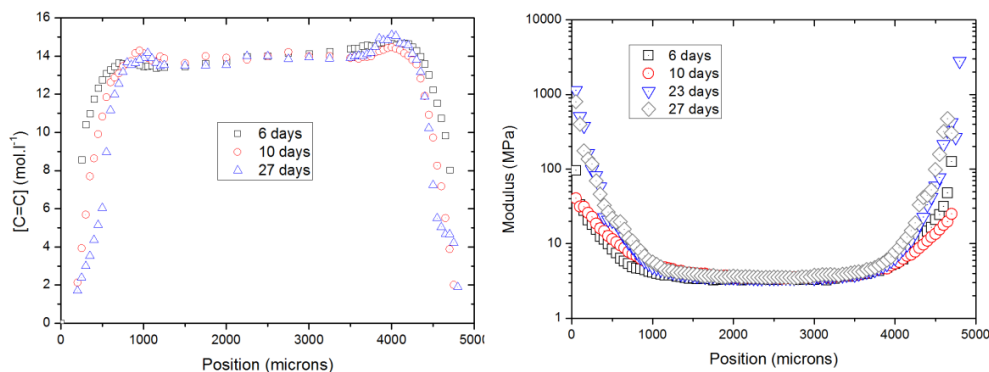


Figure 4.17: Profile of double bonds (a) and modulus (b) through the thickness of a 4.8 mm thick sample during oxidation at 120°C in air.

Modulus profiles in Figure 4.17b show that the modulus in the bulk is not affected during ageing at 120°C even for long durations such as 27 days. This is a clear validation of the fact that thermal degradation (without oxygen) can be neglected and all modulus changes are induced by oxidation. At the same time large modulus increases, up to several GPa, are observed at the edges; these observations confirm measurements performed in homogeneous conditions. The question now is whether the model can predict quantitatively these profiles. In order to perform such modelling oxygen diffusion has to be taken into account, so first it is necessary to measure the actual oxygen diffusion coefficient in this material.

#### 4.4.1.2 Oxygen permeability

Permeation of oxygen through a rubber sheet has been measured at different temperatures; results are plotted in Figure 4.18. Permeability has been measured using a stabilized sample and at relatively low temperature, in order to avoid any oxidation of the rubber during the test. Oxygen diffusivity is calculated from this permeability measurement considering that the solubility coefficient is equal to  $3 \cdot 10^{-8} \text{ mol.l}^{-1} \cdot \text{Pa}^{-1}$  [1] and temperature independent. This last point could be refined, in fact it seems that solubility might be slightly influenced by temperature [113] but this effect is considered to be of second order here. Oxygen diffusivity can be expressed as follows:

$$D = D_0 \cdot \exp\left(\frac{-E_{P_{ox}}}{R \cdot T}\right) \quad (4.7)$$

With  $D_0$  equal to  $3 \cdot 10^{-4} \text{ m}^2 \cdot \text{s}^{-1}$  and  $E_{P_{ox}}$  equal to 39 kJ/mol. Then at 120°C, oxygen diffusivity is equal to  $1.9 \cdot 10^{-9} \text{ m}^2 \cdot \text{s}^{-1}$ . This value is in accordance with data available in the literature ([69], [1]).

It has to be noted that oxygen diffusion has been characterized on unaged polychloroprene and it has been postulated that this value does not change with oxidation. This point is an assumption that could be discussed, in fact because of the increase in crosslink density and the appearance of possible glassy areas with oxidation the value of oxygen diffusivity might be affected. This point would need further experiments in order to take it into account in the modelling.

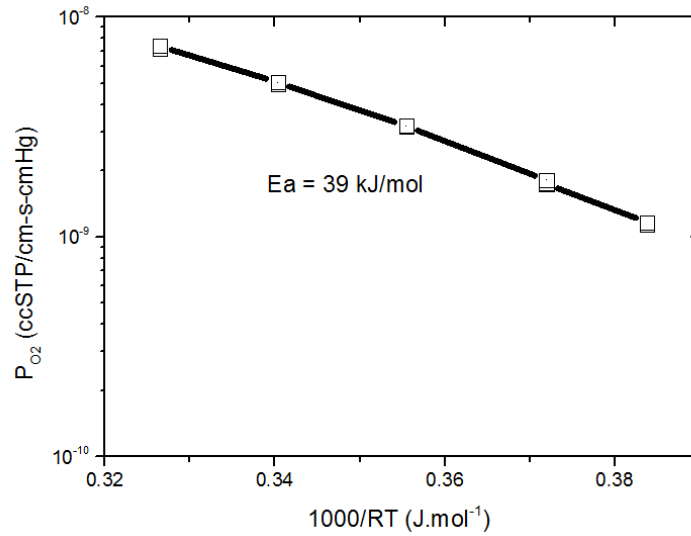


Figure 4.18: Oxygen permeability coefficient as a function of temperature.

#### 4.4.2 Modelling

The model used with thick samples is exactly the same as for homogeneous oxidation except for the fact that the oxygen concentration depends on time due to both consumption by the oxidation and increase due to diffusion from external media. These phenomena can be written in mathematical terms using the following equation that has been added to the entire model described previously:

$$\frac{\partial [O_2]}{\partial t} = -k_2 \cdot [P^o] \cdot [O_2] + k_6 \cdot [PO_2^o]^2 + D \cdot \frac{\partial^2 [O_2]}{\partial z^2} \quad (4.8)$$

Where  $D$  is oxygen diffusion coefficient (in  $m^2 \cdot s^{-1}$ ),  $[O_2]$  is the oxygen concentration and  $z$  the position in the sample thickness and  $t$  the time.

Considering this differential equation with the value of diffusivity measured on the unaged sample it is possible to model oxidation as a function of time and position in a thick polychloroprene rubber. Results obtained at 120°C for both double bond consumption and modulus changes are plotted in Figure 4.19. As expected a strong DLO is observed with large double bond consumption coupled with a large modulus increase localized at the sample edges. A comparison between experimental data and predicted values (in Figure 4.20) shows that both are in agreement, indicating that the kinetic model is suitable for prediction of heterogeneous degradation. However for low degradation levels, i.e. modulus under 10 MPa, the results are not exactly the same; the measured profile is sharper than the predicted one. This means that oxidation is more localized on the surface than predicted by the model; this behaviour

could be due to a decrease of the oxygen diffusivity with ageing. In fact the effect of the value of oxygen diffusion coefficient  $D$  on the predicted profile shape is plotted in Figure 4.21, a higher value of  $D$  leads to a sharper profile. This means that if oxidation leads to a reduction of the oxygen diffusivity (through an increase of the crosslink density), the degradation profile will be more localized close to the surface. By taking into account this potential evolution of diffusivity with oxidation a better description of experimental results might be possible. This would require measurements of oxygen permeability at several oxidation levels. It is important to note that a modification of the oxygen solubility might also occur during degradation. This effect of oxidation on both oxygen solubility and diffusion is still an open field for research and would also require time dependent DLO models.

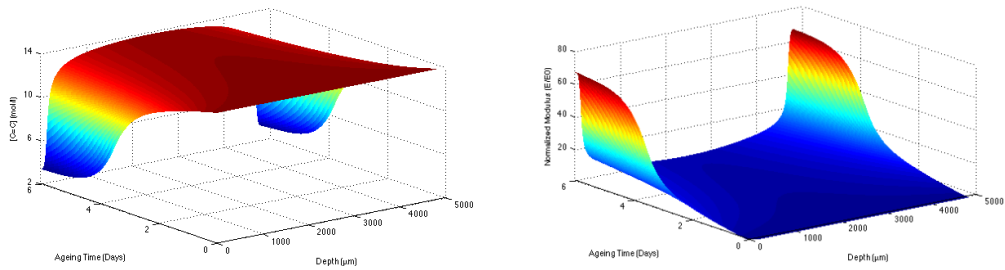


Figure 4.19: Typical modelling results with evolution of double bonds (left) and increase in modulus (right) as a function of time and position at 120°C.

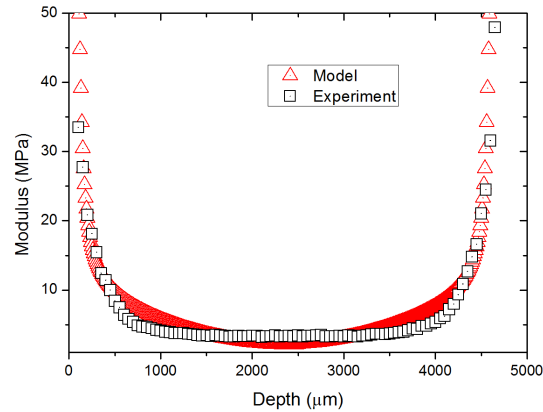


Figure 4.20: Comparison between predicted and measured modulus profile through thickness after 6 days of ageing at 120°C.

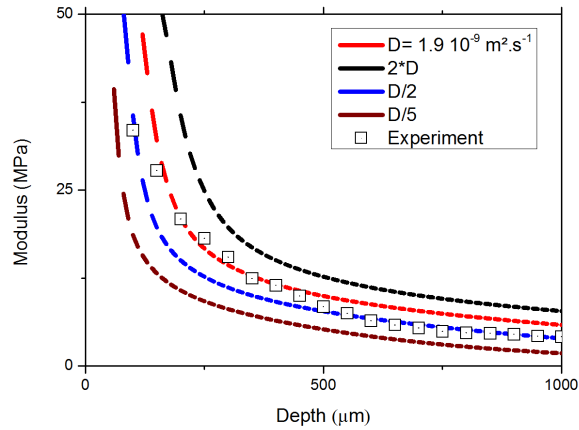


Figure 4.21: Effect of the oxygen diffusivity value on the modulus profile at 120°C.

The comparison between experiments and modelling is limited to one ageing time; in fact for longer durations the modulus of the oxidized layer is considerably higher than 50 MPa, which was taken as the upper limit in terms of prediction. It would be useful to perform ageing for shorter durations in order to make comparisons at different ageing times. Prediction for very high oxidation levels needs to consider more reactions and physical phenomena such as formation of glassy regions in the rubber. This is out of the scope of this work but would be interesting for the future.

## 4.5 Conclusion

Homogeneous oxidation of vulcanized polychloroprene without any stabilizers or reinforcing fillers has been studied first using FTIR, oxygen consumption and in-situ modulus changes in order to set up a kinetic model and predict the observed large increase in modulus.

Because of the vulcanization process and more especially the presence of sulfur within the rubber, the oxidation rate is much lower compared to that of uncured material. This sulfur effect has been integrated in the oxidation scheme and oxidation rate has been determined using the double bond consumption, meaning that a mechanistic model of the oxidation of a vulcanized polychloroprene is now available. The sulfur effect has been integrated through two reactions in which POOH reacts directly with the sulfur bonds, however due to the complexity of the vulcanization process that leads to the presence of several types of sulfur bonds; a more detailed study on the relationship between the oxidation of rubber and the nature of sulfur bonds would be interesting. This sulfur effect might explain the difference observed between measured and predicted oxygen absorption.

Based on network modification at the macromolecular scale predicted by the kinetic model coupled with the rubber theory, a modulus prediction has been performed and compared with experimental results in the range of 140 to 100°C. A good agreement is observed when a fixed ratio is used between double bond consumption and formation of new crosslinks, this ratio is equal to 0.35 and independent of temperature in the range determined here, however there is not much data published to compare with. A comparison with other rubbers with different double bond concentrations (polyurethane based on PBHT for example) would be interesting to study in detail.

In spite of minor limitations this kinetic model is the first prediction of modulus changes in polychloroprene during homogeneous oxidation. The temperature effect has been considered for each chemical reaction considered in the oxidation scheme; despite the complexity of the oxidation process, the overall process of polychloroprene oxidation displays Arrhenius behaviour based on oxygen consumption rate. Both measured and predicted temperature effects are similar with an activation energy about 65 kJ/mol. This value is low, especially at high temperature, compared to other rubbers. This point is a clear validation of the modelling approach in order to predict the temperature effect on oxidation and so predict the behaviour of rubber at service temperature. Moreover, using data from Celina [62] on stabilized polychloroprene it appears that the observed non-arrhenian behaviour is probably due to a stabilization effect, but the comparison between both studies is limited by the fact that the vulcanization process was not the same. It seems thus necessary to consider stabilization effects on the oxidation rate at several temperatures; this has not

been considered here due to lack of time.

Oxygen diffusion in the rubber has also been considered and implemented in the model in order to be able to predict modulus change in thick samples. A relatively good agreement between experimental data and the predicted profile is observed. However, a sharper profile is observed experimentally, that could be attributed to a reduction of oxygen diffusivity in the rubber due to an increase of the crosslink density induced by oxidation. Moreover, high oxidation degree has not been considered here. In fact the model is suitable only for modulus values up to 50 MPa, this fact limits the prediction of the modulus for long durations at high temperature.

In this chapter, the only mechanical property that has been considered is the modulus and its evolution induced by oxidation. However life time prediction in rubbers is usually based on evolution of fracture properties, and more especially elongation at break. The next chapter will therefore be devoted to the effect of oxidation on fracture behaviour of rubbers.



## Chapter 5

# Oxidation effect on fracture properties of rubbers

This chapter was originally intended to present the prediction of fracture properties of CR when undergoing oxidation. However, results presented below show a very complex evolution of the fracture energy in mode I with ageing time. So an emphasis has instead been placed on the understanding of such behaviour, using model rubbers. In the first part, a brief description of existing knowledge on rubber fracture properties is proposed. Then, the experiments that have been set up and used for this study are described. Next, results are presented, and these are discussed in the last part of the chapter.

## 5.1 Introduction

This chapter deals with fracture properties of elastomers, their relationships with structure, and the consequences of oxidative ageing on these properties. There is a relatively abundant literature on the effect of crosslink density on fracture properties of elastomers. These studies have been performed essentially on network families of well controlled architecture such as crosslinked polydimethyl siloxanes [78] and [114] or polyurethane elastomers [115], in which all the additives likely to modify the mechanical behaviour, especially fillers, were avoided. Particular attention has been paid to the quasi equilibrium properties which could be deduced from the network theory and the theory of entropic elasticity applied to quasi ideal networks in which the length distribution of elastically active chains (EAC) would be unimodal. In such cases, a key characteristic is the number of chains crossing a unit area in an unloaded state [116]; according to Lake [73], there is a simple relationship with the molar mass  $M_c$  of EACs (that is defined as the reciprocal of crosslink density):

$$G_{IC_0} = K \cdot M_c^{1/2} \quad (5.1)$$

where  $G_{IC_0}$  is the threshold tear strength that characterizes fracture free of viscoelastic or strain induced crystallization (SIC) effects.  $K$  is mainly related to the rupture energy of a single chain.

This kind of relationship has been experimentally checked by various authors [74], [75] and [76], but counter-examples have also been found. For instance Yanyo observed that in polydimethyl siloxane networks, the fracture behaviour depends also on the length distribution of EACs [77]. This was confirmed by Mark and co-workers [78] and [114] who studied a series of polydimethyl siloxane networks based on long chains to which variable quantities of short chains were added. It appeared that the modulus increased regularly with the average crosslink density. In contrast, the ultimate elongation does not vary with the crosslink density except at high concentrations of short chains, showing that in a wide interval of crosslink densities, for a bimodal network, the fracture behaviour remains controlled by the extension of long chains. In such systems, indeed, the fracture energy increases regularly with crosslink density as long as ultimate elongation remains constant. "Equilibrium" fracture properties are interesting from a theoretical point of view but they do not correspond to the real use conditions of rubbers. Under such conditions, viscoelastic effects cannot be ignored.

Persson [117] proposed a simple equation to represent the contribution of viscoelasticity to toughness:

$$G_{IC} = G_{IC_0} \cdot [1 + \phi_{T,v}] \quad (5.2)$$

where  $G_{IC_0}$  is the “equilibrium”  $G_{IC}$  value and  $\phi_{T,v}$  is a function of temperature  $T$  and crack velocity  $v$  expressing the contribution of dissipative, viscoelastic processes to fracture energy. This approach has been used recently in a study of fracture properties of polyurethane elastomers by Cristiano et al. [115]. The fracture behaviour depends not only on crosslink density but also on the type of crosslinks [118].

Some elastomers, e.g. natural rubber at elongations higher than c.a. 200%, undergo strain induced crystallization (SIC) [119], [120], [121], [122], [123] and [124], because they have a regular chain structure and, due to entropic effects linked to chain orientation, their melting point tends to become higher than the test temperature. Crystallization at the crack tip increases the crack propagation energy significantly. In other words, SIC improves the fracture strength substantially [119]. The technological interest of SIC has resulted in a large number of studies which were recently reviewed by Huneau [124] who concluded that there is an optimum crosslink density of the order of 0.13 mol/kg to obtain the highest SIC effect. At low crosslink densities, crosslinks favour chain orientation upon tensile loading because they prevent loss of orientation by chain relaxation. At high crosslink density, crosslinks appear as defects limiting crystallinity.

For the family of unsaturated elastomers, oxidative crosslinking is often the major mode of atmospheric thermal ageing because in these polymers, macro-radical addition to double bonds is an important propagation process for radical oxidation. Indeed, intermolecular addition, responsible for crosslinking, coexists with intramolecular addition, responsible for cycle formation and also with other processes such as chain scission, but in several cases, among which the polychloroprene (CR) and polyurethane (PU) studied here, crosslinking predominates. It seemed to us interesting to study its consequences on fracture behaviour; this can bring valuable data, both in the domain of structure–property relationships and in the domain of rubber ageing.

The fracture properties of elastomers have already been studied from this point of view [28], [72], [54], [125], [126], [127] and [128], including studies on polychloroprene [72] and [54], but unfortunately the measurements were made on thick samples. In these cases oxidation is diffusion controlled [62] in such a way that an aged sample tends to adopt a sandwich structure with an undegraded core and two degraded superficial layers. Indeed, the change in fracture properties of such samples is not easy to interpret. For this reason it seemed to us interesting to study the effect of oxidative ageing on thin sam-

ples either undergoing crosslinking or not, and either displaying SIC or not. For the interpretation of oxidation mechanisms and kinetics, we used classical theories [44] [43] but powerful numerical tools are available for the resolution of kinetic schemes [100].

In this study three types of model rubbers have been used, a detailed description of these materials is made in Chapter 2, but let us recall the nature and characteristics of these elastomers (Table 5.1).

Elastomer	Acronym	$M_c$ ( $\text{kg}\cdot\text{mol}^{-1}$ )	$T_g$ °C	Presence of dou- ble bonds	Crystallize when streched
Polychloroprene	CR	5.50	-40	Yes	Yes
Chlorinated Polyethylene	CPE	2.99	-21	No	Yes
Polyurethane	PU	1.77	-63	Yes	No

Table 5.1: Initial characteristics of rubbers used in this study.

## 5.2 Crack propagation experiments

In order to evaluate the effect of oxidation on fracture properties of polychloroprene rubber a new experimental test has to be set up. Because we want to work with homogenously degraded samples, these have to be thin, in order to avoid DLO. Also this characterization has to be possible at several temperatures in order to control the strain induced crystallization phenomena. This first part of the chapter is focused on the presentation of the methodology used to measure fracture properties in rubber.

### 5.2.1 Description of the experiments

#### 5.2.1.1 Machine

The machine used to measure  $G_{IC}$  on thin films was a Metravib DMA 150 N, but in order to increase the load sensitivity of the testing device, a 2 N load cell (XF3TC300) from Measurement Specialists has been added. Tests were performed inside a transparent oven, in order to record experiments with a high resolution camera (Camera Basler PIA 2400-12GM) (see Figure 5.1). Images from the camera were used to measure the ligament length (L) before testing, and fracture energy was measured from the load/displacement curve. The following expression was used to determine  $G_{IC}$ :

$$G_{IC} = \frac{\int P dU}{t \cdot L} \quad (5.3)$$

where P is the load in Newtons, U is displacement in m, t is sample thickness in m and L distance between the two notches in m.

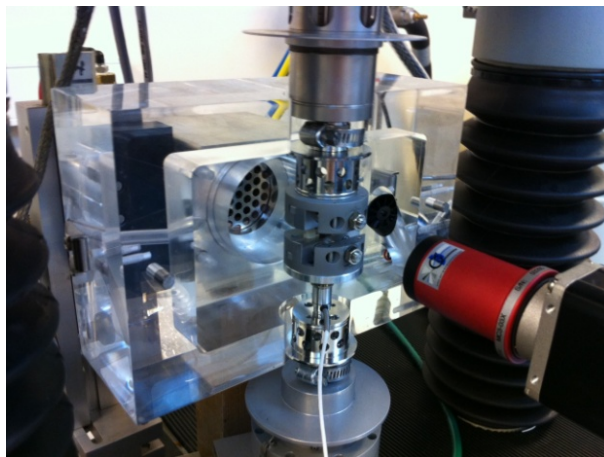


Figure 5.1: Experimental set-up used to characterize fracture properties of rubbers in this study.

### 5.2.1.2 Sample geometry

The samples used here were double notched as shown in Figure 5.2. Sample dimensions were defined as a function of machine limitations, sample preparation and mechanical considerations for the test. In fact in order to avoid any transition between plane stress and plane strain the ligament length, i.e. the distance between the two cracks was defined according to the EWF rules [129] [130]. Typical sample dimensions in this study are:  $H = 10\text{mm}$ ,  $w = 5\text{mm}$ ,  $L = 1\text{mm}$  and  $e = 0.2\text{mm}$ .

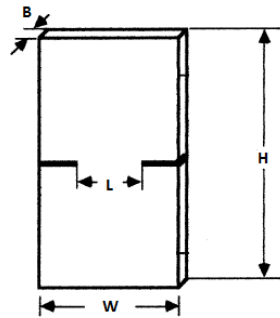


Figure 5.2: Schematic representation of DENT sample used in this study.

## 5.2.2 Influence of experimental parameters

In a preliminary study the influence of several experimental parameters was characterized in order to evaluate their influence on the measured fracture energy.

### 5.2.2.1 Influence of ligament length

When considering the energy to propagate an existing crack in a polymer, the ligament length (distance between the two crack tips) is a very important parameter due to the formation of a plastic zone close to the crack tip. Because of this ligament length dependence a methodology called Essential Work of Fracture has been developed, in order to separate the essential work of fracture that is dissipated in the process zone and which does not depend on ligament length, from the non-essential work of fracture that is dissipated in the plastic zone and which depends on ligament length. Here, the effect of ligament length has been tested with CR at both  $25^\circ\text{C}$  and  $100^\circ\text{C}$ , results are plotted in Figure 5.3 and it appears that for these testing conditions there is no large effect of the ligament length on the measured  $G_{IC}$  value meaning that testing could be performed at one  $L$  value only.

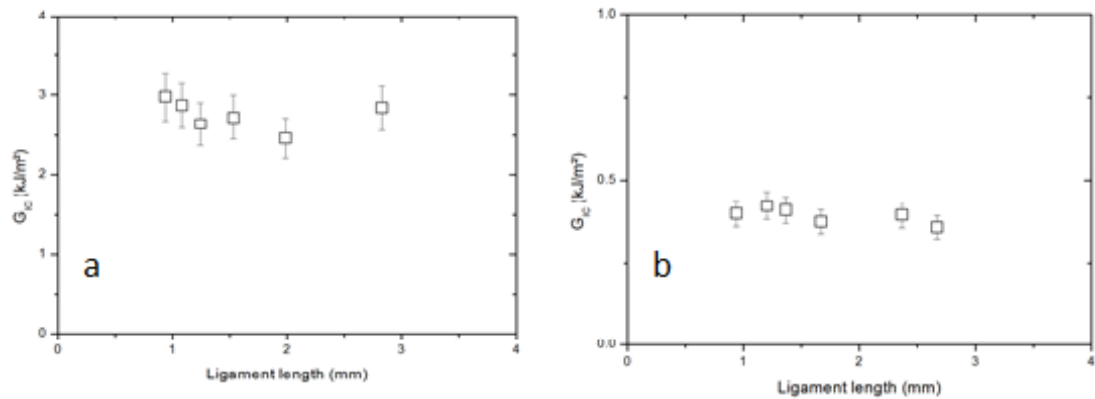


Figure 5.3: Ligament length effect on  $G_{IC}$  values at 25°C (a) and 100°C (b).

### 5.2.2.2 Effect of sample thickness

Usually fracture properties of rubber are measured with 2 mm thick samples, however due to the DLO effect it is not possible use such thick materials if we want to have a homogeneous oxidation through the thickness, which raises the question of possible sample thickness effects. Figure 5.4 shows the effect of sample thickness on the  $G_{IC}$  measurement in the range of 100 to 500  $\mu\text{m}$ , no significant effect is observed. It should be noted that it was not possible to increase the thickness further to limit edge effects.

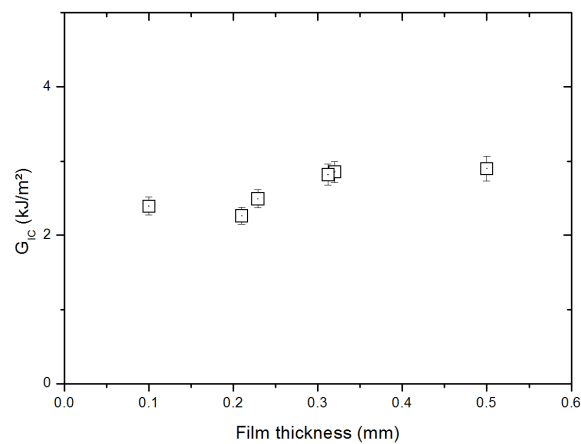


Figure 5.4: Effect of sample thickness on  $G_{IC}$  measurement with virgin CR.

### 5.2.2.3 Temperature effect

The temperature effect on the fracture energy in CR has also been considered, because this rubber undergoes strain induced crystallization (SIC) and it is known that crystallites can melt when the temperature is increased. Figure 5.5 shows the effect of testing temperature on fracture energy in polychloroprene rubber, it appears that  $G_{IC}$  decreases almost exponentially from 2.8 kJ/m<sup>2</sup> at 25°C to 0.9 kJ/m<sup>2</sup> at 100°C, due to the fact that SIC does not occur at high temperature [124]. In this study the testing temperature will be used to characterize the contribution of the crystallization to the fracture energy.

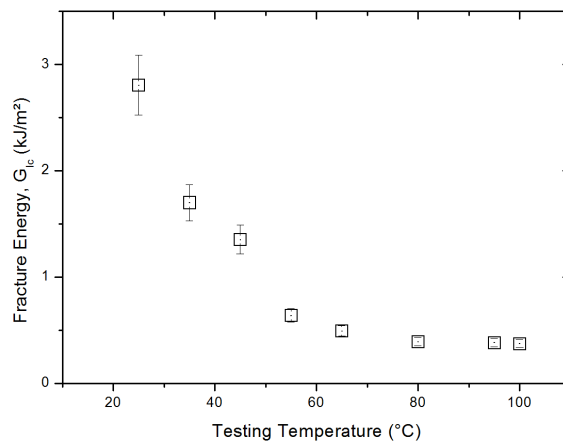


Figure 5.5: Evolution of fracture energy of unaged CR with testing temperature.

#### 5.2.2.4 Influence of strain rate

Because rubber visco-elasticity is involved in the fracture energy measurement it is necessary to evaluate the effect of strain rate on the measurement, in order to choose an appropriate value. Figure 5.6 shows the influence of strain rate on  $G_{IC}$  measurement at both 25°C and 100°C. In both cases a reduction of the strain rate leads to a reduction of the energy, however we observe a plateau only at 100°C. The fact there is no plateau at 25°C is probably because strain rate has a role in both viscous properties of rubber and also in the formation of crystallites. For the rest of this study strain rate was chosen equal to  $6.7 \cdot 10^{-4} \text{ s}^{-1}$ , in order to limit the viscous contribution, but also to keep testing time reasonably short.

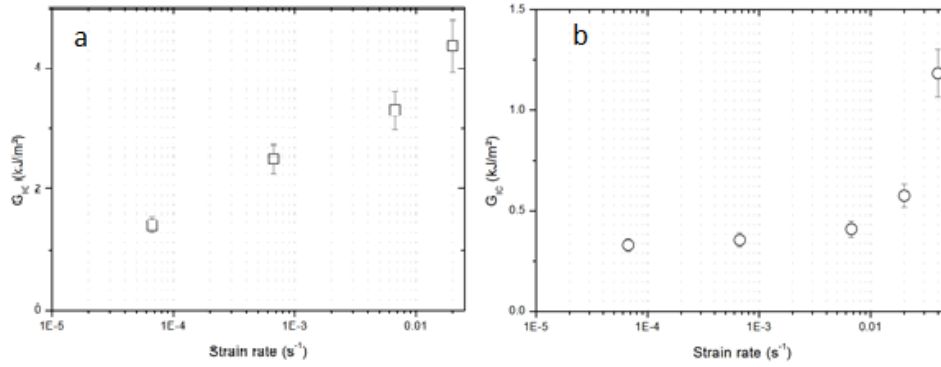


Figure 5.6: Effect of strain rate on  $G_{IC}$  values measured at 25°C (a) and 100°C (b).

Based on the results shown above, a new methodology of  $G_{IC}$  measurement in rubber has been set up in order to be able to characterize the effect of oxidation on the fracture energy in rubbers, and more particularly in polychloroprene rubber. Testing conditions have been determined based on an experimental study of the influence of the sample thickness, temperature, strain rate and ligament length. For the rest of this study,  $G_{IC}$  measurements were performed with a strain rate of  $6.7 \cdot 10^{-4} \text{ s}^{-1}$ , on  $200 \mu\text{m}$  thick samples with a length of 10 mm and a width of 5 mm. They were notched on each side using a new razor blade, distance between the two notches (ligament length,  $L$ ) was about 1 mm. For additional tests performed on CR and CPE, fracture energy was measured at two different temperatures (25 and 100°C) in order to evaluate the contribution of strain induced crystallization (which does not occur at 100°C) to the  $G_{IC}$  measurement. A typical standard deviation of 10% of the mean fracture value was observed for each measurement, this standard deviation was determined at three different ageing stages by performing the same experiment on different specimens.

## 5.3 Results

### 5.3.1 Fracture properties from tensile test

This section is devoted to the evolution of elongation at break measured in unidirectional tensile tests on dumbbell specimens. Tensile results are plotted as a function of oxidation in Figure 5.7. Here again a large increase of the modulus is observed attributed to crosslinking during oxidation, this behaviour is mainly induced by the presence of the double bonds in the rubber as discussed in previous chapters.

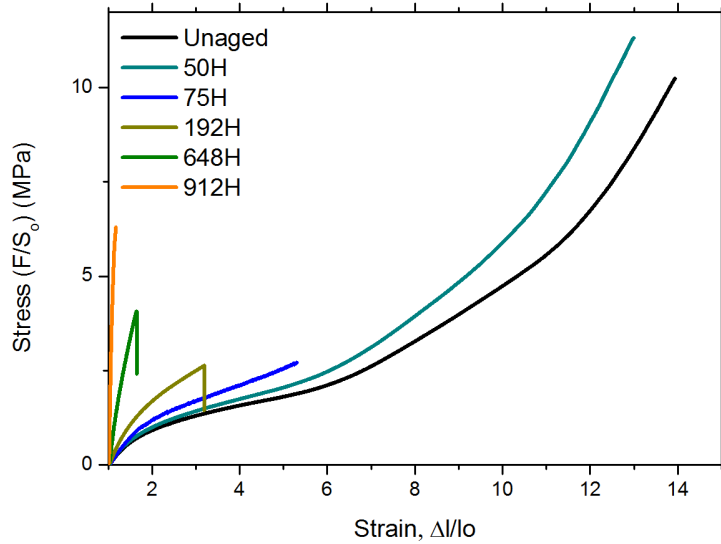


Figure 5.7: Change in tensile behaviour during CR oxidation at 100°C.

Considering now elongation at break, a large decrease is observed. In fact the ultimate stretching ratio  $\lambda_{break}$  and the strain energy density at rupture  $W_r$  i.e. the area under the tensile curve, have been plotted against exposure time in Figure 5.8. After a short (about 50 h) “induction period”, the ultimate strain and the strain energy density at rupture drop off abruptly by about one order of magnitude. This change can be attributed to the disappearance of the portion of the tensile curve (Figure 5.7) having a positive curvature, which was attributed to the hardening effect of SIC. After this period, the ultimate properties continue to decrease, first slowly, but with a slight tendency to accelerate at long term. Because elongation at break measured with dumbbell samples is sensitive to sample preparation it is more a sample characteristic than a material characteristic, this limitation can be overcome by considering fracture energy with notched samples.

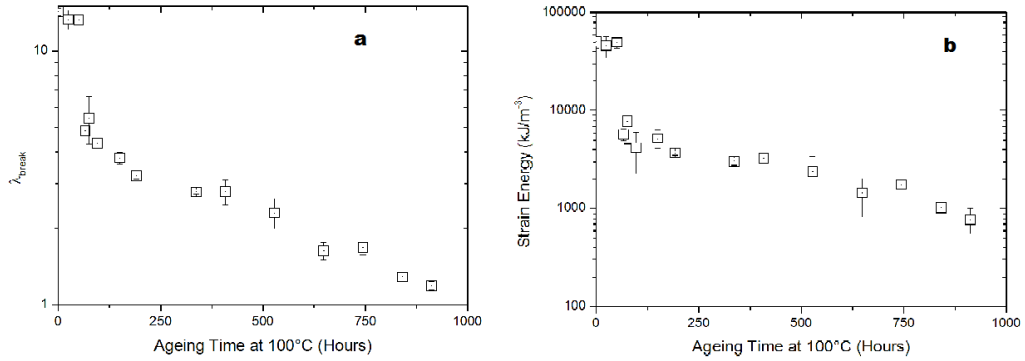


Figure 5.8: Evolution of fracture properties (elongation at break and strain energy) obtained in tensile tests during oxidation at 100°C.

### 5.3.2 Fracture properties of CR from crack propagation characteristics

Both values of  $G_{IC}$  measured at 25°C and 100°C on CR samples have been plotted against exposure time at 100°C in Figure 5.9. These figures allow at least three periods to be distinguished: period I 0 to 200 h; period II 200 to 600–700 h; period III > 600–700 h.

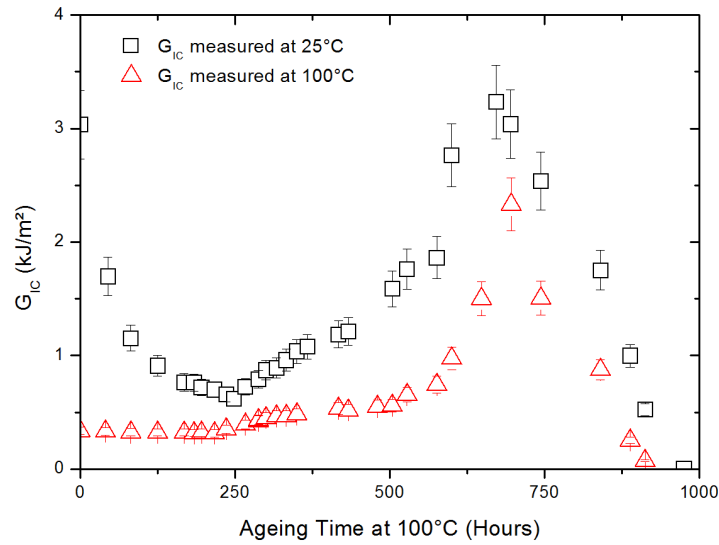


Figure 5.9:  $G_{IC}$  evolution during CR oxidation at 100°C.

The period I, during which  $G_{IC_{25^\circ C}}$  decreases almost exponentially, closely corresponds to the period of fast decay of ultimate tensile properties with however one difference: No “induction period” is observed here. In the same period, no significant variation was observed for  $G_{IC_{100^\circ C}}$ .

During the period II, both  $G_{IC_{25^{\circ}C}}$  and  $G_{IC_{100^{\circ}C}}$  increase up to a maximum after 600–700 h of exposure.

During the period III, both  $G_{IC_{25^{\circ}C}}$  and  $G_{IC_{100^{\circ}C}}$  decay rapidly to reach values lower than 0.1 kJ/mol after 900 h of exposure.

The same behaviour can be observed on samples exposed at 120°C or 140°C (Figure 5.10). A typical Arrhenius behaviour can be used to build a master curve of  $G_{IC}$  evolution independent of ageing temperature (in the 100–140°C range – Figure 5.10). This approach cannot be used to make reliable life time prediction for lower temperatures because of a possible non Arrhenian behaviour for lower temperature but is still interesting to highlight the fact that ageing temperature does not change the trend but only the kinetics.

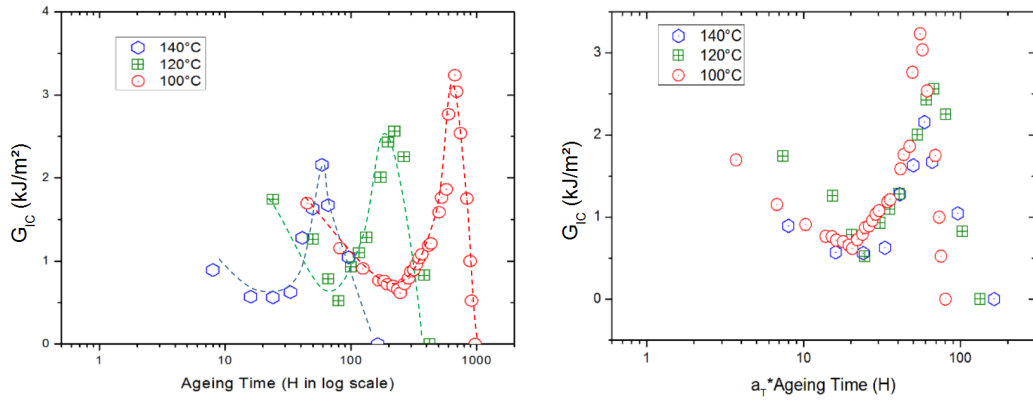


Figure 5.10: Effect of ageing temperature on  $G_{IC}$  evolution measured at 25°C during CR oxidation (a) Raw data, (b) Shifted plots.

From these measurements it appears that the change in  $G_{IC}$  during polychloroprene oxidation is not simple and has to be examined more closely. Therefore, oxidation effects on fracture properties of two other model elastomers have been considered.

### 5.3.3 Comparison of CR with other elastomers

Some elements of comparison of CR with chlorinated polyethylene (CPE) and isocyanate cured polybutadiene (PU) are summarized in Figure 5.11: Figure 5.11-a shows the modulus changes during exposure at 120°C. It can be seen that both unsaturated polymers, CR and PU undergo crosslinking whereas CPE, in which there is an initial modulus decrease, undergoes first predominant chain scission. Toughness changes are displayed in Figure 5.11-b for CR, Figure 5.11-c for CPE and Figure 5.11-d for PU.

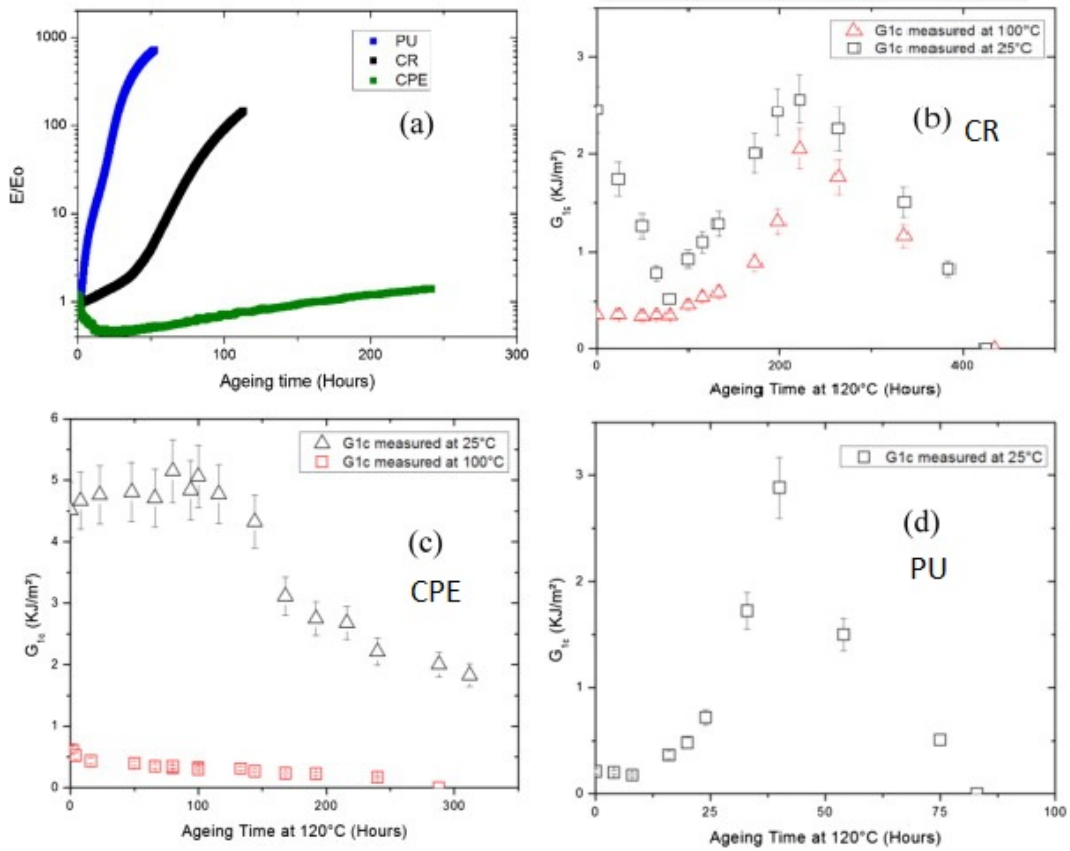


Figure 5.11: Effect of oxidation on normalized modulus variation for PU, CR and CPE (a) aged at 120°C and modification of  $G_{IC}$  measured at 25 and 100°C during oxidation at 120°C for CR (b), CPE (c), PU (d).

The following comments may be made:

- In CPE, the strong difference between  $G_{IC}$  values at 25°C and 100°C indicates, the existence of SIC. The SIC effect does not disappear: it remains almost constant during an early period of exposure of about 120 h and then decreases but remains active, even after 300 h at 120°C. It can be recalled that CPE does not undergo predominant crosslinking.

- PU ( $G_{IC}$  at 25°C) behaves as CR ( $G_{Ic}$  at 100°C):  $G_{IC}$  increases rapidly during the early period of exposure, reaches a maximum after about 40 h at 120°C and then decreases rapidly. It should be recalled that CR and PU have in common that both can undergo large crosslinking.

In this experimental section, the oxidation effect on the fracture energy of CR during oxidation has been characterized and reveals a complex behaviour with a first decrease, then an increase and finally a drop off of  $G_{IC}$  measured at 25°C. In order to understand this unexpected behaviour during CR oxidation, two other elastomers have been considered, results will be discussed in the next part of this chapter.

## 5.4 Discussion

It is clear that CR and PU undergo predominant crosslinking, as shown by modulus changes (Figure 5.11-a). In these rubbers, oxidation induced changes can be tentatively used to appreciate the effect of crosslinking on fracture properties. In the case of CPE, the initial modulus decrease indicates a decrease of crosslink density presumably linked to predominant chain scission. A description of the oxidative crosslinking process would involve a relatively complex set of reactions. Crosslinking results predominantly from additions of  $P^\circ$  and  $POO^\circ$  radicals to double bonds but these additions can be either intermolecular or intramolecular and only the former participate in crosslinking as shown in previous chapters.

### 5.4.1 Period I: Decrease in $G_{IC}$

Let us first consider the initial decay of fracture properties (both  $\lambda_b$  and  $G_{IC_{25^\circ C}}$ ) for CR. The comparison with PU shows that it involves SIC and the comparison with CPE shows that it is due to crosslinking. In other words, crosslinking, even at low conversion, would inhibit SIC. This is not surprising, we know that for a linear polymer undergoing crosslinking, gelation occurs for a small number  $x_g$  of crosslinking events [131] and [132]:

$$x_g = \frac{1}{M_{w0}} \quad (5.4)$$

where  $M_{w0}$  is the initial weight average molar mass of the polymer. A small number of crosslinking events are thus required to increase the viscosity considerably and then significantly reduce the crystallization rate, explaining thus the observed behaviour of CR.

### 5.4.2 Period II: Increase in $G_{IC}$

It seemed to us interesting to check a basic result of the simple network theory for period II for which, for affine deformations, in the absence of viscoelasticity, fracture would occur when the chains reach their maximum extension, i.e.:

$$\lambda_{break} = K' \cdot M_c^{1/2} \quad (5.5)$$

Since  $M_c$  can be determined from modulus, we have plotted  $\lambda_b$  against  $M_c^{1/2}$  in Figure 5.12-a. There are several ways of interpreting this figure. According to the simplest one, the following relationship would be obeyed:

$$\lambda_{break} = (2 \pm 0.4) \cdot M_c^{1/2} \quad (5.6)$$

However, the plot displays a positive curvature which could be linked to a specificity of the crosslinking process and can be explained as follows: random crosslinking creates a new population of chains shorter than initial ones. It is interesting to compare this trend with the one of model networks having a bimodal distribution of chain lengths [78] and [114] (Figure 5.12-a). In this latter case, it can be seen that the long chains control the ultimate elongation, even at relatively high concentrations of short chains so that  $\lambda_{break}$  appears almost independent of  $M_c$  over a large interval of  $M_c$  values. One can consider that crosslinking creates a new population of short chains (of average length half of that of the initial ones), but the behaviour differs from the preceding one since  $\lambda_{break}$  decreases at low conversions of the crosslinking process (Figure 5.12). A possible explanation is that if crosslinking is a random process, it must preferentially affect the longer chains. Thus, if these chains controlled the ultimate elongation, the latter would be expected to decrease as soon as crosslinking begins.

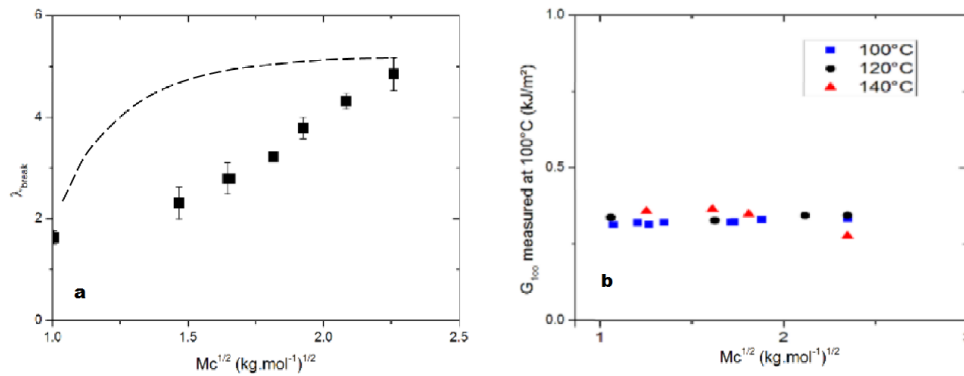


Figure 5.12: Elongation at break during oxidation at 100°C (a) dashed curves represent evolution with bimodal chain lengths (see text) and  $G_{IC_0}$  (b) as a function of  $M_c^{1/2}$  in CR.

To appreciate the effect of crosslinking on fracture properties, it is convenient to determine these latter at high temperature, for instance 100 °C, in order to eliminate SIC effects.

The relatively fast toughness increase for CR at 100°C and PU at 25°C (absent for CPE) indicates that crosslinking plays a favourable role in fracture, in contradiction with many published works according to which rubber toughness is mainly linked to chain extensibility so that:

$$G_{IC} = K'' \cdot M_c^{1/2} \quad (5.7)$$

Here,  $G_{IC}$  increases rapidly when  $M_c$  decreases as a result of oxidative crosslinking, for CR (Figure 5.11-b) and PU (Figure 5.11-c).

It can be noted that, in the case of Llorente's model for bimodal networks [114], the strain energy density at rupture in tension  $W_r$  is also a decreasing function of  $M_c$ . Assuming that  $W_r$  and  $G_{IC}$  are closely related, we reach the following conclusion: oxidative crosslinking, due to its bimodal character, does not affect (at low conversions) ultimate elongations but induces an increase of stresses as expected from the theory of rubber elasticity. The existence of a compromise between stiffness and strength in certain rubbers has been recently reported by Roland [133]. As a result, the fracture energy increases with the crosslink density where it would decrease in the case of networks with unimodal distributions of chain lengths.

### 5.4.3 Period III: Drop off in $G_{IC}$

The last period, common to all materials undergoing crosslinking and at all testing temperatures, where the samples undergo a steep, irreversible, and fast embrittlement remains to be explained. In CPE, embrittlement is also observed but it is more progressive. In CR and PU, crosslinking is no doubt the primary cause of the final toughness decay. An explanation can be envisaged. It is once again offered by Llorente's results on bimodal networks [78] and [114]. One sees in these results that when the fraction of short chains increases, the strain energy density at rupture first increases, as previously quoted, but beyond a certain concentration, the ultimate elongation becomes controlled by the short chains, and the fracture energy begins to decrease. The maximum of  $G_{IC}$  could then correspond to the point where short chains created by the oxidative crosslinking process, begin to take control of ultimate elongation. The various changes in fracture behaviour are summarized in Table 4.2. In the meantime the final drop could be related to the very low mobility in highly cross-linked materials.

Rubber	Testing temperature (°C)	Step I: sense of variation of $G_{IC}$	Step I : mechanism	Step II: sense of variation of $G_{IC}$	Step II mechanism	II
CR	25	↘	SIC inhibition by oxidative crosslinking	↗	Oxidative crosslinking	
CR	100	none	No SIC	↗	Oxidative crosslinking	
PU	25	none	No SIC	↗	Oxidative crosslinking	
CPE	25	none	No crosslinking	↘	No crosslinking	
CPE	100	none	No crosslinking	↘	No crosslinking	

Table 5.2: Summary of the observed changes in fracture properties and their explanation.

#### 5.4.4 Life time prediction

Although fracture energy changes in CR during oxidation are not in accordance with the theory developed in the literature, a life time prediction is still possible. This life time prediction of fracture could be performed considering an arbitrary end of life of  $G_{IC_{25}}$  less than  $1 \text{ kJ/m}^2$  i.e. 3 times lower than the initial value. For the three tested temperatures (140, 120 and  $100^\circ\text{C}$ ), the crosslink density when  $G_{IC_{25}}$  is less than  $1 \text{ kJ/m}^2$  is about  $0.3 \text{ mol/kg}$ . This means that it is possible to define a critical value for the crosslink density that corresponds to the end of life criterion. Because the model can predict the crosslink density in the rubber as a function of oxidation and there exists a critical value for this crosslink density, it is thus possible to propose for the first time a non-empirical life time prediction based on crack propagation in rubber.

## 5.5 Conclusion

We have investigated the fracture properties of three rubbers chosen in order to distinguish between the effects of strain induced crystallization and crosslinking on fracture behaviour, this latter being examined both by tensile testing and crack propagation studies, at 25°C and 100°C.

The evolution of fracture properties reveals the existence of three consecutive steps of which the last is always a steep embrittlement. The most important phenomenon is SIC because it ensures, initially, a high toughness, with  $G_{IC}$  values of the order of several  $\text{kJ/m}^2$  against a few hundred  $\text{J/m}^2$  in the absence of SIC. However, SIC is inhibited by oxidative crosslinking so that its reinforcing effect disappears rapidly in the early period of exposure.  $G_{IC}$  decreases by a factor of about 10 so that, at the end of this step, most users would consider that the material has reached the end of its life. Therefore, the first practical conclusion of this study is that the best rubbers, from this point of view, are those which, like CPE, undergo SIC but do not crosslink during their oxidative ageing.

There is however a second step during which, in unsaturated rubbers such as CR and PU, the toughness increases as a result of crosslinking while, according to the basic network theory, it would be expected to decrease. It has been proposed here that this peculiar behaviour is linked to the bimodal character of networks resulting from oxidative crosslinking.

This bimodal character is also presumably the cause of the fast final catastrophic embrittlement.

From this study it appears that fracture property changes during oxidation are complex in rubber, especially when SIC is involved. However considering an arbitrary end of life criteria ( $G_{IC_{25}} < 3G_{IC_{25_{initial}}}$ ), it is possible to define a critical value for the crosslink density. This critical value could be used to make a life time prediction using the kinetic model developed here.



## Chapter 6

# Long term behaviour of polychloroprene in sea water

This last chapter is devoted to the behaviour of polychloroprene when immersed in sea water. The initial idea was to generate data during accelerated ageing in heated sea water for a fully formulated CR with the aim to adapt the oxidation model developed in air to the marine environment. This adaptation would need to take into account eventual coupling mechanisms between water absorption and oxidation, such as stabilization leaching. However first results during ageing revealed that this CR undergoes a large water absorption, that leads to a significant reduction in mechanical properties. Due to this unexpected behaviour a specific study on water absorption in CR has been performed.

In the first part of this chapter, results obtained during accelerated ageing in heated sea water with a fully formulated CR will be presented. Then in the second part, we will focus on polymer-water interaction mechanism in polychloroprene rubber, i.e. formation of water clusters induced by the presence of water. A brief reminder of existing knowledge on this subject will be presented first, then experimental results will be discussed leading to a proposal for a new way to predict water absorption in rubbers.

## 6.1 Accelerated ageing of fully formulated CR in sea water

Fully formulated polychloroprene (i.e. with stabilizers and reinforcing fillers see Chapter 2 for details) samples were immersed in sea water at different temperatures in order to generate the data needed to adapt the existing oxidation model for air to the marine environment. Unexpectedly the rubber absorbed a large amount of water, for example at 60°C for 2 mm thick samples, the water absorption after almost 3 years was about 60% (Figure 6.1). Moreover it appears that water uptake depends on sample thickness (even when immersion time is normalized according to the Fickian mechanism) meaning that the water absorption kinetics are more complex than Fickian behaviour. This large water absorption in the rubber leads to a swelling of the material that generates cracks on the sample surface (as shown in Figure 6.2).

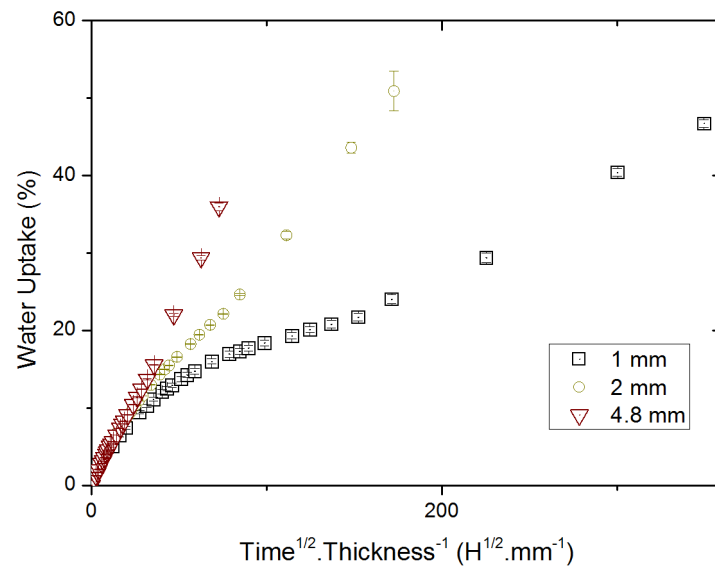


Figure 6.1: Water absorption in a fully formulated polychloroprene rubber immersed in natural sea water at 60°C.



Figure 6.2: Crack formation on polychloroprene surface after 6 months at 80°C in sea water.

In order to evaluate the influence of damage induced by the presence of such a large amount of water, uniaxial tensile properties were measured as a function of ageing time. Results are plotted in Figure 6.3, the stress is calculated using the section of wet sample. A decrease of elongation at break is observed as immersion time increases whereas no large modulus variation occurs. This behaviour is not reversible, if samples are dried the tensile properties are still degraded although no modifications induced by oxidation have been detected by FTIR.

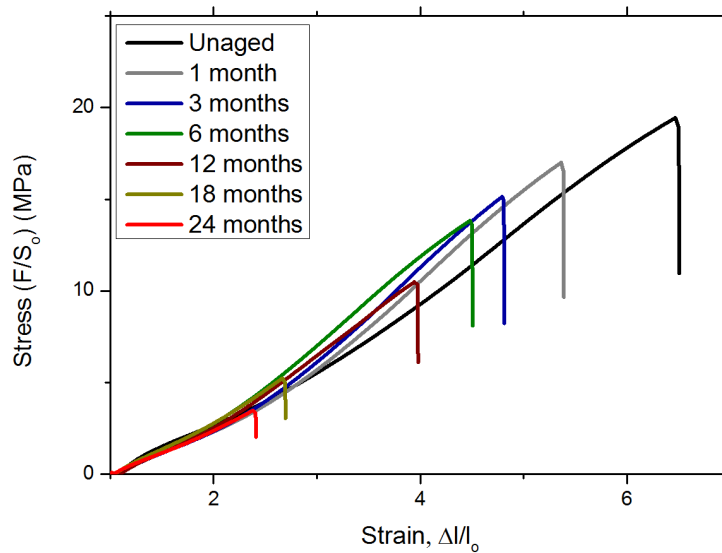


Figure 6.3: Change in tensile behaviour of 2mm thick polychloroprene samples as a function of ageing time in sea water at 60°C.

Instead of studying this water absorption effect on mechanical properties further, it was then decided to work with a rubber with a much simpler formulation in order to focus on the origin the phenomenon. The next section will describe water clustering in polychloroprene with a brief reminder of existing knowledge, then a description and discussion of experimental results.

## 6.2 Water clustering in polymers: a literature review

Elastomers are generally polymers of low polarity, a condition to have a low cohesive energy density and thus a low glass transition temperature. Since water interacts with polymers through hydrogen bonds with polar groups it is expected to have a relatively low solubility in elastomers as is generally observed. But low solubility is not necessarily synonymous with a simple dissolution mechanism. It was observed 50 years ago that in many elastomers, the equilibrium water volume fraction,  $u$ , varies non-linearly with water activity,  $a$ , while the water diffusivity appears as a decreasing function of  $a$  [134]. Both characteristics are generally attributed to clustering [135], [136], [137] and [138]. As will be shown, this term covers a variety of processes having in common the fact that a part of the water molecules establishes preferentially bonds with previously solvated water molecules rather than with polar sites of the polymer.

The most trivial cause of clustering is the presence of pores in the elastomer matrix. When these pores are small enough, water condenses in the pores at water activities lower than unity owing to confinement effects and the sorption isotherm displays a positive curvature in the domain of high activities. Adsorption at the pore surface can have the same consequences as condensation. In the case under study, porosity can be considered negligible; water is first dissolved into the superficial layer of the elastomer but tends to adopt an inhomogeneous spatial distribution characterized by the existence of water-water bonds when, at the concentrations under consideration, each water molecule would be isolated from all the others in the case of an homogenous distribution.

One can envisage at least two mechanisms of clustering in non-porous polymers. The first one involves the presence of an extrinsic driving force, for instance a thermal shock inducing a sudden decrease of the water solubility in the polymer or the release of small hydrophilic organic molecules resulting for instance from matrix degradation. In such cases, a de-mixing process occurs; liquid micro-pockets are formed, creating a situation favorable for the propagation of an osmotic cracking process. Blistering of composite boat hulls, for instance, results from polyester hydrolysis [139] and [140].

The second mechanism does not need the existence of a driving force, clustering can be schematically explained by the fact that water molecules have more affinity for themselves than for polymer sites. Here, clusters can be chains or networks [141] and [142] of hydrogen bonded water molecules rather than quasi-spherical aggregates and it is not unreasonable to imagine relatively large clusters not phase separated from the polymer matrix contrary to quasi-spherical clusters.

The present study deals with water absorption mechanisms of vulcanized chloroprene in the 25–80°C temperature range. Long term aging experiments at constant temperature and hygrometric ratio will be combined with short

term measurements in order to record sorption isotherms. Particular attention will be paid to clustering processes using a vulcanized polychloroprene without MgO (see Chapter 2 for details), because MgO is known to be an initiator of the osmotic process [13].

### 6.3 Results and discussion

The curves of mass gain against exposure time at constant temperature and hygrometry (CTH) are presented in Figure 6.4 for samples of 1.8 mm thickness and in Figure 6.5 for samples of 3.8 mm thickness. Immersion in sea water is considered, here, as pure water with an activity of 0.98 according to Robinson [79]. These curves display a negative curvature in their initial part and a quasi-linear asymptote of which the slope is an increasing function of temperature and seems almost independent of sample thickness. The asymptotic rate values  $r_s = \frac{1}{m_0} \cdot \left(\frac{dm}{dt}\right)_\infty$  are listed in Table 6.1. An Arrhenius plot of  $r_s$  values for both sample thicknesses is given in Figure 6.6. At first sight, these plots appear non-linear, that would indicate the coexistence of at least two mechanisms. Indeed, the number of points is very small but the close similarity of both curves does not result from a coincidence and suggests that effectively, an Arrhenius law is not obeyed here.

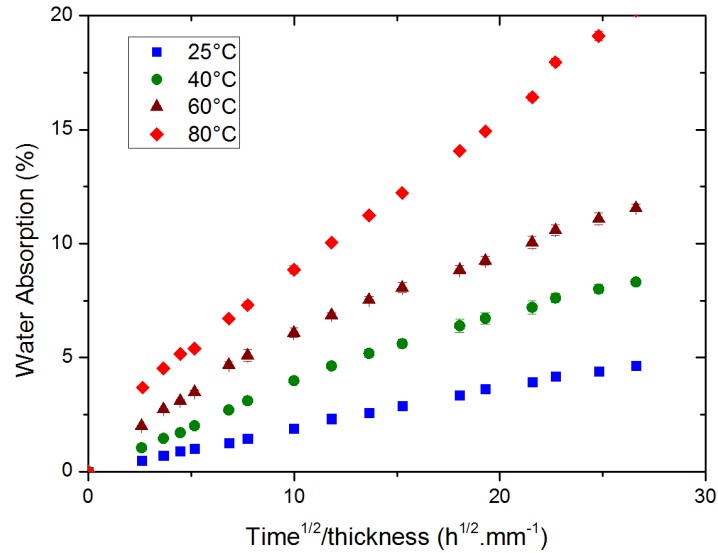


Figure 6.4: Water absorption in 1.8 mm thick sample of CR at different temperatures.

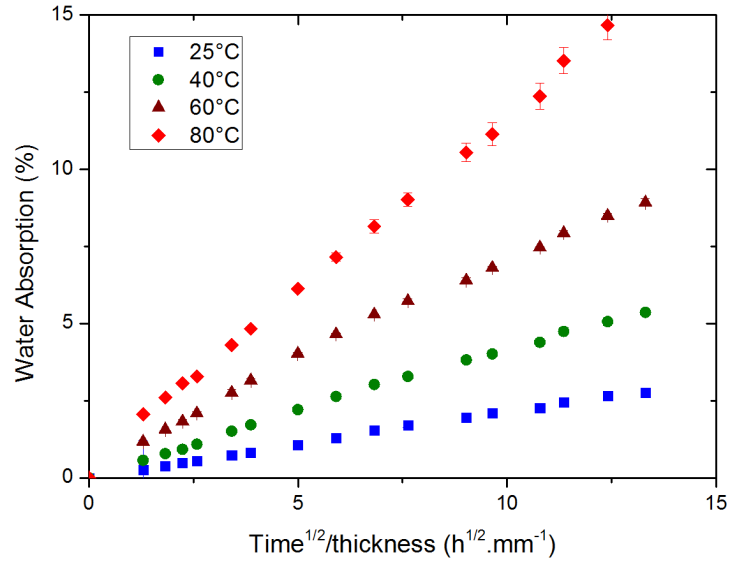


Figure 6.5: Water absorption in 3.8 mm thick sample of CR at different temperatures.

Sample thickness (mm)	Temperature (°C)	$r_s \cdot 10^9$ ( $s^{-1}$ )	$b \cdot 10^2$	$B \cdot L$ (mm)	$v_0 \cdot 10^8$ ( $m \cdot s^{-1/2}$ )	$D \cdot 10^{13}$ ( $m^2 \cdot s^{-1}$ )
1.8	25	$2.26 \pm 0.04$	$2.67 \pm 0.17$	$5.07 \pm 0.32$	$3.23 \pm 0.17$	$2.9 \pm 0.7$
1.8	40	$3.56 \pm 0.33$	$5.23 \pm 0.44$	$9.94 \pm 0.83$	$6.77 \pm 0.44$	$3.3 \pm 0.1$
1.8	60	$3.70 \pm 0.35$	$8.13 \pm 0.47$	$15.45 \pm 0.89$	$13.00 \pm 0.19$	$5.0 \pm 0.1$
1.8	80	$8.80 \pm 0.08$	$12.07 \pm 0.53$	$22.93 \pm 1.01$	$23.83 \pm 0.50$	$7.7 \pm 0.1$
3.8	25	$1.46 \pm 0.31$	$1.47 \pm 0.05$	$5.58 \pm 0.19$	$3.48 \pm 0.09$	$11.0 \pm 1.3$
3.8	40	$2.97 \pm 0.16$	$2.74 \pm 0.15$	$10.41 \pm 0.57$	$7.41 \pm 0.08$	$14.4 \pm 1.8$
3.8	60	$3.79 \pm 0.21$	$5.46 \pm 0.08$	$20.75 \pm 0.30$	$15.20 \pm 0.07$	$15.2 \pm 0.6$
3.8	80	$8.37 \pm 0.05$	$7.95 \pm 0.11$	$30.21 \pm 0.41$	$26.70 \pm 0.54$	$22.1 \pm 1.5$

Table 6.1: Kinetic parameters of water absorption (see text) in CTH experiments.

The initial parts of the curves call for the following comments: At the lowest temperatures, 25°C and 40°C, mass gain increases proportionally to the square root of time in the first days of exposure. At the highest temperatures 60°C and 80°C, mass gain is proportional to a power of time ranging between 0.5 and 1.0. It can be reasonably supposed that here also, there is an initial period where mass gain is proportional to the square root of time but this period is shorter than 24 h. What is observed here is essentially the transition between the regime characterized by an exponent value of 0.5 and the “steady

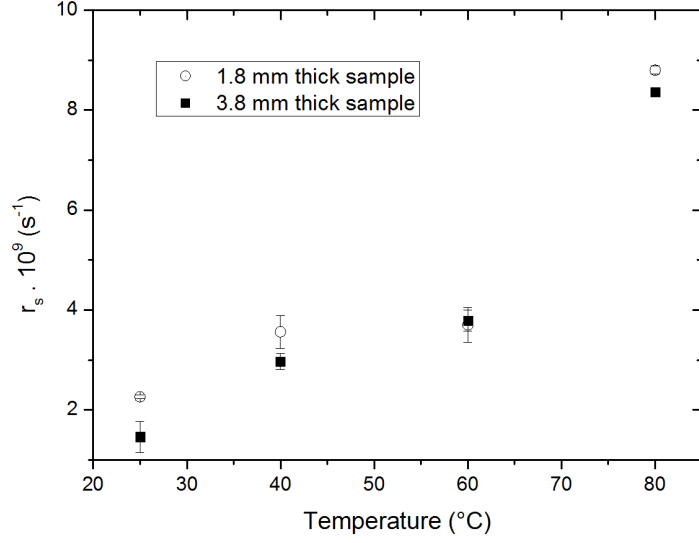


Figure 6.6: Temperature dependence of  $r_s$  (values are given in Table 6.1).

state” regime characterized by an exponent of unity. We have determined a pseudo-initial slope  $v_{24h} = \frac{1}{m_0} \cdot \frac{\Delta m_{24h}}{L \cdot (24 \cdot 3600)^{1/2}}$  where  $L$  is sample thickness. In the case of the lowest temperatures (25°C and 40°C),  $v_{24h}$  is effectively the initial slope  $v_0$ . In the case of the highest temperatures (60°C and 80°C), it can be supposed that  $v_0 > v_{24h}$  but the difference is presumably small and one can consider, in a first approach, that  $v_{24h}$  is effectively the initial slope. Contrary to  $r_s$ ,  $v_0$  varies significantly with the sample thickness (Table 6.1), but the product  $V_0 = L \times v_0$  is almost independent of the thickness  $L$ . It can be recalled that, in the context of a Fickian diffusion process,  $V_0$  is an important component of the expression of the diffusion coefficient

$$D = \frac{\pi}{16} \cdot \frac{V_0^2}{\left(\frac{\Delta m_\infty}{m_0}\right)^2} \quad (6.1)$$

The kinetic curves of mass gain can thus be considered as resulting from two processes: a (relatively fast) pseudo-fickian sorption process characterized by a virtual equilibrium mass gain  $\Delta m_\infty$  (see below) and a (relatively slow) unknown process of apparent zero order, occurring at the same rate in all the sample layers. Let us first consider the equation of the linear asymptote:

$$\frac{\Delta m}{m_0} = r_s \cdot t + b \quad (6.2)$$

The values of  $b$  are listed in Table 6.1. This intercept value can be interpreted, at least in a first approach, as the (virtual) equilibrium value for the initial fickian process

$$b = \frac{\Delta m_\infty}{m_0} \quad (6.3)$$

From the values of  $V_0$  and  $b$ , it is possible to determine the value of the coefficient of diffusion  $D$  using equation 6.1 (Table 6.1).  $D$  appears to be about three times higher for the sample of 3.8 mm thickness than for the sample of 1.8 mm. This is exclusively due to the difference in  $b$  values, which increase almost linearly with temperature :

$$b = \frac{\Delta m_\infty}{m_0} \sim A \cdot (T - 13) \quad (6.4)$$

where  $A \sim 2.0 \cdot 10^{-1} \text{ K}^{-1}$  for samples of 1.8 mm and  $1.1 \cdot 10^{-3} \text{ K}^{-1}$  for samples of 3.8 mm. As will be seen below, the physical meaning of this dependence is not obvious. What is sure is that the values of  $\frac{\Delta m_\infty}{m_0}$  do not correspond to the true water solubility in polychloroprene, the latter being considerably lower.

In order to provide more information on this abnormal sorption process, we have first performed cyclic tests in which the samples were maintained at constant temperature and periodically dried after exposure in humid atmosphere. The results (Figure 6.7) can be summarized as follows: water absorption is fully reversible and there is no significant change of the diffusion coefficient from one cycle to the next. The fact that  $D$  remains constant indicates the absence of irreversible damage resulting for instance from osmotic cracking. If there is a polymer–water phase separation, we are forced to imagine that the water pockets become voids upon drying, these latter would then collapse and heal in such a way that the polymer homogeneity was restored at the end of the drying period. But what could be the driving force of phase separation? Osmotic cracking would need the presence of small polar molecules soluble in water but having diffusivity values significantly lower than that of the water in the polymer. We have imagined that hydrolyzable C–Cl bonds could be present in irregular structures and that the released HCl would induce osmotic cracking. An experiment of sample immersion in a bath of pure boiling water was therefore performed, but no HCl was found in the bath after an exposure time of 200 h, which eliminates the hypothesis of hydrolysis of labile C–Cl bonds.

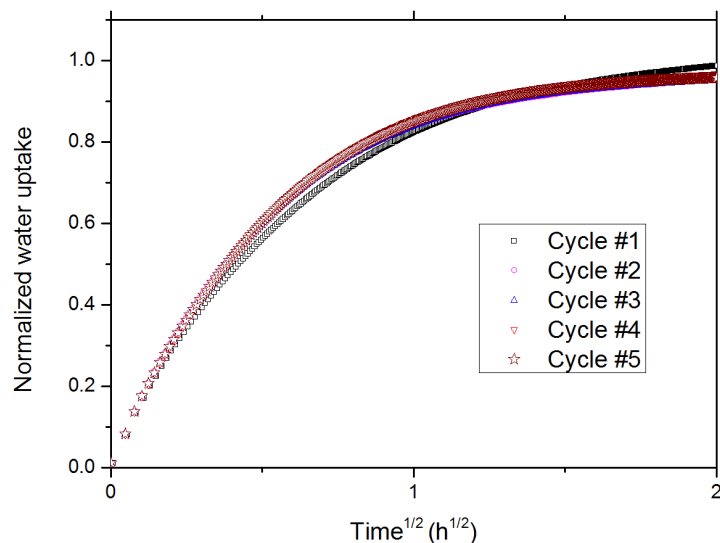


Figure 6.7: Cyclic tests of water absorption in CR.

Polymer hydrolysis could explain the observed behaviour, provided that water molecules are incorporated in the polymer structure without mass loss. It can be noted that mass gain reaches values higher than 20% in 1.8 mm samples and that corresponds to 1 mol of water per mole of monomer unit. The only possible hydrolysis event would be thus the addition of the water molecule to the double bond but that is unlikely, at least in the temperature range under consideration. The hypothesis of hydrolysis to explain the abnormal mass gain must thus also be rejected.

At the end of this set of investigations, it has been shown that the mechanism of water absorption responsible for the continuous mass increase at long term is neither hydrolysis nor osmotic cracking, it is fully reversible and able to incorporate in polychloroprene more than one water molecule per monomer unit. The questions which remain unanswered lead us to investigate sorption mechanisms at the molecular level. The analysis of sorption isotherms could bring interesting information on this aspect; for this reason Dynamic Vapor Sorption (DVS) experiments were performed.

A typical sorption curve is shown in Figure 6.8 and the sorption isotherm obtained at 40°C on a sample of 100  $\mu\text{m}$  thickness is shown in Figure 6.9. The most striking difference between this curve and those of Figure 6.4 and Figure 6.5 is that equilibrium is reached in less than 10 h while it is not reached after more than 2500 h during the experiment at constant temperature and hygrometry (CTH). Within a Fickian diffusion mechanism, the time to reach equilibrium would be proportional to the square of thickness so that equilibrium would be reached in less than  $19^2 = 361$  h for the sample of 1.8 mm and  $38^2 = 1444$  h for the sample of 3.8 mm thickness. It is clear that the effect

of sample thickness on the sorption behaviour cannot be simply derived from Fick's law.

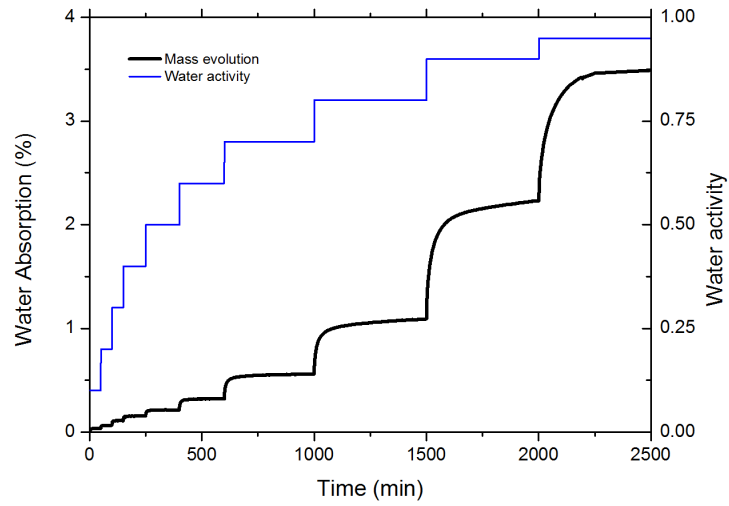


Figure 6.8: Water absorption in 100  $\mu\text{m}$  thick film for several water activities at 40  $^{\circ}\text{C}$ .

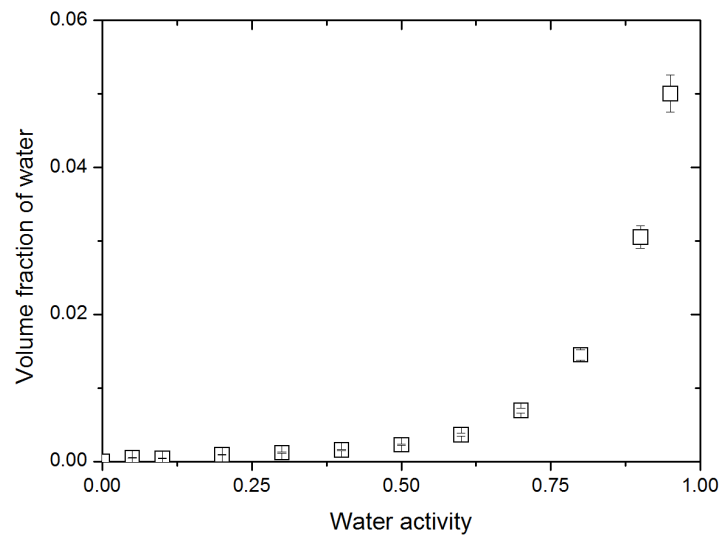


Figure 6.9: Volume fraction of water in 100  $\mu\text{m}$  thick film at 40 $^{\circ}\text{C}$  for different water activities.

The sorption isotherm displays a strong positive curvature in the domain of high activities. There are to our knowledge, two main ways to interpret this behaviour. In the first, the relationship between the water volume fraction,  $u$ , and water activity,  $a$ , would obey the well-known Flory–Huggins equation; in the second, water dissolution would obey Henry’s law and the isotherm curvature would be explained by clustering.

- Let us consider the first hypothesis. By linear regression on the earlier points of the isotherm, one can determine the initial slope  $H$ .

$$H = \left( \frac{\delta u}{\delta a} \right)_{a=0} = 4.6 \cdot 10^{-3} \quad \text{with} \quad (R^2 = 0.956) \quad (6.5)$$

where  $u$  is the volume fraction of water and  $a$  is the water activity. According to the Flory–Huggins equation

$$H = \exp(-(1 + \chi)) \quad (6.6)$$

where  $\chi$  is the polymer–water interaction coefficient. Application of this equation would give  $\chi = 4.38$ . For such a value, the Flory–Huggins isotherm would be almost linear over the whole activity scale and the water volume fraction at saturation would be close to  $4.6 \times 10^{-3}$  compared to the experimental value of  $71 \times 10^{-3}$ . It is thus clear that the isotherm curvature does not correspond to the Flory–Huggins equilibrium.

- Let us now examine the second hypothesis. The isotherm shape can be then analyzed with the Zimm–Lundberg theory [143]. These authors define a clustering function  $f_{ZL}$  defined by

$$f_{ZL} = -(1 - u) \cdot \left( \frac{\delta \left( \frac{a}{u} \right)}{\delta a} \right) - 1 \quad (6.7)$$

Clusters are present when  $f_{ZL} > -1$  and the average cluster size  $l$  is given by  $l = u_{f_{ZL}} + 1$ .

The isotherms can be fitted by the sum of a Henry’s term and a power term representing the cluster contribution, in order to have an analytical representation of isotherms facilitating calculations [144]:

$$u = H \cdot a + B \cdot a^n \quad (6.8)$$

$B$  and  $n$  were determined from experimental results. The regression analysis leads to  $B = 67 \times 10^{-3}$  and  $n = 9.1$  ( $R^2 = 0.999$ ). This relationship

leads to particularly simple expressions of Zimm–Lundberg quantities at saturation ( $u = u_s = H + B$  at  $a = 1$ )

$$f_{ZL_s} = B \cdot (m - 1) \cdot \frac{(1 - u_s)}{u_s^2} \quad \text{and} \quad l_s = (1 - u_s) \cdot \left[ \frac{B \cdot (m - 1)}{u_s} + 1 \right] \quad (6.9)$$

The numerical application leads to  $l_s = 7.1$ .

The coefficient of diffusion  $D$  has been determined and plotted against hygrometric ratio  $HR$  at  $40^\circ\text{C}$  in Figure 6.10.  $D$  is almost independent of  $HR$  between about 10 and 50%  $HR$  and decreases rapidly with  $HR$  above 50%  $HR$ . The  $D$  value at 100%  $HR$  (about  $3 \times 10^{-13} \text{ m}^2 \text{ s}^{-1}$ ) is not very different from the one obtained in the CTH experiment for the sample of 1.8 mm thickness.

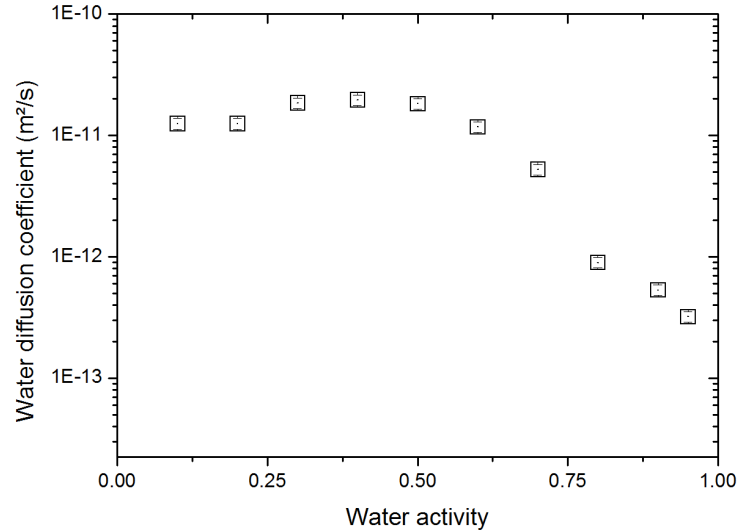
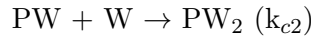
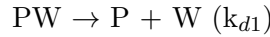
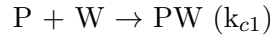


Figure 6.10: Water diffusion coefficient measured at  $40^\circ\text{C}$  on  $100 \mu\text{m}$  thick film for different water activities.

To conclude on DVS results: polychloroprene is characterized by a very low water solubility (obeying Henry’s law with a dimensionless solubility coefficient  $H = 4.6 \times 10^{-3}$ ). But it is also characterized by the formation of clusters at moderate–high activities, to which the Zimm–Lundberg theory applies. Since the hypothesis of osmosis has been rejected, we have to find a proposal for another clustering mechanism. At high water activity values, the clusters slow down the diffusion rate as previously observed [135], [136] and [137], the diffusion coefficient being about 30 times lower at 100%  $HR$  than at 10–20%  $HR$ .

It is possible to envisage clustering from the (purely physical) formation of polymer–water complexes involving several water molecules. Water clustering occurs frequently in polymers of low polarity because water molecules bound to the polymer compete efficiently with polymer polar sites to “capture” new water molecules. An interesting theory of clustering was developed at the beginning of the 1960s [145] and [146], it considers that a water molecule is able to establish 4 hydrogen bonds and then behaves as a tetrafunctional monomer of type  $A_4$  forming a network. Gelation would then correspond to saturation and the Flory’s theory for network formation would be applicable. An important parameter in this theory is the equilibrium constant for the formation–dissociation of hydrogen bonds. Clustering conditions can be illustrated by a simpler model in which cluster growth is limited to two water molecules



where  $P$  is a polymer polar site,  $W$  is the water molecule,  $[W]$  is the concentration of non-bonded water in the polymer, presumably proportional to water activity.  $PW$  and  $PW_2$  are polymer-water complexes with respectively one and two water molecules.  $k_{c1}$  and  $k_{c2}$  are (second order) rate constants for complex formation;  $k_{d1}$  and  $k_{d2}$  are (first order) rate constants for complex decomposition. The number  $N$  of bound water molecules is given by:

$$N = [PW] + 2 \cdot [PW_2] \quad (6.10)$$

The complex concentration varies according the following equations:

$$\frac{d[PW]}{dt} = k_{c1} \cdot [P] \cdot [W] - k_{d1} \cdot [PW] - k_{c2} \cdot [W] [PW] \quad (6.11)$$

$$\frac{d[PW_2]}{dt} = k_{c2} \cdot [W] [PW] - k_{d2} [PW_2] \quad (6.12)$$

In stationary state  $N$  is constant so that:

$$\frac{d[PW]}{dt} + 2 \cdot \frac{d[PW_2]}{dt} = 0 \quad (6.13)$$

The equilibrium cluster ( $PW_2$ ) is then:

$$[PW_2]_{\infty} = \frac{k_{c1} \cdot k_{c2} \cdot [W]^2 \cdot [P]}{3k_{c2} \cdot k_{d2} \cdot [W] - k_{d1} \cdot k_{d2}} \quad (6.14)$$

Clustering exists only if  $[PW_2] > 0$  i.e. if  $3k_{c2} [W] > k_{d1}$  thus two conditions appear:

- The first one is on rate constants, if the following equation was not obeyed, no clustering would occur whatever the water activity:

$$R_1 = \frac{3k_{c2} \cdot [W]_s}{k_{d1}} > 1 \quad (6.15)$$

where  $[W]_s$  is the water concentration at saturation.

- The second one illustrates the existence of a critical water concentration  $[W]_c$ , therefore a critical water activity  $a_c$  below which no cluster is formed

$$[W] > [W]_c = \frac{k_{d1}}{3k_{c2}} \quad (6.16)$$

With this analytical model of sorption isotherms, it is effectively possible to define arbitrarily a critical water activity  $a_c$  such that the ratio power term/Henry's term is equal to the relative uncertainty on water volume fraction (or mass uptake):

$$\frac{B \cdot a_c^2}{H \cdot a_c} = \frac{\Delta u}{u} \quad (6.17)$$

Taking arbitrarily a relative uncertainty of 1% one obtains  $a_c \sim 0.41$ .

Obviously the above model is an oversimplification of the reality. However it is difficult for us to imagine another configuration than the one consisting of the presence of clusters with a certain size distribution determined by their stability i.e; their ability to decompose by releasing successively water molecules or by splitting into smaller units. Among the infinite diversity of possible configurations, the above model describes the simplest one but it differs only qualitatively from a more complex model of the same type. It is not proposed here as the definitive solution of the problem but rather as an interesting point of departure towards more realistic models. The most difficult problem here will not be to find a good solution; it is rather to demonstrate that there is no other solution. Two important points should be considered here.

- First about the existence or not of a phase separation: if the clusters were almost spherical, centered on a polar site of the polymer, it would be difficult to imagine the formation of large clusters without phase separation, and the existence of this latter without irreversible damage. But in fact,  $PW_n$  clusters can be linear, possibly branched, as found by molecular dynamics simulation [142] but also by dielectric or NMR measurements [147] and [148], and can reach relatively large sizes without phase separation, which could solve the problem of full reversibility.

- Second concerning equilibrium, DVS results show that an apparent equilibrium is established rapidly i.e. that the rate constants  $k_{cj}$  and  $k_{di}$  have relatively high values. In this case, the explanation could be linked to the high water concentration reached in samples at high activities: more than 15%, predominantly in clusters. A rubber sample swelled by a large quantity of clustered water is no doubt a fragile object in De Gennes' sense [149], i.e. it is expected to undergo significant changes under small stimuli, for instance linked to swelling stresses. This stress-water absorption coupling could explain the observed effect of sample thickness, for instance the slow increase of water concentration at almost constant rate could be linked to polymer creep under swelling stresses. This aspect has been investigated many years ago, for instance Crank [150] found that swelling stresses could explain an increase of water diffusivity with the sample thickness, as observed here (Table 6.1). However some aspects observed here, for instance the continuous mass increase at constant rate do not appear in Crank's work and will need further study.

## 6.4 Conclusion

When a fully formulated CR is immersed in sea water, large water absorption occurs even if the formulation has been chosen with great care. Due to this large water absorption, the oxidation model developed in air cannot be adapted to sea water in this study. It has been chosen to focus on water absorption mechanisms in CR and so the water absorption by polychloroprene has been studied at various temperatures and constant hygrometric ratios (CTH experiments) for long times (up to 2500 h) on thick samples (1.8 and 3.8 mm). It has also been examined at fixed temperature (40°C) and various water activities (DVS experiments) for short times (a few hours) on thin samples (100  $\mu\text{m}$ ). In CTH experiments, water absorption begins as a fickian process but does not display equilibrium, the water concentration continues increasing linearly with time when the diffusion process has apparently reached its equilibrium. It was demonstrated that this abnormal process is neither due to hydrolysis nor osmotic cracking. In DVS experiments, in contrast, equilibrium is apparently reached. The shape of the sorption isotherm plotted as the variation of water diffusivity with its activity clearly indicates the existence of a water clustering process, responsible for the major part of the absorbed water at high activities. For instance, at saturation, water mass uptake can reach values of the order of 15–20% by weight whereas water dissolution in the polymer contributes only for 0.46%. Cyclic experiments have shown that mass changes are fully reversible, i.e. that the abnormal sorption process does not induce damage. There is no other clustering mechanism to explain the observed behaviour than the formation of polymer–water complexes carrying several (seven on average) water molecules per polar site of the polymer. These complexes remain miscible to the polymer which explains the full reversibility of absorption curves in cyclic experiments. A possible way to explain the differences of behaviour between thin and thick samples could be the existence of a relatively strong coupling between swelling stresses and water absorption.

# Conclusions

The aim of this study is to contribute to the characterization, understanding and prediction of the long term behaviour of polymers, and more particularly elastomers, in a marine environment. The polymer studied here is polychloroprene (vulcanized or not), this elastomer has properties similar to natural rubber and durability often announced to be better than the latter.

The analysis of results from a literature study showed that when elastomers are correctly formulated they absorb little water and this water has little effect on physical properties. However, osmotic cracking can cause absorption of large quantities of water, and change properties. In addition, irreversible chemical degradation can occur through hydrolysis or oxidation. The former is well known and can be controlled by appropriate choice of polymer, but oxidation cannot be avoided. At best it can be slowed down, so attention must be paid to this degradation mechanism, all the more so as the polydienes in elastomers are particularly sensitive to oxidation.

In spite of widespread interest in oxidation of polymers from the scientific community for more than 50 years there is no agreement on a simple and reliable method to predict how mechanical properties of polychloroprene evolve during oxidation. In this work a new kinetic model is proposed first based on the reactions which govern oxidation. The particularity of this approach is that all the chemically important reactions are described and their kinetic rates are identified. In order to determine these parameters independently a step by step approach has been used with increasing complexity. In the first step the raw material was studied. Both literature data and experimental measurements were used to identify the important mechanisms. Two chemical particularities of polychloroprene are the presence of chlorine and of a carbon-carbon double bond. The role of chlorine can be neglected but the consumption of the double bonds is characteristic of the oxidation process and must be included. Finally a mechanistic scheme with 9 elementary reactions has been proposed in order to describe the evolutions. By using experimental results at different partial oxygen pressures the kinetics of the elementary reactions were determined, first at 100°C, then the effect of temperature was integrated in the kinetic model.

In a second step vulcanized polychloroprene was studied. A significant reduction in oxidation rate was measured and attributed to the anti-oxidant properties of sulfur, which decomposes hydroperoxides. This mechanism was included in the kinetic model through the introduction of two new chemical reactions. The results were compared to experimental oxygen absorption data from Sandia National Laboratories in order to establish the limits of the model.

Oxidation of polychloroprene results in a large increase in modulus due to the addition reaction of radicals with the double bonds. These variations in modulus have been quantitatively predicted for the first time up to 50 MPa, by considering the evolution of cross-link density and chain scissions induced by oxidation. From this the modulus has been predicted based on rubber elasticity theory. This prediction requires the introduction of a ratio between the number of new cross-link points and the number of double bonds. A ratio of 0.35 was determined and found to be independent of aging temperature (over the range considered here: 140 to 100°C). Oxygen diffusion has been included in the model so that it may be also applied to predict the behaviour of thick components. Predictions from this origin approach show good overall agreement with experimental results up to a modulus of 50 MPa.

The network modifications induced by oxidation of CR also have a strong influence on fracture behaviour. An unexpected behaviour was noted as aging progressed, with a rapid decrease in crack propagation energy ( $G_{IC}$ ) then an increase and finally a large drop. These results have been explained by using model materials, polyurethane and chlorinated polyethylene, in order to separate the roles of cross-linking and crystallization. It appears that the first drop is linked to the inhibition of induced crystallization, which results in a drop in  $G_{IC}$  from several  $\text{kJ/m}^2$  to a few hundred  $\text{J/m}^2$ . The subsequent increase has been attributed to a cross-linking mechanism at high conversion in the elastomers containing double bonds. The final drop is related to the very low mobility in highly cross-linked materials. Although the behaviour has not been predicted from theoretical considerations of elastomer embrittlement an end of life criterion has been proposed which allows lifetime to be predicted.

Finally, in order to adapt the oxidation model in air to a marine environment samples have been subjected to accelerated aging in sea water. The results show a large water absorption in CR which do not allow the direct application of the kinetic model. The origins of this large water absorption have been investigated using DVS and a mechanism of water cluster formation in polychloroprene has been proposed. This is based on a stronger affinity of water molecules with each other than with the polymer.

## Future work

Following this contribution to the understanding and the prediction of the long term behaviour of polychloroprene in a marine environment, further work is required at different levels: a) to examine in more detail the consequences of vulcanization by sulfur on the oxidation kinetics; b) to characterize the addition of stabilizers on the kinetics and incorporate them in the kinetic model; c) to refine the structure-mechanical property relationships in order to include the roles of fillers (carbon black) and induced crystallization; d) to study the role of other additives found in the industrial formulation (MgO) in the water absorption.

a) The model for modulus prediction during oxidation has been developed for a CR with only one type of vulcanization. In order to generalize this model to all polychloroprenes an improved understanding of the role of sulfur is required, and in particular the influence of sulfur concentration and the different types of bonds (mono-sulfur, poly-sulfur) on oxidation kinetics.

b) In order to move closer to industrial materials it is important to account for both fillers and stabilizers. The introduction of stabilizers in the model is possible, and has already been done in other studies. Here, part of the identification has been performed, for example Figure 6.11 shows the effect of anti-oxidants on the kinetics of increase of the modulus at 150°C. It is also necessary to perform oxygen absorption measurements on stabilized CR in order to confirm (or not) the role of stabilizers in the non-Arrhenian oxidation behaviour. This is an important open question.

c) The role of reinforcing fillers is also a vast subject. This has been briefly studied but in insufficient detail to report here. Nevertheless at low strain the modulus of a CR with carbon black filler can be predicted using the expression developed by Guth et al. [151]. The validity of this approach during oxidation remains to be verified, and more generally the integration of aging in the behaviour laws. A strong inhibition by oxidation of the induced crystallization in elastomers was observed using indirect methods. It would be interesting to examine this effect more closely by direct characterization such as X-ray

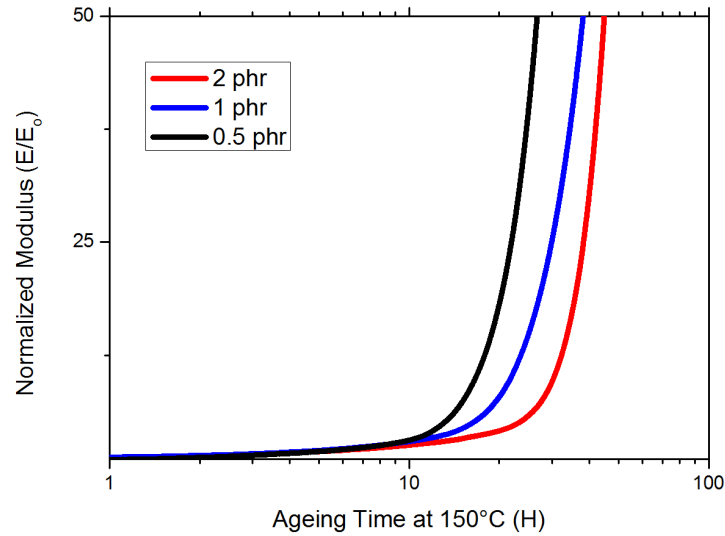


Figure 6.11: Effect of anti-oxidants (in parts per hundred of rubber) on the kinetics of increase of the modulus at 150°C.

diffraction, on different elastomers which either crystallize (NR, CR, CPE) or don't (SBR, EPDM) in order to better understand the SIC phenomenon.

d) The final objective of this work is to be able to predict the long term behaviour of elastomers when they are used in marine applications. For that it is necessary to study in more detail the mechanisms involved in osmotic degradation, and in particular the role of the different additives in order to develop design rules to avoid large water absorption.

In addition to these short term objectives which will lead to a lifetime prediction model for industrial polychloroprene, the need to take into account more realistic marine service conditions will require the study of two types of coupling:

a) Coupling between oxidation and water absorption: the water absorbed by the elastomer can contribute of extraction of stabilizers. This extraction will reduce the amount of oxidation protection remaining in the elastomer.

b) Coupling between oxidation and mechanical loading (fatigue in particular): an inhibition of SIC by oxidation has been revealed in this study. Given that SIC is one of the main reasons for the excellent fatigue resistance of CR one can imagine that fatigue lifetime may be significantly affected by oxidation

in sea water; this effect must be thoroughly investigated as it is critical for many long term applications at sea.



# Bibliography

- [1] DW Van Krevelen and K Te Nijenhuis. *Properties of polymers: their correlation with chemical structure; their numerical estimation and prediction from additive group contributions*. Elsevier, 2009.
- [2] PJ Flory. *Principles of polymer chemistry*. Cornell University Press, 1953.
- [3] AR Kemp. Purified rubber for electrical insulation. *Rubber Chemistry and Technology*, 10(3):474–491, 1937.
- [4] CR Boggs and JT Blake. Deproteinized rubber. *Industrial & Engineering Chemistry*, 28(10):1198–1202, 1936.
- [5] PY Le Gac, D Choqueuse, and D Melot. Description and modeling of polyurethane hydrolysis used as thermal insulation in oil offshore conditions. *Polymer Testing*, 32(8):1588–1593, 2013.
- [6] LA Wells, PE Cassidy, TM Aminabhavi, and RB Perry. A study of permeation and diffusion of aqueous salt solutions through polyurethane and polysiloxane and their laminates. *Rubber Chemistry and Technology*, 63(1):66–76, 1990.
- [7] BE Brokenbrow, D Sims, and J Wright. Polyurethane elastomers based on hydroxyl-terminated polyurethane. Technical report, DTIC Document, 1970.
- [8] BE Brokenbrow, D Sims, and J Wright. High performance polyurethane elastomers. part 1. laboratory ageing trials. Technical report, DTIC Document, 1972.
- [9] GJ Briggs, DC Edwards, and EB Storey. Water absorption of elastomers. *Rubber Chemistry and Technology*, 36(3):621–641, 1963.
- [10] PD Riggs, S Parker, M Braden, and S Kalachandra. Influence of additives on the water uptake of hydrosilanized silicone rubbers. *Biomaterials*, 18(10):721–726, 1997.
- [11] A Boisseau. *Long term durability of composites for ocean energy conversion systems*. PhD thesis, Université de Franche-Comté, 2011.

- [12] JA Hinkley and BS Holmes. Effect of water on the strength of filled polychloroprene vulcanizates. *Journal of applied polymer science*, 32(5):4873–4881, 1986.
- [13] BP Velayudhan. *Studies on rubber compositions as passive acoustic materials in underwater electro acoustic transducer technology-and their aging characteristics*. PhD thesis, Cochin University of Science And Technology, 2003.
- [14] GJ Lake and TJ Pond. Effects of aqueous environments on fatigue and elastic properties of rubber. In *2 nd International Conference on Polymers in a Marine Environment*, pages 141–147, 1987.
- [15] RF Fedors. Osmotic effects in water absorption by polymers. *Polymer*, 21(2):207–212, 1980.
- [16] RF Fedors. Water-treeing as an osmotic phenomenon. *Polymer*, 21(8):863–865, 1980.
- [17] JM Ball. Discontinuous equilibrium solutions and cavitation in nonlinear elasticity. *Philosophical Transactions of the Royal Society of London. Series A, Mathematical and Physical Sciences*, pages 557–611, 1982.
- [18] HA Winkelmann and EG Croakmann. Water absorption of rubber compounds. *Industrial & Engineering Chemistry*, 22(12):1367–1370, 1930.
- [19] HA Daynes. Note on the theory of water absorption by rubber. *Rubber Chemistry and Technology*, 12(3):532–534, 1939.
- [20] AG Thomas and K Muniandy. Absorption and desorption of water in rubbers. *Polymer*, 28(3):408–415, 1987.
- [21] V Miri, O Persyn, J-M Lefebvre, and R Seguela. Effect of water absorption on the plastic deformation behavior of nylon 6. *European Polymer Journal*, 45(3):757–762, 2009.
- [22] B De’Nève and MER Shanahan. Water absorption by an epoxy resin and its effect on the mechanical properties and infra-red spectra. *Polymer*, 34(24):5099–5105, 1993.
- [23] P Davies and Y Rajapakse. *Durability of Composites in a Marine Environment*. Springer, 2014.
- [24] M Arhant, PY Le Gac, and P Davies. Fatigue behavior of natural rubber in a marine environment. Technical report, IFREMER Document : Internal Report, 2013.
- [25] X Leveque. Behaviour of various elastomers in a marine environment. In *Polymers in a Marine Environment Conference*, 1900.

- [26] K Ab-Malek and A Stevenson. The effect of 42 year immersion in seawater on natural rubber. *Journal of materials science*, 21(1):147–154, 1986.
- [27] D Oldfield and T Symes. Long term natural ageing of silicone elastomers. *Polymer testing*, 15(2):115–128, 1996.
- [28] PH Mott and CM Roland. Aging of natural rubber in air and seawater. *Rubber chemistry and technology*, 74(1):79–88, 2001.
- [29] PY Le Gac, V Le Saux, M Paris, and Y Marco. Ageing mechanism and mechanical degradation behaviour of polychloroprene rubber in a marine environment: Comparison of accelerated ageing and long term exposure. *Polymer Degradation and Stability*, 97(3):288–296, 2012.
- [30] ZT Ossefort and PB Testroet. Hydrolytic stability of urethan elastomers. *Rubber chemistry and technology*, 39(4):1308–1327, 1966.
- [31] M Rutkowska, K Krasowska, A Heimowska, I Steinka, and H Janik. Degradation of polyurethanes in sea water. *Polymer Degradation and Stability*, 76(2):233–239, 2002.
- [32] V Bellenger, M Ganem, B Mortaigne, and J Verdu. Lifetime prediction in the hydrolytic ageing of polyesters. *Polymer degradation and stability*, 49(1):91–97, 1995.
- [33] C Hepburn. *Polyurethane elastomers*. Elsevier Applied Science London, 1992.
- [34] A Ballara and J Verdu. Physical aspects of the hydrolysis of polyethylene terephthalate. *Polymer degradation and stability*, 26(4):361–374, 1989.
- [35] P Gilormini, E Richaud, and J Verdu. A statistical theory of polymer network degradation. *Polymer*, 2014.
- [36] S Murata, T Nakajima, N Tsuzaki, M Yasuda, and T Kato. Synthesis and hydrolysis resistance of polyurethane derived from 2, 4-diethyl-1, 5-pentanediol. *Polymer Degradation and stability*, 61(3):527–534, 1998.
- [37] TM Chapman. Models for polyurethane hydrolysis under moderately acidic conditions: A comparative study of hydrolysis rates of urethanes, ureas, and amides. *Journal of Polymer Science Part A: Polymer Chemistry*, 27(6):1993–2005, 1989.
- [38] P Davies and G Evrard. Accelerated ageing of polyurethanes for marine applications. *Polymer Degradation and Stability*, 92(8):1455–1464, 2007.
- [39] SJ Skinner and TJ Drakeley. Water absorption by rubber. part ii. vulcanized rubber. *Rubber Chemistry and Technology*, 6(1):12–23, 1933.

- [40] M Celina. Review of polymer oxidation and its relationship with materials performance and lifetime prediction. *Polymer Degradation and Stability*, 98(12):2419–2429, 2013.
- [41] J Verdu. *Oxydative Ageing of Polymers*. John Wiley & Sons, 2012.
- [42] V Coveney. *Elastomers and components: Service life prediction-progress and challenges*. Woodhead Publishing, 2006.
- [43] AV Tobolsky, DJ Metz, and RB Mesrobian. Low temperature autoxidation of hydrocarbons: the phenomenon of maximum rates<sup>1, 2</sup>. *Journal of the American Chemical Society*, 72(5):1942–1952, 1950.
- [44] FR Mayo. Some new ideas on oxidation. *Industrial & Engineering Chemistry*, 52(7):614–618, 1960.
- [45] JR Shelton. Review of basic oxidation processes in elastomers. *Rubber Chemistry and Technology*, 45(2):359–380, 1972.
- [46] A Riaya, MT Shaw, and A Garton. Oxidation of elastomers in aqueous environments. *Rubber chemistry and technology*, 67(5):775–785, 1994.
- [47] BB Benson and D Krause Jr. The concentration and isotopic fractionation of oxygen dissolved in freshwater and seawater in equilibrium with the atmosphere. *Limnology and oceanography*, 29(3):620–632, 1984.
- [48] WL Hawkins, MA Worthington, and W Matreyek. Loss of antioxidants from polyethylene by evaporation and aqueous extraction. *Journal of Applied Polymer Science*, 3(9):277–281, 1960.
- [49] NC Billingham, PD Calvert, and G Scott. Developments in polymer stabilisation—3. *Chap*, 5:97–139, 1980.
- [50] X Colin, L Audouin, J Verdu, M Rozental-Evesque, B Rabaud, F Martin, and F Bourguine. Aging of polyethylene pipes transporting drinking water disinfected by chlorine dioxide. i. chemical aspects. *Polymer Engineering & Science*, 49(7):1429–1437, 2009.
- [51] DA Tester. The sorption of water by rubber. *Rubber Chemistry and Technology*, 29(4):1321–1331, 1956.
- [52] JL Bolland. Kinetics of olefin oxidation. *Q. Rev. Chem. Soc.*, 3(1):1–21, 1949.
- [53] M Coquillat, J Verdu, X Colin, L Audouin, and R Nevriere. Thermal oxidation of polybutadiene. part 3: Molar mass changes of additive-free non-crosslinked polybutadiene. *Polymer degradation and stability*, 92(7):1343–1349, 2007.

- [54] T Ha-Anh and T Vu-Khanh. Prediction of mechanical properties of polychloroprene during thermo-oxidative aging. *Polymer testing*, 24(6):775–780, 2005.
- [55] JM Baldwin, DR Bauer, and KR Ellwood. Accelerated aging of tires, part iii. *Rubber chemistry and technology*, 78(5):767–776, 2005.
- [56] AU Paeglis. A simple model for predicting heat aging of epdm rubber. *Rubber chemistry and technology*, 77(2):242–256, 2004.
- [57] M Celina, KT Gillen, and RA Assink. Accelerated aging and lifetime prediction: review of non-arrhenius behaviour due to two competing processes. *Polymer Degradation and Stability*, 90(3):395–404, 2005.
- [58] V Le Saux, PY Le Gac, Y Marco, and S Calloch. Limits in the validity of arrhenius predictions for field ageing of a silica filled polychloroprene in a marine environment. *Polymer Degradation and Stability*, 99:254–261, 2014.
- [59] KT Gillen, M Celina, RL Clough, and J Wise. Extrapolation of accelerated aging data: Arrhenius or erroneous? *Trends in polymer science*, 5(8):250–257, 1997.
- [60] KT Gillen, J Wise, and RL Clough. General solution for the basic autoxidation scheme. *Polymer Degradation and Stability*, 47(1):149–161, 1995.
- [61] J Wise, KT Gillen, and RL Clough. Quantitative model for the time development of diffusion-limited oxidation profiles. *Polymer*, 38(8):1929–1944, 1997.
- [62] M Celina, J Wise, DK Ottesen, KT Gillen, and RL Clough. Correlation of chemical and mechanical property changes during oxidative degradation of neoprene. *Polymer degradation and Stability*, 68(2):171–184, 2000.
- [63] LM Rincon-Rubio, B Fayolle, L Audouin, and J Verdu. A general solution of the closed-loop kinetic scheme for the thermal oxidation of polypropylene. *Polymer degradation and stability*, 74(1):177–188, 2001.
- [64] E Richaud, F Farcas, B Fayolle, and J Audouin, L Verdu. Hydroperoxide build-up in the thermal oxidation of polypropylene—a kinetic study. *Polymer degradation and stability*, 92(1):118–124, 2007.
- [65] M Coquillat. *Vieillessement des propergols à matrice polybutadiène: modélisation cinétique de l’oxydation*. PhD thesis, Arts et Métiers Paris-Tech, 2007.
- [66] GY Li and JL Koenig. A review of rubber oxidation. *Rubber Chemistry and technology*, 78(3):355–390, 2005.

- [67] JR Shelton. Aging and oxidation of elastomers. *Rubber Chemistry and Technology*, 30(5):1251–1290, 1957.
- [68] M Celina, J Wise, DK Ottesen, KT Gillen, and RL Clough. Oxidation profiles of thermally aged nitrile rubber. *Polymer degradation and stability*, 60(2):493–504, 1998.
- [69] M Celina, AC Graham, KT Gillen, RA Assink, and LM Minier. Thermal degradation studies of a polyurethane propellant binder. *Rubber chemistry and technology*, 73(4):678–693, 2000.
- [70] LRG Treloar. *The physics of rubber elasticity*. Oxford University Press, 1975.
- [71] KT Gillen, R Bernstein, and DK Derzon. Evidence of non-arrhenius behaviour from laboratory aging and 24-year field aging of polychloroprene rubber materials. *Polymer Degradation and Stability*, 87(1):57–67, 2005.
- [72] T Ha-Anh and T Vu-Khanh. Effects of thermal aging on fracture performance of polychloroprene. *Journal of materials science*, 40(19):5243–5248, 2005.
- [73] GJ Lake. Fracture mechanics and its application to failure in rubber articles. *Rubber chemistry and technology*, 76(3):567–591, 2003.
- [74] K Tsunoda, JJC Busfield, CKL Davies, and AG Thomas. Effect of materials variables on the tear behaviour of a non-crystallising elastomer. *Journal of Materials Science*, 35(20):5187–5198, 2000.
- [75] AK Bhowmick, AN Gent, and CTR Pulford. Tear strength of elastomers under threshold conditions. *Rubber chemistry and technology*, 56(1):226–232, 1983.
- [76] LC Yanyo and FN Kelley. Effect of network chain length on the tearing energy master curves of poly (dimethyldiphenyl siloxane). *Rubber chemistry and technology*, 61(1):100–118, 1988.
- [77] LC Yanyo and FN Kelley. Effect of chain length distribution on the tearing energy of silicone elastomers. *Rubber chemistry and technology*, 60(1):78–88, 1987.
- [78] JE Mark and MY Tang. Dependence of the elastomeric properties of bimodal networks on the lengths and amounts of the short chains. *Journal of Polymer Science: Polymer Physics Edition*, 22(11):1849–1855, 1984.
- [79] RA Robinson. The vapour pressure and osmotic equivalence of sea water. *Journal of the Marine Biological Association of the United Kingdom*, 33(02):449–455, 1954.

- [80] M Celina, AR Dayile, and A Quintana. A perspective on the inherent oxidation sensitivity of epoxy materials. *Polymer*, 54(13):3290–3296, 2013.
- [81] KT Gillen, RL Clough, and A Quintana. Modulus profiling of polymers. *Polymer degradation and stability*, 17(1):31–47, 1987.
- [82] Y Miyata and M Atsumi. Spectroscopic studies on the initial stages of thermal degradation of polychloroprene. *Journal of Polymer Science Part A: Polymer Chemistry*, 26(9):2561–2572, 1988.
- [83] HC Bailey. . *Rev Gen Caoutch Plast*, 44(12):1495, 1967.
- [84] JR Shelton, RL Pecsok, and JL Koenig. *Fourier Transform IR Studies of the Uninhibited Autoxidation of Elastomers*, chapter 7, pages 75–96. American Chemical Society, Washington, D.C., 1979.
- [85] D Cuccato, M Dossi, D Moscatelli, and G Storti. A density functional theory study of poly (vinyl chloride) (pvc) free radical polymerization. *Macromolecular Symposia*, 302(1):100–109, 2011.
- [86] X Colin, L Audouin, and J Verdu. Kinetic modelling of the thermal oxidation of polyisoprene elastomers. part 3: Oxidation induced changes of elastic properties. *Polymer degradation and stability*, 92(5):906–914, 2007.
- [87] F Delor, J Lacoste, J Lemaire, N Barrois-Oudin, and C Cardinet. Photo- and thermal ageing of polychloroprene: Effect of carbon black and crosslinking. *Polymer Degradation and Stability*, 53(3):361 – 369, 1996.
- [88] A Fraind, R Turncliff, T Fox, J Sodano, and LR Ryzhkov. Exceptionally high decarboxylation rate of a primary aliphatic acyloxy radical determined by radical product yield analysis and quantitative 1h-cidnp spectroscopy. *Journal of Physical Organic Chemistry*, 24(9):809–820, 2011.
- [89] G Socrates. *Infrared and Raman characteristic group frequencies: tables and charts*. John Wiley & Sons, 2004.
- [90] V Arjunan, S Subramanian, and S Mohan. Vibrational spectroscopic studies on trans-1, 4-polychloroprene. *Turkish Journal of Chemistry*, 27(4):423–432, 2003.
- [91] P Gijsman and J Sampers. The influence of oxygen pressure and temperature on the uv-degradation chemistry of polyethylene. *Polymer degradation and stability*, 58(1):55–59, 1997.
- [92] M Coquillat, J Verdu, X Colin, L Audouin, and R Nevriere. Thermal oxidation of polybutadiene. part 1: Effect of temperature, oxygen pressure and sample thickness on the thermal oxidation of hydroxyl-terminated

- polybutadiene. *Polymer degradation and stability*, 92(7):1326–1333, 2007.
- [93] FR Mayo. Relative reactivities in oxidations of polypropylene and polypropylene models. *Macromolecules*, 11(5):942–946, 1978.
- [94] S Korcek, JHB Chenier, JA Howard, and KU Ingold. Absolute rate constants for hydrocarbon autoxidation. activation energies for propagation and the correlation of propagation rate constants with carbon–hydrogen bond strengths. *Canadian Journal of Chemistry*, 50(14):2285–2297, 1972.
- [95] SW Benson. *Thermochemical kinetics*. Wiley Interscience, 1976.
- [96] JL Bolland and G Gee. Kinetic studies in the chemistry of rubber and related materials. ii. the kinetics of oxidation of unconjugated olefins. *Trans. Faraday Soc.*, 42:236–243, 1946.
- [97] JA Howard. Absolute rate constants for hydrocarbon autoxidation. xxii. the autoxidation of some vinyl compounds. *Canadian Journal of Chemistry*, 50(14):2298–2304, 1972.
- [98] KU Ingold. Inhibition of the autoxidation of organic substances in the liquid phase. *Chemical Reviews*, 61(6):563–589, 1961.
- [99] C Sinturel and NC Billingham. A theoretical model for diffusion-limited oxidation applied to oxidation profiles monitored by chemiluminescence in hydroxy-terminated polybutadiene. *Polymer international*, 49(9):937–942, 2000.
- [100] X Colin, L Audouin, and J Verdu. Kinetic modelling of the thermal oxidation of polyisoprene elastomers. part 1: unvulcanized unstabilized polyisoprene. *Polymer degradation and stability*, 92(5):886–897, 2007.
- [101] M Ben Hassine. *Modélisation du vieillissement thermique et mécanique d’une protection externe en EPDM de jonctions rétractables à froid*. PhD thesis, Arts et Métiers ParisTech, 2013.
- [102] S Kamaruddin, PY Le Gac, Y Marco, and AH Muhr. Formation of crust on natural rubber after ageing. *Constitutive Models for Rubber VII*, page 197, 2011.
- [103] D Barnard, ME Cain, JI Cunneen, and TH Houseman. Oxidation of vulcanized natural rubber. *Rubber Chemistry and Technology*, 45(2):381–401, 1972.
- [104] PY Le Gac, G Roux, J Verdu, P Davies, and B Fayolle. Oxidation of unvulcanized, unstabilized polychloroprene: A kinetic study. *Polymer Degradation and Stability*, 109:175–183, 2014.

- [105] E Richaud, C Monchy-Leroy, X Colin, Lu Audouin, and J Verdu. Kinetic modelling of stabilization coupled with stabilizer loss by evaporation. case of dithioester stabilized polyethylene. *Polymer Degradation and Stability*, 94(11):2004–2014, 2009.
- [106] M Coquillat, J Verdu, X Colin, L Audouin, and R Nevriere. Thermal oxidation of polybutadiene. part 2: Mechanistic and kinetic schemes for additive-free non-crosslinked polybutadiene. *Polymer degradation and stability*, 92(7):1334–1342, 2007.
- [107] J Pospíšil. Chemical and photochemical behaviour of phenolic antioxidants in polymer stabilization—a state of the art report, part i. *Polymer degradation and stability*, 40(2):217–232, 1993.
- [108] J Pospíšil. Chemical and photochemical behaviour of phenolic antioxidants in polymer stabilization: a state of the art report, part ii. *Polymer degradation and stability*, 39(1):103–115, 1993.
- [109] PD Calvert and NC Billingham. Loss of additives from polymers: a theoretical model. *Journal of Applied Polymer Science*, 24(2):357–370, 1979.
- [110] W Dong and P Gijssman. Influence of temperature on the thermo-oxidative degradation of polyamide 6 films. *Polymer Degradation and Stability*, 95(6):1054–1062, 2010.
- [111] KT Gillen, M Celina, and R Bernstein. Validation of improved methods for predicting long-term elastomeric seal lifetimes from compression stress–relaxation and oxygen consumption techniques. *Polymer Degradation and Stability*, 82(1):25–35, 2003.
- [112] KT Gillen, R Bernstein, R L Clough, and M Celina. Lifetime predictions for semi-crystalline cable insulation materials: I. mechanical properties and oxygen consumption measurements on epr materials. *Polymer degradation and stability*, 91(9):2146–2156, 2006.
- [113] M Celina. An overview of the inherent oxidation sensitivity and diffusion limited oxidation behavior of epoxy materials. In *The Polymer Discussion Group - Paris*, 2013.
- [114] MA Llorente, AL Andrady, and JE Mark. Model networks of end-linked polydimethylsiloxane chains. xi. use of very short network chains to improve ultimate properties. *Journal of Polymer Science: Polymer Physics Edition*, 19(4):621–630, 1981.
- [115] A Cristiano, A Marcellan, BJ Kestra, P Steeman, and C Creton. Fracture of model polyurethane elastomeric networks. *Journal of Polymer Science Part B: Polymer Physics*, 49(5):355–367, 2011.

- [116] GJ Lake and PB Lindley. The mechanical fatigue limit for rubber. *Journal of Applied Polymer Science*, 9(4):1233–1251, 1965.
- [117] BNJ Persson, O Albohr, G Heinrich, and H Ueba. Crack propagation in rubber-like materials. *Journal of Physics: Condensed Matter*, 17(44):R1071, 2005.
- [118] LC Yanyo. Effect of crosslink type on the fracture of natural rubber vulcanizates. *International journal of fracture*, 39(1-3):103–110, 1989.
- [119] S Trabelsi, P-A Albouy, and J Rault. Crystallization and melting processes in vulcanized stretched natural rubber. *Macromolecules*, 36(20):7624–7639, 2003.
- [120] S Amnuaypornsi, S Toki, B S Hsiao, and J Sakdapipanich. The effects of endlinking network and entanglement to stress–strain relation and strain-induced crystallization of un-vulcanized and vulcanized natural rubber. *Polymer*, 53(15):3325–3330, 2012.
- [121] JM Chenal, L Chazeau, L Guy, Y Bomal, and C Gauthier. Molecular weight between physical entanglements in natural rubber: A critical parameter during strain-induced crystallization. *Polymer*, 48(4):1042–1046, 2007.
- [122] M Tosaka, S Murakami, S Poompradub, S Kohjiya, Y Ikeda, S Toki, I Sics, and B S Hsiao. Orientation and crystallization of natural rubber network as revealed by waxd using synchrotron radiation. *Macromolecules*, 37(9):3299–3309, 2004.
- [123] D Goritz and AG Thomas. Effect of ageing on the ability of natural rubber to strain crystallise. In *Constitutive Models for Rubber III: Proceedings of the Third European Conference on Constitutive Models for Rubber, London, UK, 15-17 September 2003*, page 79. CRC Press, 2003.
- [124] B Huneau. Strain-induced crystallization of natural rubber: a review of x-ray diffraction investigations. *Rubber chemistry and technology*, 84(3):425–452, 2011.
- [125] S Kole, S Roy, and Anil K Bhowmick. Influence of chemical interaction on the properties of silicone-epdm rubber blend. *Polymer*, 36(17):3273–3277, 1995.
- [126] E Planes, L Chazeau, G Vigier, and J Fournier. Evolution of epdm networks aged by gamma irradiation–consequences on the mechanical properties. *Polymer*, 50(16):4028–4038, 2009.
- [127] V Gueguen. *Vieillessement d’élastomères utilisés comme isolants électriques en ambiance nucléaire*. PhD thesis, 1992.

- [128] Y Merckel, J Diani, M Brieu, and J Caillard. Effects of the amount of fillers and of the crosslink density on the mechanical behavior of carbon-black filled styrene butadiene rubbers. *Journal of Applied Polymer Science*, 129(4):2086–2091, 2013.
- [129] B Fayolle, A Tcharkhtchi, and J Verdu. Temperature and molecular weight dependence of fracture behaviour of polypropylene films. *Polymer testing*, 23(8):939–947, 2004.
- [130] T Bárány, T Czigány, and J Karger-Kocsis. Application of the essential work of fracture (ewf) concept for polymers, related blends and composites: a review. *Progress in Polymer Science*, 35(10):1257–1287, 2010.
- [131] O Saito. Effects of high energy radiation on polymers ii. end-linking and gel fraction. *Journal of the Physical Society of Japan*, 13(12):1451–1464, 1958.
- [132] A Charlesby and SHF Pinner. Analysis of the solubility behaviour of irradiated polyethylene and other polymers. *Proceedings of the Royal Society of London. Series A. Mathematical and Physical Sciences*, 249(1258):367–386, 1959.
- [133] CM Roland. Unconventional rubber networks: Circumventing the compromise between stiffness and strength. *Rubber Chemistry and Technology*, 86(3):351–366, 2013.
- [134] JA Barrie. *Diffusion in polymers*, chapter Water in polymers. Academic Press, London, 1968.
- [135] JA Barrie, D Machin, and A Nunn. Transport of water in synthetic 1, 4-polyisoprenes and natural rubber. *Polymer*, 16(11):811–814, 1975.
- [136] KA Schult and DR Paul. Water sorption and transport in a series of polysulfones. *Journal of Polymer Science Part B: Polymer Physics*, 34(16):2805–2817, 1996.
- [137] D-K Yang, WJ Koros, HB Hopfenberg, and VT Stannett. Sorption and transport studies of water in kapton polyimide. i. *Journal of applied polymer science*, 30(3):1035–1047, 1985.
- [138] S Naudy, F Collette, F Thominet, G Gebel, and Eliane Espuche. Influence of hygrothermal aging on the gas and water transport properties of nafion membranes. *Journal of Membrane Science*, 451:293–304, 2014.
- [139] KHG Ashbee, FC Frank, and RC Wyatt. Water damage in polyester resins. *Proceedings of the Royal Society of London. Series A. Mathematical and Physical Sciences*, 300(1463):415–419, 1967.

- [140] L Gautier, B Mortaigne, V Bellenger, and J Verdu. Osmotic cracking nucleation in hydrothermal-aged polyester matrix. *Polymer*, 41(7):2481–2490, 2000.
- [141] J Mijovic and H Zhang. Local dynamics and molecular origin of polymer network-water interactions as studied by broadband dielectric relaxation spectroscopy, ftir, and molecular simulations. *Macromolecules*, 36(4):1279–1288, 2003.
- [142] G Marque, S Neyertz, J Verdu, V Prunier, and D Brown. Molecular dynamics simulation study of water in amorphous kapton. *Macromolecules*, 41(9):3349–3362, 2008.
- [143] BH Zimm and JL Lundberg. Sorption of vapors by high polymers. *The Journal of Physical Chemistry*, 60(4):425–428, 1956.
- [144] E Gaudichet-Maurin. *Caractérisation et vieillissement d’une membrane d’ultrafiltration d’eau*. PhD thesis, Arts et Métiers ParisTech, 2005.
- [145] M Gordon, CS Hope, LD Loan, and R-J Roe. The polymerization of water in benzene and toluene. *Proceedings of the Royal Society of London. Series A. Mathematical and Physical Sciences*, 258(1293):215–236, 1960.
- [146] JA Barrie and B Platt. The diffusion and clustering of water vapour in polymers. *Polymer*, 4:303–313, 1963.
- [147] G Xu, CC Gryte, AS Nowick, SZ Li, YS Pak, and SG Greenbaum. Dielectric relaxation and deuterium nmr of water in polyimide films. *Journal of Applied Physics*, 66(11):5290–5296, 1989.
- [148] BS Lim, AS Nowick, K-W Lee, and A Viehbeck. Sorption of water and organic solutes in polyimide films and its effects on dielectric properties. *Journal of Polymer Science Part B: Polymer Physics*, 31(5):545–555, 1993.
- [149] PG de Gennes. Soft matter. *Rev. Mod. Phys.*, 64:645–648, Jul 1992.
- [150] J Crank. *The mathematics of diffusion*. Clarendon press Oxford, 1975.
- [151] E Guth and O Gold. On the hydrodynamical theory of the viscosity of suspensions. *Phys. Rev*, 53(322):2–15, 1938.

# Appendix I: Differential equation system

According to the mechanistic scheme described in chapter 3, the following differential equation system can be written:

$$\frac{d[P^o]}{dt} = 2 \cdot k_{1u} \cdot [POOH] + k_{1b} \cdot [POOH]^2 + k_3 \cdot [PH] \cdot [POO^o] + k_{f2} \cdot [F] \cdot [POO^o] - k_2 \cdot [P^o] \cdot [O_2] - 2 \cdot k_4 \cdot [P^o]^2 - k_5 \cdot [P^o] \cdot [POO^o]$$

$$\frac{d[POOH]}{dt} = -k_{1u} \cdot [POOH] - 2 \cdot k_{1b} \cdot [POOH]^2 + k_3 \cdot [PH] \cdot [POO^o] + (1 - \gamma_5) \cdot k_5 \cdot [P^o] \cdot [POO^o]$$

$$\frac{d[POO^o]}{dt} = k_{1b} \cdot [POOH]^2 + k_2 \cdot [P^o] \cdot [O_2] - k_3 \cdot [PH] \cdot [POO^o] - k_{f2} \cdot [F] \cdot [POO^o] - k_5 \cdot [P^o] \cdot [POO^o] - 2 \cdot k_6 [POO^o]^2$$

$$\frac{d[F]}{dt} = -k_{f1} \cdot [F] \cdot [P^o] - k_{f2} \cdot [F] \cdot [POO^o]$$

$$\frac{d[PH]}{dt} = -4 \cdot k_{1u} \cdot [POOH] - 2 \cdot k_{1b} \cdot [POOH]^2 - 2 \cdot k_3 \cdot [PH] \cdot [POO^o] - k_{f1} \cdot [F] \cdot [P^o] - 2 \cdot k_{f2} \cdot [F] \cdot [POO^o]$$

$$\frac{d[C = O]}{dt} = \gamma_1 \cdot k_{1u} \cdot [POOH] + \gamma_1 \cdot k_{1b} \cdot [POOH]^2 + k_6 \cdot [POO^o]^2$$

Differential equation system used in Chapter 4 is the same but the sulfur effect is added.



# Appendix II: French summary

## Introduction

Les océans représentent plus de 70% de notre planète et ont été, à ce jour, explorés uniquement à 5% environ. Face à la raréfaction de l'énergie, de la nourriture ou des métaux rares, l'exploration et l'exploitation durables des ressources issues de ces océans sont un enjeu majeur pour notre société. Le coût et la complexité de la maintenance en environnement marin de structures immergées ne favorisent pas l'exploitation pérenne de ces ressources. Les structures utilisées en milieu marin sont composées majoritairement de trois types de matériaux : le béton, les métaux et les polymères. Ces derniers, qui présentent l'avantage important d'avoir une faible densité, participent à l'allègement global de ces structures et facilitent ainsi leur mise en place. La durée de vie des polymères en milieu marin est un sujet encore peu connu et complexe. Cette complexité suggère probablement que la dégradation en milieu marin résulterait de nombreux mécanismes. C'est pourquoi, l'élaboration d'une méthodologie permettant d'en appréhender la durée de vie, à partir de vieillissements accélérés en laboratoire, est plus que jamais d'actualité. L'objectif de cette étude est d'analyser le comportement à long terme du polychloroprène (CR) en milieu marin et tout particulièrement d'évaluer le rôle de l'oxydation dans sa dégradation, pour ainsi mettre en place une méthodologie non empirique de prédiction de l'évolution des propriétés mécaniques.

Dans une première partie, le comportement à long terme des élastomères sera exposé à partir des connaissances et données de la littérature. On retiendra que lorsqu'un élastomère est immergé dans l'eau de mer, il absorbe, en théorie, très peu d'eau. En pratique, il apparaît qu'un processus de fissuration osmotique peut se mettre en place conduisant à une forte absorption d'eau et à une forte perte de propriétés mécaniques à la rupture. De plus, le CR peut subir des dégradations chimiques résultant notamment de l'oxydation. En effet, l'analyse d'échantillons vieillis en service a montré que l'oxydation était un des processus chimiques majeurs de la dégradation des élastomères utilisés en milieu marin. Notre étude se focalisera sur la prédiction de l'oxydation dans le polychloroprène et plus particulièrement de ses conséquences sur les prédictions des propriétés mécaniques.

Dans ce même chapitre, une description des méthodes de prédiction de durée

de vie utilisées dans le cas de l'oxydation des élastomères sera présentée. Elle conclura que la description mécanistique de l'oxydation couplée à une approche cinétique est la seule méthode permettant la prédiction de l'oxydation de façon non empirique. Cependant cette approche est complexe et nécessite donc une mise en place étape par étape. Un rappel des points bibliographiques importants sera précisé avant chaque chapitre afin de faciliter la lecture du document.

Le chapitre suivant présentera la description des matériaux et méthodes utilisés lors de cette étude. Si les méthodes pour suivre les modifications chimiques et mécaniques sont classiques (spectrophotométrie infrarouge, mesure du module d'élasticité), un effort spécifique a été déployé pour suivre ces modifications in situ au cours du processus d'oxydation en conditions accélérées.

La première étape de la mise en place d'un modèle cinétique sera présentée dans le chapitre 3, consacré à l'oxydation du polychloroprène non vulcanisé. L'objectif de cette partie de l'étude est de déterminer les mécanismes d'oxydation et notamment d'appréhender le rôle du chlore et de la double liaison caractérisant le motif monomère du polychloroprène. Après avoir proposé un schéma mécanistique pour l'oxydation du polychloroprène non vulcanisé, les constantes de vitesse associées à chacune des réactions chimiques ont été déterminées à 100°C par méthode inverse en utilisant des résultats expérimentaux à différentes pressions d'oxygène. Puis l'effet de la température a été intégré dans le modèle cinétique.

La seconde étape de la mise en place du modèle cinétique de prédiction consiste à intégrer l'effet de la vulcanisation et notamment celui du soufre (Chapitre 4). Celui-ci agit comme un antioxydant qui conduit à une réduction de la vitesse d'oxydation de l'élastomère. Cet effet a été pris en compte via l'ajout de deux nouveaux actes chimiques au modèle ainsi que la détermination des constantes de vitesse associées.

Par ailleurs, la présence de doubles liaisons dans le CR conduit à une forte réticulation au cours de l'oxydation qui se traduit par une forte augmentation du module. Ce comportement sera prédit de façon quantitative pour la première fois dans le CR grâce à l'utilisation du modèle cinétique couplé à la théorie de l'élasticité caoutchoutique.

Pour finir, ce chapitre traitera également des effets physiques impliqués dans l'oxydation notamment la diffusion de l'oxygène qui doit être prise en compte pour prédire le comportement de pièces épaisses.

Le chapitre suivant (Chapitre 5) présentera l'effet de l'oxydation sur le comportement à rupture des élastomères. L'objectif final est d'être en mesure de prédire le comportement à rupture à partir de l'approche mécanistique en considérant les changements de densité de réticulation résultant de l'oxydation. Dans un premier temps, une étude expérimentale de la fissuration dans le CR sera exposée afin d'identifier les paramètres influant sur la mesure. Dans un

second temps, l'évolution de l'énergie de fissuration avec l'oxydation indiquera un comportement inattendu avec une première chute rapide puis une augmentation et enfin une chute finale. La compréhension de ce comportement est primordiale pour réaliser une prédiction de durée de vie fiable. Afin de tester différentes hypothèses, deux autres matériaux seront comparés au CR : un polyuréthane contenant des doubles liaisons et du polyéthylène chloré. Ce dernier permet de dissocier le rôle de l'oxydation sur la cristallisation sous charge de la réticulation induite par la présence de double liaison. Les résultats obtenus seront confrontés à la théorie et une prédiction proposée.

Le dernier chapitre devait être l'adaptation du modèle d'oxydation mis en place dans l'air au milieu marin (Chapitre 6). Cependant les vieillissements accélérés en eau de mer d'un polychloroprène complètement formulé (c'est-à-dire contenant stabilisants et noir de carbone) ont mis en évidence une très forte absorption d'eau. Le chapitre est donc consacré à l'origine de cette forte absorption avec notamment des essais de sorption dynamique de vapeur d'eau qui indiquent la formation d'agrégat d'eau dans l'élastomère. La formation de ces agrégats sera exposée et modélisée.

Enfin, ce manuscrit s'achèvera par une conclusion générale sur le travail présenté ici et par des pistes de réflexion pour les futures études à mener pour compléter un modèle de prédiction à long terme des élastomères présentant une formulation industrielle.

## Résumé du chapitre 1 : Comportement à long terme des élastomères en milieu marin

Ce premier chapitre est consacré à l'étude bibliographique du comportement à long terme des élastomères en milieu marin. Dans un premier temps, les dégradations physiques subies par ce type de matériaux lorsqu'ils sont immergés en eau de mer sont décrites. Puis dans un second temps, les possibles dégradations chimiques sont détaillées et montrent que l'oxydation est l'un des phénomènes majeurs mis en jeu. Les mécanismes liés à l'oxydation des élastomères sont donc ensuite détaillés.

### Dégradation physique des élastomères en milieu marin

Lorsqu'un élastomère est immergé en eau de mer, il absorbe de l'eau en raison d'une différence de potentiel chimique entre le milieu extérieur et le polymère. L'absorption d'eau dans un polymère est généralement caractérisée par deux paramètres : la quantité absorbée qui est liée à la solubilité de l'eau dans le polymère et la vitesse à laquelle l'équilibre est atteint. Dans le cas des élastomères, en raison de la faible polarité entre les groupements chimiques qui le constituent, la quantité d'eau absorbée est, en théorie, faible : généralement inférieure à 1%. De plus, étant donné la forte mobilité dans le matériau ( $T_g < T$ ), la vitesse de diffusion devrait obéir à la deuxième loi de Fick avec une valeur de coefficient de diffusion élevée. Ce genre de comportement a été, dans la littérature, mis en évidence à plusieurs reprises : dans ce cas, les conséquences de l'absorption d'eau sur les propriétés usuelles sont généralement très faibles.

Cependant on observe également, dans la littérature, des exemples de fortes absorptions d'eau dans les élastomères lorsqu'ils sont immergés. Ceci s'explique par la présence d'un second phénomène. Un processus de fissuration osmotique peut s'établir si, pour une raison ou une autre, le matériau contient des molécules ou des ions solubles dans l'eau et de diffusivité inférieure à celle de l'eau. Ce processus conduit à la formation de 'poches' d'eau contenant le soluté en question et dans lesquelles le potentiel chimique de l'eau est différent de celui de l'eau du bain. Cette différence de potentiel chimique est à l'origine d'un processus osmotique qui entraîne une très forte absorption d'eau. Elle peut conduire à une très importante dégradation des propriétés des élastomères allant jusqu'à la ruine du matériau. Ceci montre l'importance du choix de la formulation et des additifs utilisés lorsque les élastomères sont employés en milieu marin.

## Dégradation chimique des élastomères en milieu marin

En plus des dégradations physiques induites par la présence d'eau, les élastomères peuvent subir des dégradations chimiques irréversibles lorsqu'ils sont utilisés en milieu marin, la plus connue étant l'hydrolyse. L'hydrolyse des élastomères est, de façon générale, assez bien évaluée notamment dans le cas des polyuréthanes. On retiendra qu'un choix judicieux d'élastomère et de formulation permet d'éviter les problèmes d'hydrolyse. L'autre dégradation chimique importante pour les élastomères est l'oxydation. En effet, ce type de matériau est très sensible à l'oxydation en raison de la structure moléculaire du monomère (Energie de dissociation de la liaison CH en  $\alpha$  du chlore, et de la présence de double liaison dans le cas des élastomères insaturés). L'analyse d'échantillons vieillis naturellement a montré que l'oxydation est l'une des dégradations majeures lorsque les élastomères sont utilisés en milieu marin. Ce mécanisme est donc au centre de la problématique de la durabilité du polychloroprène en milieu marin.

### L'oxydation des polymères

L'oxydation est une dégradation chimique radicalaire qui fait intervenir l'oxygène et conduit à une importante modification des propriétés mécaniques du polymère. Cette dégradation est en fait composée de nombreux actes chimiques élémentaires qui se répartissent en trois étapes, l'amorçage des chaînes radicalaires, la propagation et la terminaison. Chacune de ces trois étapes est décrite dans le chapitre. On retiendra que le polychloroprène a la particularité de posséder une double liaison dans le squelette carboné qui conduit à une complexification des mécanismes d'oxydation. L'objectif étant, ici, de réaliser des prédictions de durée de vie à basse température, il est indispensable de considérer l'aspect cinétique de la dégradation. Trois différentes approches de prédiction sont décrites et comparées:

- La superposition temps/température : une approche simple mais qui peut être erronée dans la mesure où plusieurs phénomènes sont mis en jeu dans la dégradation des matériaux ;
- Une approche mécanistique avec de nombreuses hypothèses qui permettent une résolution analytique. Les hypothèses sont discutées dans ce chapitre, notamment le fait que le modèle disponible ne prend pas en compte le rôle de la double liaison présente dans le CR ;
- Une approche mécanistique couplée à une résolution numérique afin de limiter les hypothèses. Elle est développée à l'ENSAM depuis 20 ans et sera la base de la prédiction de la durée de vie dans ce document. Elle a pour principal inconvénient d'être complexe et nécessite donc une mise en place étape par étape, c'est-à-dire partant du cas le plus simple (le polymère linéaire, non vulcanisé, sans additifs) et allant vers le cas le

plus complexe (le matériau industriel) en ajoutant à chaque étape un élément supplémentaire de la formule.

Ce modèle a pour objectif de prédire l'évolution du comportement mécanique au cours de l'oxydation d'un polychloroprène en utilisant la théorie de l'élasticité caoutchoutique ; deux caractéristiques seront particulièrement étudiées, le module d'élasticité et les propriétés à rupture. Dans le cas du module, une forte augmentation de raideur est observée dans la littérature. On peut l'attribuer au mécanisme de réticulation associé à l'addition de macroradicaux aux doubles liaisons. Mais l'oxydation dans le CR conduit aussi à des coupures de chaînes ayant un effet opposé sur les propriétés élastiques.



Mécanisme de réticulation lors de la consommation de la double liaison dans le polychloroprène.

Pour conclure, un élastomère utilisé en milieu marin avec une formulation adaptée devrait rapidement absorber une faible quantité d'eau sans détérioration majeure des propriétés mécaniques. Cependant, l'existence d'un processus osmotique pourrait conduire à une forte absorption d'eau avec des effets défavorables sur le comportement mécanique. Dans le même temps, des dégradations chimiques irréversibles peuvent avoir lieu, les deux principales étant l'hydrolyse et l'oxydation. L'hydrolyse des élastomères en milieu marin peut être évitée par un choix adéquat de formulation. L'oxydation, quant à elle, est un processus extrêmement important dans le cas des élastomères et ne peut pas être ignorée.

L'objectif de ce travail est donc de mettre en place un modèle mécanistique d'oxydation dans l'air pour le polychloroprène permettant de prédire l'évolution des propriétés mécaniques. Puis dans un second temps, d'adapter ce modèle au milieu marin en considérant d'éventuels couplages.

## Résumé du chapitre 2 : Matériaux et Méthodes

Le chapitre 2 décrit les matériaux et techniques utilisés dans cette étude.

### Matériaux

Cette étude est principalement réalisée sur du polychloroprène avec différentes formulations. On retiendra que :

- Le chapitre 3 porte sur le polychloroprène linéaire non vulcanisé.
- Les chapitres 4 et 5 sont dédiés à l'oxydation du polychloroprène vulcanisé au soufre.
- Le chapitre 6 fait intervenir un CR complètement formulé avec noir de carbone et stabilisant ainsi qu'un CR vulcanisé sans MgO.

### Techniques

Les techniques de caractérisation utilisées dans cette étude sont 'classiques' lorsque l'on considère le vieillissement des polymères. Une attention particulière a été portée à l'utilisation de mesures in situ, soit en infrarouge via l'utilisation d'une cellule de vieillissement fonctionnant à différentes pressions d'oxygène, soit à la mesure de module au cours de l'oxydation. D'autre part, une méthodologie de mesure de l'énergie de fissuration dans les films élastomères a été développée.

## Résumé du chapitre 3 : Oxydation du CR cru

Ce chapitre présente un modèle mécanistique qui peut être utilisé pour l'oxydation d'un polychloroprène vulcanisé. Tout d'abord les mécanismes d'oxydation dans le CR sont considérés puis les résultats expérimentaux issus de cette étude sont décrits. Par la suite, un modèle mécanistique de l'oxydation du CR non vulcanisé est proposé et les paramètres cinétiques déterminés. Pour finir, une comparaison avec les valeurs disponibles pour d'autres élastomères insaturés est réalisée afin de mettre en évidence les spécificités du CR.

### Mécanismes d'oxydation

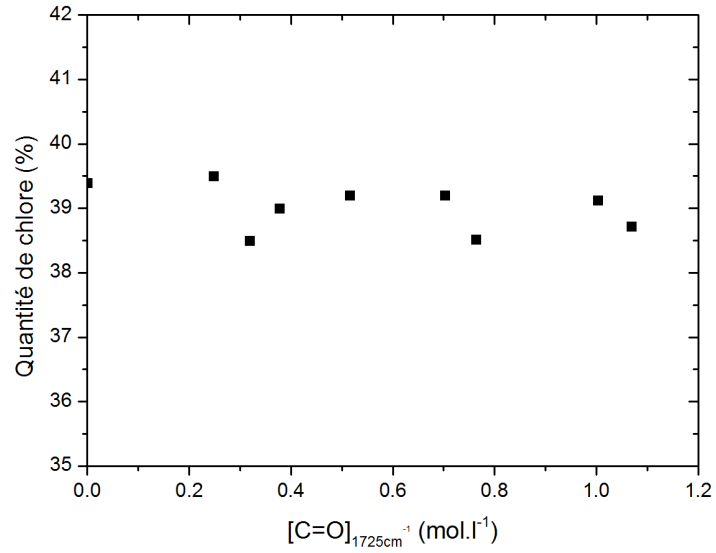
Etant donné sa nature chimique, le CR possède deux caractéristiques qui peuvent affecter largement les mécanismes d'oxydation par la présence : d'un atome de chlore et d'une double liaison :

- Le rôle du chlore dans l'oxydation n'est pas évidente dans la littérature car selon les auteurs, il agit ou non sur l'oxydation du matériau. Dans la mesure où le chlore jouerait un rôle, il y aurait formation de radicaux  $Cl^\circ$  et donc de HCl résultant de l'arrachement d'hydrogènes par  $Cl^\circ$ .
- L'existence de réactions impliquant les instauration est moins controversée. Il est connu que les radicaux libres peuvent réagir sur la double liaison via une réaction d'addition qui constitue un mode de propagation de la chaîne radicalaire d'oxydation autre que l'arrachement d'hydrogène. Cette étape devra être intégrée dans le modèle.

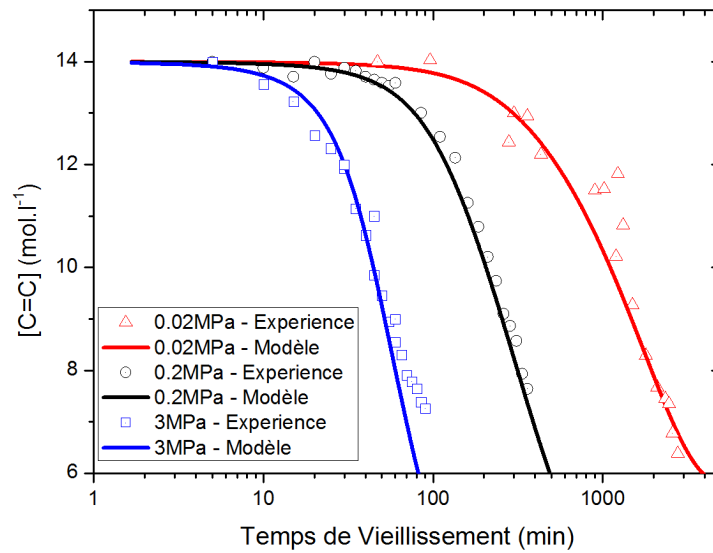
### Résultats expérimentaux

Un dosage du chlore au cours de l'oxydation du CR a été effectué afin d'évaluer son rôle. Les résultats sont présentés dans la figure ci-dessous. Dans la limite de détection de la mesure (0.6%), le taux de chlore ne varie pas. On peut donc considérer légitimement qu'il n'est pas nécessaire d'intégrer une possible formation de  $Cl^\circ$  dans le modèle mécanistique.

A l'inverse, une forte consommation de la double liaison est observée au cours de l'oxydation. Ce processus devra donc être intégré au modèle. La Figure met également en évidence le rôle prépondérant de la pression d'oxygène sur la cinétique d'oxydation. L'effet de la pression d'oxygène sera utilisé pour simplifier la détermination des constantes cinétiques du modèle.



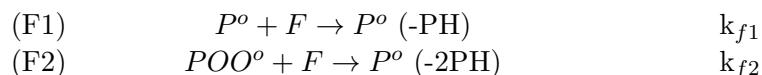
Dosage du chlore au cours de l'oxydation du CR cru à 80°C.



Effet de la pression d'oxygène sur la consommation de la double liaison au cours de l'oxydation du CR cru à 100°C.

## Mise en place du modèle

Le modèle mécanistique mis en place est basé sur le mécanisme général d'oxydation des polymères avec deux réactions de décomposition des hydroperoxydes lors de l'amorçage et l'intégration de la propagation via les doubles liaisons :



A chacun des actes chimiques est associée une constante de vitesse. Les constantes de vitesse de propagation  $k_2$  et  $k_3$  sont extraites de la littérature. Les autres constantes de vitesse sont déterminées en plusieurs étapes à partir des résultats expérimentaux, par méthode inverse. Les résultats obtenus par modélisation sont tracés en ligne continue sur la figure précédente.

## Comparaison avec les autres polydiènes

Une comparaison des constantes déterminées dans cette étude avec celles connues sur le polyisoprène et le polybutadiène montre que dans le CR :

- Les hydroperoxydes sont très instables. Cet effet est attribué à la présence de l'atome de chlore en position  $\alpha$ .
- La réaction des radicaux  $POO^o$  sur la double liaison est largement plus rapide que l'arrachement d'hydrogène par ces mêmes radicaux.
- La propagation est plus lente dans le CR que dans les autres polydiènes.

Un modèle cinétique d'oxydation du polychloroprène cru a été développé en intégrant l'effet de la présence des doubles liaisons. Les constantes déterminées ont pu être comparées à celles connues pour d'autres élastomères insaturés afin de mettre en relief les particularités du CR. Ce modèle cinétique est la base du modèle permettant la prédiction du module sur le CR vulcanisé présenté dans le chapitre suivant.

## Résumé du chapitre 4 : Oxydation du CR vulcanisé

En raison de la complexité du modèle cinétique à mettre en place, il est nécessaire de décomposer cette mise en place étape par étape. Après avoir mis en place le modèle cinétique sur le CR cru, l'effet de la vulcanisation sera ici considéré. Dans un premier temps, l'oxydation du CR vulcanisé est considérée avec une présentation des résultats expérimentaux et du modèle cinétique permettant de prédire le module dans le cas de films homogènes à 100°C. Puis l'effet de la température de vieillissement est étudié en détail. Enfin le rôle de la diffusion de l'oxygène est intégré au modèle afin de faire des prédictions sur pièces épaisses.

### Oxydation homogène à 100°C

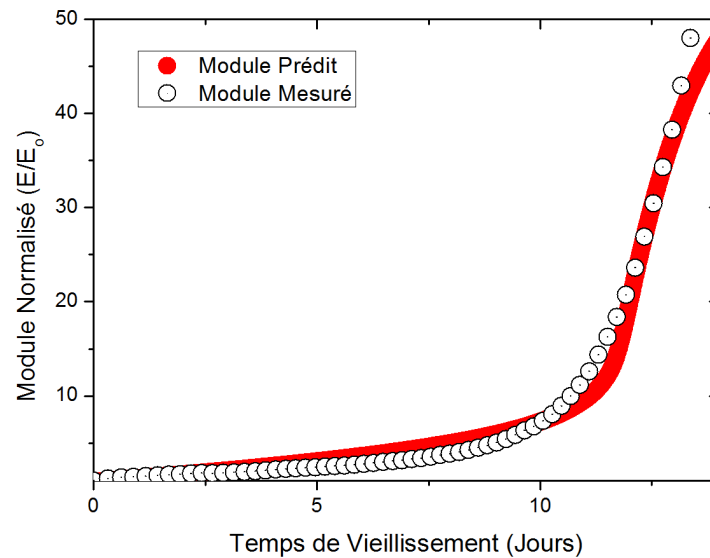
#### Mécanismes d'oxydation

L'oxydation du CR vulcanisé a été caractérisée par suivi FTIR au cours du temps. La comparaison des résultats obtenus avec ceux présentés dans le chapitre précédent montre que :

- La présence de ZnO conduit à une modification des produits d'oxydation qui ne sera pas considérée ici mais qui implique que le modèle sera basé uniquement sur la consommation des doubles liaisons.
- La cinétique d'oxydation est très largement ralentie en raison de la présence de soufre. Cet effet s'explique par une décomposition non radicalaire des POOH par les sulfures qui agissent donc comme un fort stabilisant.

#### Conséquence de l'oxydation sur le module

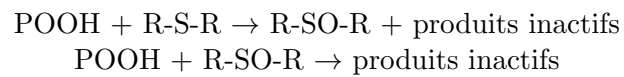
Le suivi in situ du module à 100°C montre une très forte augmentation de celui-ci au cours de l'oxydation. Cela s'explique notamment par la formation de nouveaux points de réticulation lors de la réaction des macro-radicaux sur la double liaison. Cependant les valeurs atteintes (plus de 200 MPa) par le module ne peuvent pas s'expliquer uniquement par cette réticulation. Des analyses DMA montrent un étalement de la transition vitreuse vers les hautes températures pouvant être attribué à la formation de domaines vitreux. En raison de cette complexité supplémentaire à fort taux de conversion, la prédiction du module sera considérée uniquement jusqu'à 50 MPa en première approche.



Augmentation du module au cours de l'oxydation du CR à 100°C.

### Mise en place du modèle

L'effet du soufre a été intégré au modèle cinétique en considérant deux nouveaux actes chimiques :



Les constantes de vitesse associées à ces actes chimiques ont été déterminées par méthode inverse. Les limites de ce modèle ont ensuite été évaluées pour la première fois en comparant l'absorption d'oxygène prédite avec des données expérimentales générées au laboratoire de Sandia (Albuquerque, USA). On observe que l'ordre de grandeur prédit est en accord avec les données expérimentales. Cependant une légère surestimation apparaît, l'origine en est discutée.

## Prédiction du module

A partir du modèle cinétique, il est possible de décrire les coupures de chaînes et les réticulations qui interviennent au cours de l'oxydation du CR vulcanisé. Ici deux types de coupures sont considérés : les coupures aléatoires lors de l'amorçage ainsi que les coupures sélectives lors de la décomposition des POOH sur le soufre aux nœuds de réticulation. Dans le même temps, deux types d'acte de réticulation sont pris en compte : le couplage des radicaux lors de la terminaison et l'addition des macro-radicaux sur les doubles liaisons. Dans ce cas, la densité de réticulation au cours du temps peut s'écrire (à faible degré de conversion) :

$$\nu(t) = \nu_0 - \delta \cdot s(t) + x_{\text{terminaison}}(t) + 2 \cdot \tau \cdot x_{C=C}(t) \quad (6.18)$$

Avec  $\nu_0$  la densité de réticulation initiale,  $s(t)$  le nombre de scission de chaîne,  $x_{\text{termination}}$  le nombre de réticulation lors des réactions de terminaisons,  $x_{C=C}$  le nombre de réticulation lors des additions sur la double liaison. Un rendement  $\tau$  de création des points de réticulation par rapport à la consommation des doubles liaisons est introduit pour prendre en compte de possibles réactions parallèles comme les réactions intramoléculaires. Connaissant la densité de réticulation dans un élastomère non renforcé, il est possible de prédire le module à partir de la théorie de l'élasticité caoutchoutique. Les résultats du modèle sont représentés sur la figure au dessus. Un bon accord entre la prédiction et les données expérimentales est observé pour un rendement de 0.35.

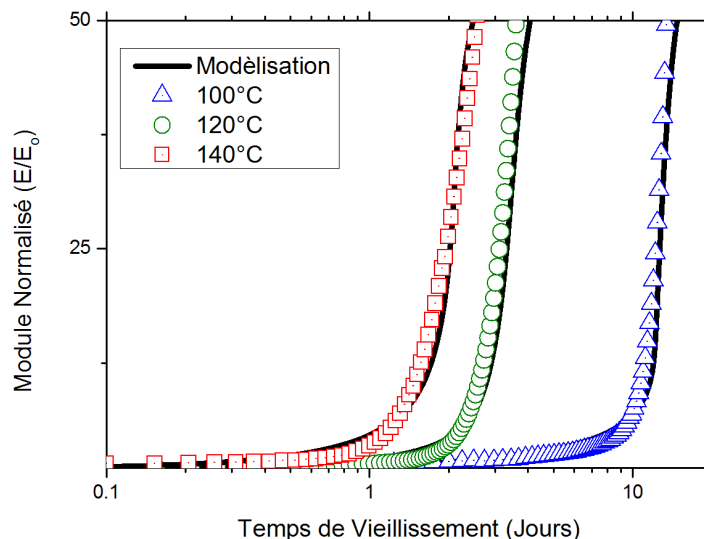
Pour la première fois, un modèle cinétique de prédiction du module au cours de l'oxydation du polychloroprène a été mis en place et validé à 100°C. L'effet de la température est maintenant considéré pour pouvoir faire des prédictions sur le long terme (et donc à basse température).

## Effet de la température

L'effet de la température est considéré sur différents aspects qui peuvent se résumer ainsi :

- Les variations des constantes de vitesse associées à la réaction du POOH sur le soufre avec la température sont déterminées à partir de résultats de mesures Infra Rouge dans une gamme de températures variant de 60°C à 140°C. Un comportement Arrhenien est observé avec des énergies d'activation de 130 et 85 kJ/mol.
- Le rendement  $\tau$  des réticulations créées lors de la consommation de la double liaison est indépendant de la température dans une gamme de 100°C à 140°C. En supposant que ce rendement reste constant à plus

basse température, il est donc possible de faire une prédiction du module pour des températures de service.



Effet de la température sur l'augmentation du module au cours de l'oxydation du CR.

- L'effet de la température sur la vitesse de consommation d'oxygène est étudié en détail à partir de résultats expérimentaux, des prédictions du modèle et de données issues de la littérature. Cette comparaison indique que l'oxydation du CR non stabilisé suit un comportement Arrhenien avec une énergie d'activation de 66 kJ/mol. Ce comportement est correctement prédit par le modèle. La littérature nous révèle que, dans le cas d'échantillons industriels, le comportement cesse d'obéir à la loi d'Arrhenius, les résultats ci-dessus semblent indiquer que cette déviation est liée à la présence de stabilisants.

Les deux premières parties de ce chapitre étaient dédiées à l'oxydation homogène. Cependant en service, les échantillons sont épais. La notion d'oxydation limitée par la diffusion de l'oxygène depuis l'air environnant dans le matériau doit donc être considérée. C'est le but de la partie suivante.

### Oxydation limitée par la diffusion

Dans cette partie dédiée à l'oxydation d'échantillons épais, les résultats expérimentaux sont tout d'abord exposés avec la mise en évidence de profil d'oxydation induit par l'effet DLO (Diffusion Limited Oxidation) puis les mesures de perméabilité à l'oxygène ainsi que son évolution avec la température. Dans un second temps, une modélisation de ce couplage entre la diffusion de

l'oxygène par une diffusion de type Fickien (dont les valeurs sont tirées des mesures de perméabilité) et la consommation induite par l'oxydation est mise sous la forme d'une équation différentielle et intégrée dans le modèle. Les profils de doubles liaisons et d'augmentation de modules sont présentés. Afin d'évaluer la pertinence de ces résultats, une comparaison des profils après 6 jours de vieillissement est proposée.

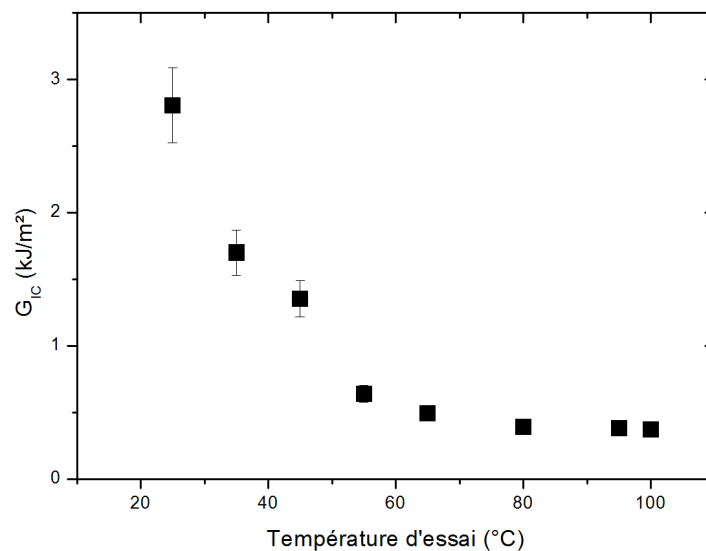
On observe d'un point de vue global un bon accord entre les résultats expérimentaux et les résultats prédits. Cependant il apparaît que le profil mesuré est un peu plus prononcé que celui prédit. Cet effet pourrait s'expliquer par une diminution du coefficient de diffusion avec l'oxydation.

## Résumé du chapitre 5 : Evolution des propriétés à rupture

Ce chapitre est dédié à la caractérisation, la compréhension et la prédiction des propriétés à rupture dans le polychloroprène non chargé au cours de l'oxydation. Après une introduction sur la mécanique de la rupture dans les élastomères, le montage expérimental mis en place dans cette étude est décrit. Les résultats expérimentaux sont ensuite présentés avec l'introduction de deux nouveaux élastomères modèles (un polyuréthane et un polyéthylène chloré) dans le but de mieux comprendre l'évolution de l'énergie de fissuration en mode I ( $G_{IC}$ ) due à l'oxydation. Dans une dernière partie, les résultats sont confrontés à la théorie et une prédiction est proposée.

### Mise en place d'un essai de propagation de fissure sur élastomère

Afin de pouvoir étudier l'effet de l'oxydation homogène sur la propagation de fissure, un moyen expérimental a été adapté et les paramètres influant aussi bien au niveau de la géométrie de l'échantillon (épaisseur, longueur de ligament) que de la vitesse de sollicitation, ont été étudiés. L'effet de la température de l'essai sur la valeur de  $G_{IC}$  a également été caractérisé,  $G_{IC}$  décroît de façon quasi exponentielle avec la température d'essai de  $2.8 \text{ kJ/m}^2$  à  $25^\circ\text{C}$  à  $0.9 \text{ kJ/m}^2$  à  $100^\circ\text{C}$ . Ce comportement s'explique par la présence ou non de cristallisation induite (SIC) dans le CR. En effet à  $100^\circ\text{C}$ , les cristallites induites par déformation fondent et ne peuvent donc pas jouer leur rôle renforçant. Cette particularité est utilisée par la suite pour comprendre l'effet de l'oxydation sur l'évolution du  $G_{IC}$ .



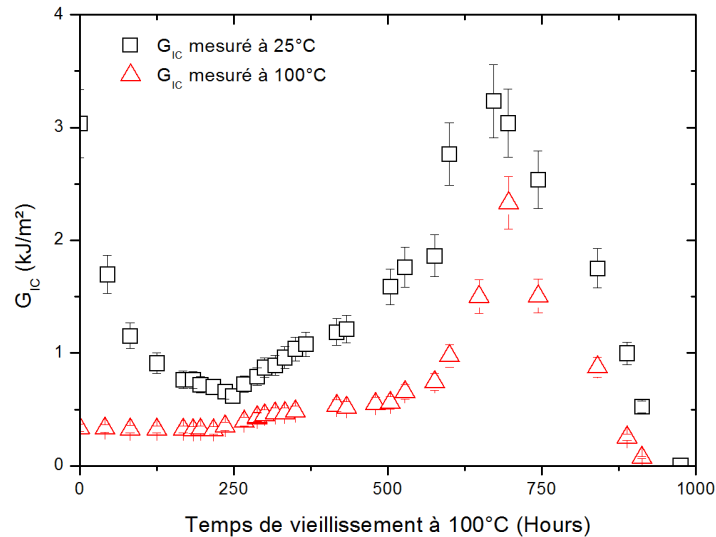
Evolution de  $G_{IC}$  en fonction de la température d'essai.

## Influence de l'oxydation sur la valeur de $G_{IC}$

L'évolution du  $G_{IC}$  avec et sans SIC (c'est-à-dire mesurée à 25 et 100°C) est présentée sur la figure ci-contre. Trois périodes peuvent être distinguées : la première jusqu'à 200 heures, la seconde entre 200 et 600-700 heures et enfin la dernière après 700 heures.

Lors de la première période,  $G_{IC}$  mesuré à 25°C décroît très vite alors que le  $G_{IC}$  mesuré à 100°C ne varie pas. Ce comportement est attribué à une inhibition de la cristallisation par l'oxydation. Ce point est confirmé par la suite.

Lors de la seconde période, les deux mesures de  $G_{IC}$  augmentent fortement, c'est la conséquence d'une forte réticulation dans l'élastomère induit par l'oxydation. La dernière période constitue un effondrement de la valeur de  $G_{IC}$  dans les deux cas.



Evolution de  $G_{IC}$  mesurés à 25 et 100°C en fonction du temps de vieillissement à 100°C.

## Comparaison avec d'autres élastomères

Deux autres élastomères modèles sont introduits afin de mieux comprendre l'effet de l'oxydation sur la propagation de fissure dans ce type de matériaux. Le premier, un polyuréthane à base de polybutadiène, ne cristallise pas sous charge mais possède une insaturation qui induit une forte réticulation lors de l'oxydation. Le second, un polyéthylène chloré qui cristallise sous charge mais ne possède pas d'insaturation. Les résultats sont conformes aux interprétations précédentes : la chute initiale est bien due à la disparition de la SIC, inhibition attribuée à la réticulation. En absence d'insaturation, elle ne se produit pas. Bien sûr, si la SIC n'existe pas au départ (cas du polyuréthane), la chute initiale n'est pas observée.

## Discussion et prédiction de durée de vie

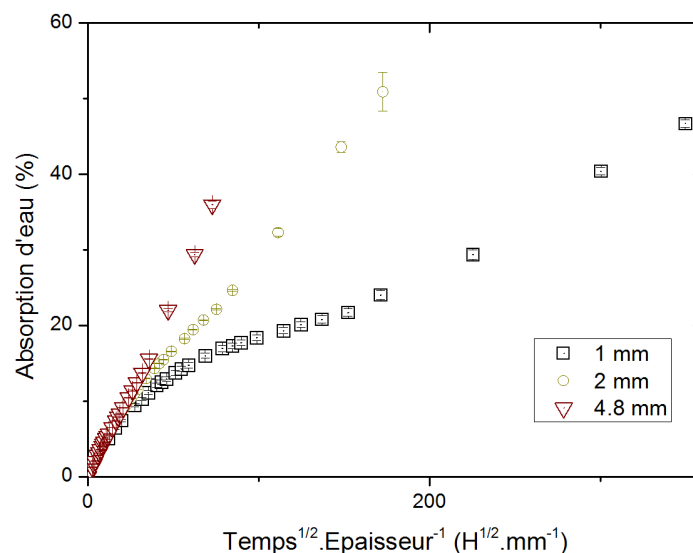
Les résultats expérimentaux résumés ci-dessus sont confrontés à la théorie de la mécanique de la rupture dans les élastomères. Il apparaît que  $G_{IC}$  sans SIC (c'est-à-dire mesurée à 100°C) ne varie pas linéairement avec la racine de la masse molaire entre nœuds. Ceci pourrait s'expliquer par la présence d'un réseau bimodal dans le matériau. Cependant en définissant une fin de vie lorsque  $G_{IC}$  est inférieure à 1 kJ/m<sup>2</sup> (de façon arbitraire), il est possible de mettre en évidence l'existence d'une densité de réticulation critique de 0.3mol/kg. Etant donné que le modèle peut prédire la densité de réticulation, il est donc possible pour la première fois de faire une prédiction de durée de vie non empirique sur une valeur d'énergie de propagation de fissure.

## Résumé du chapitre 6 : Comportement du polychloroprène en eau de mer

Le comportement à long terme en immersion du polychloroprène est considéré dans ce dernier chapitre. La première partie est dédiée à la présentation de résultats expérimentaux obtenus lors de l'immersion de CR complètement formulé en eau de mer à 60°C. Ils montrent une forte absorption d'eau qui conduit à une large dégradation des propriétés mécaniques du matériau au cours du temps. L'origine de cette forte absorption d'eau a été étudiée en détail en utilisant une formulation améliorée (c'est-à-dire sans MgO) grâce à des résultats de « Dynamic Vapor Sorption (DVS) » couplés à des immersions en eau de mer.

### Vieillessement en eau de mer d'un CR complètement formulé

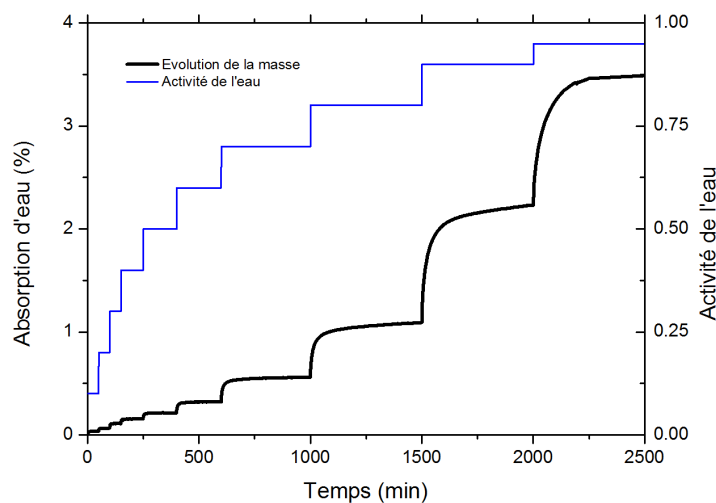
Des échantillons de CR complètement formulés, c'est-à-dire avec charges renforçantes et stabilisants ont été immergés dans de l'eau de mer naturelle et renouvelée pendant 2 ans. Les résultats obtenus montrent une très forte absorption d'eau dans le matériau sans saturation (Figure ci-dessous) qui conduit à une importante chute des propriétés en traction du matériau. Une étude plus fondamentale sur l'origine de cette forte absorption dans le CR est présentée par la suite.



Absorption d'eau dans le polychloroprène immergé dans l'eau de mer à 60°C.

## Résultats

Une nouvelle formulation de polychloroprène vulcanisé a été utilisée ici afin d'éliminer le rôle connu du MgO. Les échantillons ont été immergés en eau de mer à des températures comprises entre 25 et 80°C. Les résultats ont mis en évidence une forte absorption d'eau sans saturation. Ces résultats ont été complétés par une étude d'absorption cyclique en DVS à 40°C sur films de 100 $\mu\text{m}$  qui montre une réversibilité totale de l'absorption d'eau avec un coefficient de diffusion constant. Le fait que le coefficient de diffusion reste inchangé au cours du cyclage montre que l'absorption d'eau n'est pas due à un processus osmotique. Une autre hypothèse a alors été émise : l'hydrolyse de la liaison C-Cl aurait pu introduire un phénomène de fissuration osmotique associée à un relargage de HCl dans le milieu. Cette hypothèse est rejetée à partir des données de dosage de HCl dans le milieu d'exposition. Dans le but d'évaluer ce phénomène d'absorption d'eau, des essais de sorption à différentes activités d'eau ont été réalisés. Ils montrent que, contrairement aux essais d'immersions, une saturation est atteinte.



Absorption d'eau dans un film de 100 $\mu\text{m}$  de CR à 40°C pour niveau d'activité.

De plus, on observe que la quantité d'eau absorbée par le film de CR ne suit pas la loi de Henry. Après avoir tenté, sans succès, de décrire ce comportement par la loi de Flory-Huggins, l'approche de Zimm Lundberg a été utilisée. Cette approche basée sur la description de la formation de « clusters » d'eau dans l'élastomère permet de décrire le comportement observé mais également de décrire la taille moyenne de ces « clusters ».

### **Tentative de justification par le modèle**

Une tentative de justification de la formation de « clusters » dans le CR est proposée en considérant que ce phénomène est la conséquence d'une plus grande affinité de l'eau avec elle-même, plutôt que de l'eau avec le polymère. Bien que ce modèle soit une simplification de la réalité, il permet de valider les mécanismes mis en jeu et de définir des critères de formation de clusters tels qu'une activité critique.

## Conclusions

L'objectif de cette étude est de contribuer à la caractérisation, la compréhension et la prédiction du comportement à long terme des polymères et plus particulièrement des élastomères en milieu marin. Notre polymère d'étude a été le polychloroprène (vulcanisé ou non). Cet élastomère présente des propriétés mécaniques similaires au caoutchouc naturel et une durabilité souvent annoncée comme supérieure à celui-ci.

Un état de l'art sur les connaissances et les données concernant la durabilité des élastomères en milieu marin a été réalisé. L'analyse des résultats issus de la littérature montre que, lorsqu'un élastomère est correctement formulé il absorbe peu d'eau et ses propriétés physiques sont donc peu modifiées. Cependant, il apparaît également que de fortes absorptions d'eau peuvent se produire en raison d'un processus de fissuration osmotique. Dans ce cas, les propriétés de l'élastomère sont largement modifiées lors de l'immersion.

De plus, dans tous les cas, les élastomères peuvent subir des dégradations chimiques irréversibles telles que l'hydrolyse ou l'oxydation. L'hydrolyse est relativement connue et peut être maîtrisée par un choix adéquat de polymère. L'oxydation, en revanche, ne peut être supprimée. Elle peut être néanmoins ralentie dans le meilleur des cas. L'appréhension de ce type de dégradation est donc primordiale, d'autant plus que les élastomères polydiéniques y sont très sensibles en raison de la structure moléculaire du monomère.

Les mécanismes d'oxydation ont donc été décrits dans ce premier chapitre ainsi que les approches existantes utilisées pour la prédiction des propriétés mécaniques à long terme. Malgré un très large intérêt de la communauté scientifique pour l'oxydation des polymères depuis plus de 50 ans, il n'existe pas de consensus sur un éventuel moyen simple et fiable pour prédire l'évolution d'une propriété mécanique d'un polychloroprène au cours de l'oxydation. Nous avons mis en place une modélisation cinétique se basant sur les actes gouvernant l'oxydation du polymère. La spécificité de notre approche consiste à décrire chacun des actes chimiques cinétiquement importants à partir des mécanismes d'oxydation puis de déterminer chacune des constantes de vitesse associées à ces actes. Afin d'identifier d'une façon indépendante chacun des paramètres, la modélisation doit être mise en place étape par étape avec une complexité croissante.

La première étape a été de considérer le matériau cru. Les mécanismes chimiques essentiels ont été déterminés à partir de la littérature et des données expérimentales. Le polychloroprène possède deux particularités chimiques importantes : la présence de chlore dans la chaîne carbonée et la présence d'une double liaison carbone-carbone. A partir des résultats expérimentaux, il apparaît que le rôle du chlore peut être négligé alors que la consommation de la double liaison est caractéristique du processus d'oxydation. Il a été alors proposé un schéma mécanistique composé de 9 réactions élémentaires permettant de rendre compte de ces évolutions. En utilisant les résultats

expérimentaux à différentes pressions partielles d'oxygène, les cinétiques de ces réactions élémentaires ont d'abord été déterminées à 100°C. Puis l'effet de la température de vieillissement a été intégré au modèle cinétique.

Dans une seconde étape, le polychloroprène vulcanisé a été étudié. Une forte réduction de la vitesse d'oxydation a été mesurée et attribuée au pouvoir antioxydant du soufre qui décompose les hydroperoxydes. Ces décompositions ont été implémentées dans le modèle cinétique par l'intermédiaire de deux nouvelles réactions chimiques. Le modèle ainsi développé a été confronté à des résultats expérimentaux d'absorption d'oxygène générés au laboratoire de Sandia National Laboratories afin de mettre en évidence les limites du modèle. L'oxydation du polychloroprène conduit à une très forte augmentation du module en raison, de la réaction d'addition des radicaux sur la double liaison. Ces variations de module au cours de l'oxydation du CR ont été prédites de façon quantitative jusqu'à une valeur de 50 MPa pour la première fois, en considérant l'évolution de densité de réticulation induite par l'oxydation. En effet, en prenant en compte à la fois les réticulations et les coupures de chaîne, il est possible de prédire la densité de réticulation dans l'élastomère et donc le module via la théorie de l'élasticité caoutchoutique. Cette prédiction nécessite l'introduction d'un rapport entre le nombre de nouveaux points de réticulation et le nombre de doubles liaisons. Ce rapport est égal à 0.35 et indépendant de la température de vieillissement (dans la gamme considérée : 140 à 100°C). Les phénomènes de diffusion d'oxygène ont été intégrés dans ce modèle afin de pouvoir prédire le comportement de pièces épaisses. On observe que la prédiction est globalement en accord avec les résultats expérimentaux mais reste limitée à une augmentation de module de 50MPa.

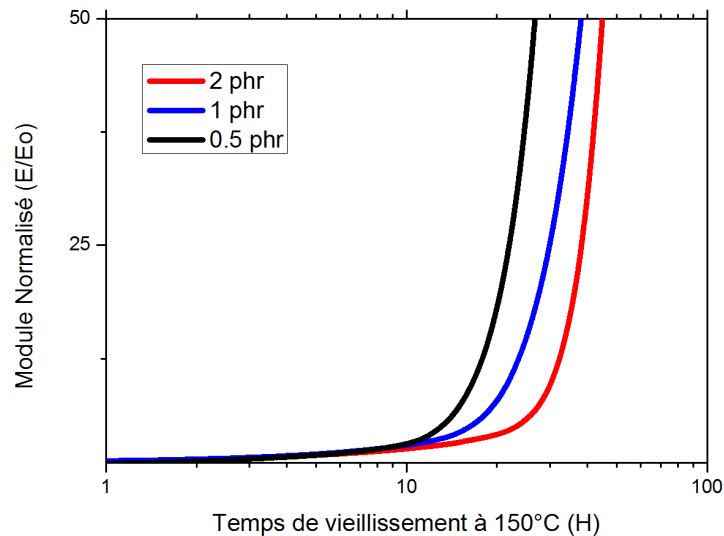
Les modifications au sein du réseau, induites par l'oxydation du CR conduisent à une forte modification du comportement à rupture. Dans le cas du polychloroprène, un comportement inattendu caractérisé par une diminution rapide de l'énergie de fissuration ( $G_{IC}$ ) puis une augmentation et enfin une chute dramatique, a été observé. Ces résultats ont pu être expliqués grâce à l'utilisation de matériaux modèles tels que le polyuréthane ou le polyéthylène chloré afin de découpler le rôle de la réticulation et de la cristallisation induite dans les matériaux. Il apparaît que la première diminution est liée à l'inhibition de la cristallisation induite qui conduit à une baisse de  $G_{IC}$  de quelques  $\text{kJ/m}^2$  à quelques centaines de  $\text{J/m}^2$ . L'augmentation, quant à elle, a été attribuée au mécanisme de réticulation à la forte conversion dans les élastomères contenant des doubles liaisons. Enfin, la chute finale de  $G_{IC}$  serait liée à la très faible mobilité dans les matériaux très réticulés. Bien que ce comportement n'ait pas pu être prédit à partir de considérations théoriques sur la fragilisation dans les élastomères, un critère de fin de vie a été proposé permettant une prédiction de durée de vie.

Afin d'adapter le modèle d'oxydation mis en place en air au milieu marin, des échantillons ont été vieillis de façon accélérée en eau de mer. Les résultats expérimentaux ont mis en évidence une forte absorption d'eau dans le CR ne permettant pas l'adaptation du modèle cinétique au milieu marin. L'origine de cette absorption d'eau a été étudiée en détail avec notamment l'utilisation d'essais DVS qui a permis de proposer un nouveau mécanisme de formation de « cluster » dans le polychloroprène. Ce mécanisme s'explique par une affinité de l'eau avec elle-même plus forte qu'avec le polymère.

## Perspectives

Il existe, suite à cette contribution à la compréhension et à la prédiction du comportement à long terme du polychloroprène en milieu marin, des perspectives à différents niveaux : a) vérifier les conséquences de la vulcanisation au soufre sur les cinétiques d'oxydation; b) caractériser l'ajout de stabilisants sur les cinétiques et les incorporer dans la modélisation cinétique; c) affiner les relations structures propriétés mécaniques comme la prise en compte des charges renforçantes (noir de carbone) et le processus de cristallisation induite; d) étudier l'influence des additifs contenus dans la formulation industrielle (MgO) sur les mécanismes d'absorption d'eau.

- Le modèle de prédiction du module au cours de l'oxydation a été réalisé pour un type de CR faisant intervenir un seul type de vulcanisation. Une généralisation de ce modèle à tous les polychloroprènes nécessite une meilleure compréhension du rôle du soufre. Notamment l'influence de la concentration et des différents types de liaisons issues de la vulcanisation (monosoufre, polysoufre) sur les cinétiques d'oxydation.
- Bien évidemment, pour se rapprocher des matériaux industriels, il est nécessaire de prendre en compte à la fois les effets des charges renforçantes et des stabilisants. L'intégration des stabilisants dans le modèle d'oxydation est possible, elle a déjà été réalisée dans d'autres études. Ici une partie des données nécessaires à cette étape a été faite, par exemple la figure ci-dessous montre l'effet des antioxydants sur la cinétique d'augmentation du module à 150°C. Il paraît également nécessaire de réaliser des mesures d'absorption d'oxygène sur le CR stabilisé afin de confirmer (ou non) le rôle des stabilisants dans le comportement non Arrhenien de l'oxydation. La nature des stabilisants et leur effet (ou non) sur un comportement Arrhenien reste une question ouverte.
- La prise en compte de l'effet des charges renforçantes est également une question importante. Ce point a été étudié ici mais de façon trop sommaire pour être présenté. On retiendra tout de même que le module aux faibles déformations d'un CR chargé en noir de carbone peut être prédit à partir de l'utilisation de la loi proposée par Guth et al. La validité de cette loi au cours de l'oxydation reste à démontrer. En outre, la question plus générale de l'intégration du vieillissement dans les lois de comportement reste ouverte. Par ailleurs, l'étude a mis en évidence une inhibition forte de la cristallisation induite dans les élastomères par l'oxydation en utilisant des caractérisations indirectes. Il semble intéressant d'étudier plus finement cette perte de capacité à cristalliser via des mesures directes telles que la diffraction des rayons X sur différents types d'élastomères présentant (NR, CR, CPE) ou non (SBR, EPDM) ce phénomène de SIC.



Effet de la quantité de stabilisant dans le CR sur l'augmentation de module au cours de l'oxydation à 150°C.

- L'objectif final de travail est d'être en mesure de pouvoir prédire le comportement à long terme des élastomères lorsqu'ils sont utilisés en milieu marin. Pour cela il paraît nécessaire d'étudier de façon plus poussée les mécanismes mis en jeu lors d'une dégradation osmotique et notamment le rôle de chacun des additifs afin de pouvoir définir des règles de conception et ainsi éviter les fortes absorptions d'eau.

Outre ces perspectives à court terme permettant de construire un modèle de prédiction de durée de vie du polychloroprène industriel, la nécessité de se rapprocher des conditions d'utilisation de l'élastomère en milieu marin nous conduit à considérer deux types de couplage :

- Le couplage entre l'oxydation et l'absorption d'eau : l'eau absorbée par l'élastomère peut contribuer au processus d'extraction des stabilisants initialement présents. Cette extraction conduirait alors à réduire la concentration en stabilisant disponible pour protéger l'élastomère contre l'oxydation.
- Le couplage entre l'oxydation et une sollicitation de type fatigue : une inhibition de la SIC par l'oxydation a été mise en évidence dans ce travail. Etant donné que la cristallisation induite est l'origine des très bonnes propriétés en fatigue, on peut s'attendre à ce que l'oxydation réduise d'une manière drastique la durée en fatigue.

## Durabilité du polychloroprène pour application marine

**RESUME :** La prédiction de la durée de vie des polymères en milieu marin est devenue, ces dernières années, indispensable afin de limiter les coûts de maintenance des structures utilisées en mer. Le polychloroprène est un élastomère très employé en milieu marin en raison de ses propriétés intrinsèques proches de celles du caoutchouc naturel, avec une durabilité supérieure. Ce travail de thèse a pour objectif de caractériser, comprendre et prédire l'évolution des propriétés mécaniques (module et rupture) au cours du vieillissement et plus particulièrement de l'oxydation, l'un des mécanismes de dégradation majeurs pour ce type de matériaux. Cette prédiction est basée sur l'utilisation d'une description mécanistique de l'oxydation couplée à l'utilisation de relations structure/propriétés issues de la théorie caoutchoutique. Dans un premier temps, un modèle cinétique d'oxydation a été mis en place sur le polychloroprène cru et les constantes associées déterminées par méthode inverse. L'effet de la vulcanisation est, par la suite, intégré au modèle cinétique permettant ainsi une prédiction du module au cours de l'oxydation, ce type de dégradation conduisant à une forte augmentation du module dans le CR en raison de la présence de doubles liaisons dans le matériau. Afin de proposer une prédiction basée sur les propriétés à rupture, l'influence de l'oxydation sur l'énergie de propagation de fissure en mode I ( $G_{Ic}$ ) a été étudiée en détail avec notamment une comparaison entre différents types d'élastomère. Cette étude a permis de mettre en évidence une chute importante de  $G_{Ic}$  en raison d'une inhibition de la cristallisation induite au cours de l'oxydation. La dernière partie de ce travail est dédiée à la diffusion de l'eau dans le polychloroprène et plus particulièrement les mécanismes de formation d'agrégat d'eau dans le matériau qui se traduit par une forte absorption et donc une perte de propriétés mécaniques à la rupture.

**Mots clés :** Polychloroprène, Oxydation, Prédiction, Propriétés mécanique, Eau, Fissuration.

## Durability of polychloroprene rubber in marine applications

**ABSTRACT :** The prediction of the lifetime of polymers in a marine environment is becoming increasingly important in order to limit maintenance costs for structures at sea. Polychloroprene is an elastomer which is widely used in marine structures due to its properties which are similar to natural rubber but with improved durability. The aim of the work described in this thesis is to characterize, understand and predict the evolution of mechanical properties (modulus and rupture) during aging, and in particular during oxidation, one of the main degradation mechanisms in this type of material. The prediction is based on the use of a mechanistic description of oxidation coupled with the use of theoretical structure/property relationships. First a kinetic model of oxidation has been set up for raw polychloroprene, and the associated rate constants have been found by an inverse method. The effect of vulcanization was then included in the model, enabling modulus to be predicted during oxidation. As a result of the presence of double bonds oxidation causes a significant increase in modulus of CR. Then, in order to predict fracture properties, the influence of oxidation on the mode I crack propagation energy ( $G_{Ic}$ ) has been studied in detail, with a comparison between different types of elastomer. This study has revealed a strong drop in  $G_{Ic}$  due to inhibition of induced crystallization during oxidation. In the last part of the document the diffusion of water in polychloroprene has been examined, and the mechanisms of cluster formation have been described: These lead to large water absorption and a loss of mechanical properties.

**Keywords :** Polychloroprene, Oxidation, Prediction, Mechanical properties, Water, Fracture, Life Time